Structural Behaviour of Lapped Cold-Formed Steel Z-Shaped Purlin Connections with Vertical Slotted Holes

by

Jingnan Liu

A thesis
presented to the University of Waterloo
in fulfillment of the
thesis requirement for the degree of
Master of Applied Science
in
Civil Engineering

Waterloo, Ontario, Canada, 2014

AUTHOR'S DECLARATION

I hereby declare that I am the sole author of this thesis. This is a true copy of the thesis, including any required final revisions, as accepted by my examiners.

I understand that my thesis may be made electronically available to the public.

Abstract

Lapped joints of cold-formed steel (CFS) Z-shaped purlins are extensively used in metal building roof systems. The research that has been carried out so far for these lapped connections is primarily focused on connections with round holes. However, the lapped connections with vertical slotted holes are extensively used in current construction practice to simplify the erection of continuous Z-shaped roof purlins. There is no design guideline or recommendation available for CFS Z-purlin lapped connections with vertical slotted holes.

Presented in this paper are the results of an experimental study and analysis of the structural behaviour of lapped CFS Z-shaped purlin connections with vertical slotted holes. 42 flexural tests were performed on lapped CFS Z-shaped purlins with vertical slotted connections with different lap lengths, purlin depths, thicknesses and spans. The flexural strength and deflection of each specimen were measured. The characteristics of moment resistance and flexure stiffness of the lapped purlins were computed. The test results show that the lapped purlins with vertical slotted holes may be more flexible than the lapped purlins with round holes or continuous purlins without lapped joint. Thus, the slotted connections may need greater lap lengths to achieve full stiffness of continuous purlins. The results also indicate that the characteristics of moment resistance and flexural stiffness in the slotted connections are dependent on the ratio of lap length to purlin depth, the ratio of lap length to purlin thickness, the ratio of purlin depth to purlin thickness, and the ratio of lap length to span. Based on the results, design recommendations for evaluating the moment resistance and flexural stiffness of lapped slotted connections were proposed.

Acknowledgements

First and foremost I would like to thank my supervisor Professor Lei Xu for his guidance, support, patience, and encouragement throughout the course of the research. His insight and expertise in the field of cold-formed steel design was essential to the completion of this thesis.

I would also like to thank the Canadian Sheet Steel Building Institute (CSSBI) for funding this project and the Steelway Building System for providing all the test materials. Without their generous support, this project would not have been possible. In particular, I would like to express my profound gratitude to Dr. Steven Fox for his help and guidance with this research.

Also, I would like to thank the Civil Engineering Structures Lab technicians; Mr. Doug Hirst, Mr. Michael Burgetz, Mr. Richard Morrison, and Mr. Rob Sluban, as well as three undergraduate research assistants, Mr. Anthony Norwell, Mr. Ping Gong, and Mr. Xi Chen for their assistance and support on the heavy testing portion of this research.

Thanks also go to my dear friends, Yi Zhuang, Xiaoli Yuan, Sigong Zhang, and Shijun Yang for listening, offering me advice, and supporting me through this process.

Last but not least, I would like to give a special thanks to my wife Alice for her understanding and love during the past few years. I am very grateful for her spending hours reading the draft of my thesis and giving me useful feedback. Her tolerance of my occasional vulgar moods is a testament in itself of her unyielding devotion and love.

Table of Contents

List of Figures

List of Tables

List of Notations

a	Clear distance between transverse stiffeners of reinforced web elements
A_f	Cross-sectional area of the compression flange plus edge stiffener about an x-y axis located at the centroid of the flange, with the x-axis measured positive to the right form the centroid, and the y-axis positive down from the centroid
A_w	Gross area of web element
b	Flange width
C	Bearing factor
C_{wf}	Warping torsion constant of the flange
d	Depth of section
d_b	Nominal bolt diameter
E	Modulus of elasticity of steel
F_d	Elastic distortional buckling stress
F_u	Tensile strength of steel
F_v	Nominal shear stress
F_y	Yield stress of steel
G	Shear modulus of steel
h	Length of lip
h_0	Out-to-out web depth
h_g	Gross section depth of flat portion of web
h_n	Net section depth of flat portion of web
h_{xf}	x distance from the centroid of the flange to the flange / web junction
I_e	Effective moment of inertia
I_g	Gross Moment of Inertia
I_{xf}	x-axis moment of inertia of the flange

I_{xyf} Product of the moment of inertia of the flange

I_{yf} y-axis moment of inertia of the flange

J_f St. Venant torsion constant of the compression flange, plus edge stiffener about an x-y axis located at the centroid of the flange, with the x-axis measured positive to the right from the centroid, and the y-axis positive down from the centroid

k_ϕ Rotational stiffness provided by a restraining element to the flange / web juncture of a member

$k_{\phi fe}$ Elastic rotational stiffness provided by the flange to the flange/web juncture

$\tilde{k}_{\phi fg}$ Geometric rotational stiffness demanded by the flange from the flange/web juncture

$k_{\phi we}$ Elastic rotational stiffness provided by the web to the flange/web juncture

$\tilde{k}_{\phi wg}$ Geometric rotational stiffness demanded by the web from the flange/web juncture

K_d Calculated stiffness

K_t Test stiffness

L_{cr} Cortical unbraced length of distortional buckling

L_m Distance between discrete restrains that restrict distortional buckling

L_p Lap length

L_t Span length

m_f Modification factor for type of bearing connection

M_n Nominal flexural strength

M_{nd} Nominal distortional buckling flexural strength

M_{nl} Nominal local buckling flexural strength

M_t Ultimate test moment

$P_{40\%}$ 40% of Ultimate load

$P_{60\%}$ 60% of Ultimate load

$P_{80\%}$ 80% of Ultimate load

P_n Bearing strength

P_s	Service load
P_t	Ultimate test load
r	Average bend inside radius
S_e	Effective section modulus, calculated at f = F_y (causing compression in top flange)
S_f	Elastic section modulus of full unreduced cross-section relative to extreme compression fiber
S_{fy}	Elastic section modulus of full unreduced cross-section relative to extreme fiber in first yielding
t	Thickness of steel
V_n	Shear buckling strength
V_{ny}	Shear yielding strength
x_{of}	x distance from the centroid of the flange to the shear centre of the flange
y_{of}	y distance from the centroid of the flange to the shear centre of the flange
α	Effective flexural rigidity ratio
α_d	Predicted effective flexural rigidity ratio
α_t	Test effective flexural rigidity ratio
β	Lap length to test span ratio
Δ_t	Test mid-span deflection
Δ_d	Predicted mid-span deflection
λ_d	Slenderness factor
μ	Poisson's ratio of steel
ξ_{web}	Stress gradient in the web

Chapter 1
Introduction

1.1 Background

Cold-formed steel (CFS) has been extensively used as an excellent construction material for mid- and low-rise residential and commercial buildings around the world, including sport arenas, shopping centres, and warehouses. It is an economical material in building construction because it is cold-formed in various shapes from steel sheets, strips or plates by roll framing. Compared to traditional hot-rolled steel, the main advantages of CFS are light weight, effective stacking, ease of transportation, storage, fabrication and mass production, and high structural efficiency.

In particular, CFS C and Z sections have been widely used as secondary structural members such as purlins in metal roof systems. Among various purlin systems to support the roof sheathing, multi-span purlin systems are the most structurally efficient system. Because the Z-section purlins can be lapped and nested at the supports to provide a structurally continuous line along the length of the building, and to create a more compact bundle for the convenience of shipping than can be achieved with C-sections, the Z-section purlins have been more popular than C-sections as design solutions for multi-span roof systems. Demonstrated in Figure 1-1 is the typical arrangement of lapped Z-shaped purlins for a multi-span system.

The use of bolted connections is one of the most common methods for joining two lapped purlins at the supports. Conventional design practice assumes that the lapped bolted sections do not affect the continuity of the purlins. The strength and stiffness checking of the lapped connection is often performed by treating it as a homogeneous section and calculating the cross-sectional properties of the lapped sections to be double that of a single section. However, this assumption could lead to unsafe design because it neglects or oversimplifies the effects of the bolted connections. As a result, the behaviour and performance of these metal roof systems were not appropriately assessed. In the worst case, inadequate design of the purlin may directly lead to roof collapses.

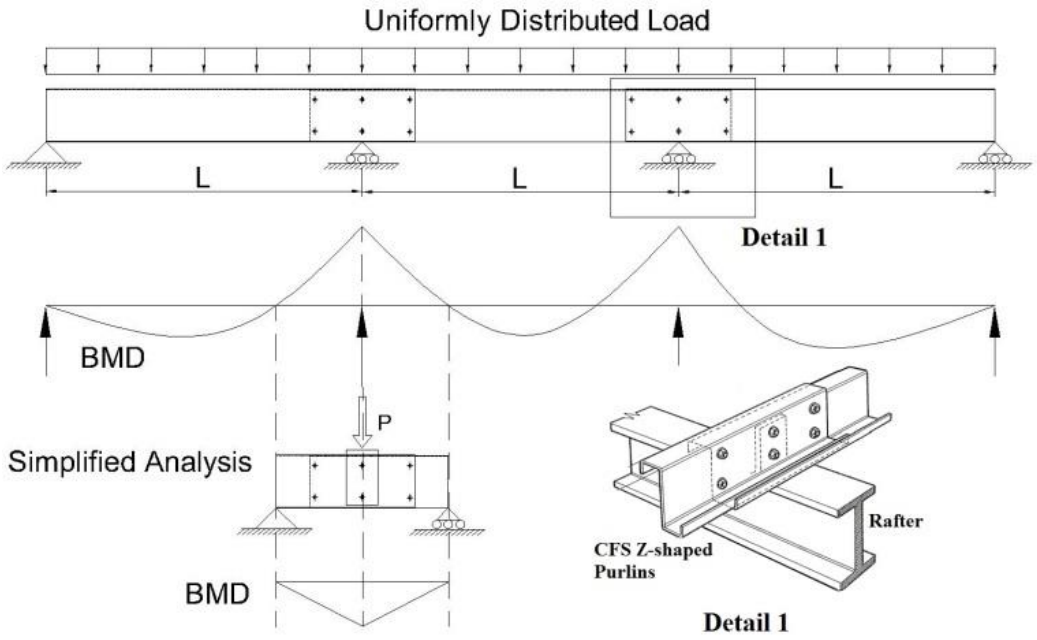

Figure 1-1 Multi-span CFS Z-shaped Purlin System

In the past two decades, an increasing number of studies have been conducted on the structural behaviour of the lapped CFS Z-shaped purlins with bolted connections. However, previous research is primarily focused on lapped purlins with unequal top and bottom flange widths, and connections with round holes. In current construction practice, vertical slotted holes are commonly used at the connections. By using vertical slotted holes, the extra erection tolerance at the connections allows two identical purlins with the same top and bottom flange width to nest together. It simplifies the fabrication, provides more effective stacking to lower the transportation and storage cost, and also expedites the erection of continuous Z-shaped roof purlins. However, there is no explicit design guideline or recommendation available for CFS Z-purlin lapped connections with vertical slotted holes. Therefore, the purpose of this research program is to acquire a better understanding of the structural performance of lapped CFS Z-shaped purlins with vertical slotted connections.

1.2 Objectives and Scope of Research

The main objectives of the research are:

- To theoretically and experimentally investigate the effects of slotted holes on the structural behaviour of lapped connections between cold-formed steel Z-shaped purlins.
- To develop design guidelines or recommendations for the design of lapped purlins with slotted connections.

Presented in this thesis are the results of research program performed on CFS Z-shaped purlins at the University of Waterloo. The research program consists of 54 laterally restrained tests including 6 tests on non-lapped purlins, 6 tests on the lapped purlins with round holes at the connections, and 42 tests on the lapped purlins with vertical slotted holes at the connections. The experimental investigations specifically focused on studying the flexural strength and stiffness of lapped purlins. A static analysis was performed to determine the internal forces at the connections. The influence of various parameters on the capacity of the slotted connections was also studied. The parameters include: the lap length to section depth ratio, the lap length to web thickness ratio, the lap length to span ratio, and the section depth to thickness ratio. Additionally, design procedures and recommendations for lapped purlins with slotted connections were proposed.

1.3 Organization of Thesis

This thesis is divided into six chapters. A review of the relevant literature on the structural behaviour of lapped Z-shaped purlins with bolted connections is presented in Chapter 2. The test program of the experimental investigation is described Chapter 3. The test results and analysis are presented in Chapter 4, as well as Appendices C and F. Design procedures and recommendations are proposed in Chapter 5 based on the test results and analysis. Finally, conclusions and recommendations for future work are presented in Chapter 6.

Chapter 2
Literature Review

2.1 General

Lapped joints of cold-formed steel (CFS) Z-shaped purlins with bolted connections are one of the most popular design solutions for providing the continuity of purlins in multi-span roof systems. Extensive research has been conducted on studying the structural behaviour of lapped connections in multi-span roof systems. However, existing research primarily focused on connections with round holes. Very limited research is available for lapped connections with vertical slotted holes. In this chapter, a literature review of previous studies and test programs of lapped connections with round holes will be conducted. Also, the current specification on design of cold-formed steel Z-sections will be discussed.

2.2 Research on Structural Behaviour of Lapped Connections

Ghosn and Sinno (1995) performed twenty-eight tests on stiffened Z-section beams with various section sizes and lapped lengths. For the test specimens, the web depth to thickness ratios ranged from 79 to 132, and the lap length to span ratios from 0.25 to 1.00. Beams were tested in pairs with braces at both top and bottom flanges to avoid torsional and/or lateral buckling effects caused by the shear flow characteristics of Z-sections. All specimens were firmly nested and clamped before drilling, so the slippage due to the bolted connection at lap joint was limited. All bolts were tightened at a torque 90 ft ·lb (122 N·m).

The results showed that the flexural strength and the stiffness of the Z-section beams were both enhanced by the lapped section when the lap to span ratio was no more than 0.5. Limited or no enhancement was found when the lap to span ratios were higher than 0.5. Failure occurred outside of the lap for beams with lap-to-span ratios less than 0.5 and in the lap section for higher ratios. The local buckling of the compressive flange was the most common failure of the lapped connections, and the load-carrying capacity of the lapped connections is governed by the moment resistance of these sections. A moment reduction factor, R_s, was introduced as a function of the lap to span ratio to evaluate the ultimate moment capacity of lapped Z-section beams. The ratios between the test ultimate moments and the predicted ultimate moments were found to range from 0.85 to 1.23. The

test results also showed that the ultimate moment capacity of lapped Z-section beams seemed to be insensitive to the depth to thickness ratios for the range tested in the study.

Ho and Chung (2004) carried out an experimental study on the structural behaviour of lapped CFS Z sections. 26 tests were performed on the lapped Z-sections with two connection configurations (4 or 6 web bolts connected lapped sections) at various lap lengths and test spans. The specimens were designed with the lap to section depth ratios ranging from 1.2 to 6.0 and the lap to span ratios ranging from 0.05 to 0.38. Two CFS Z sections with the web depth to thickness ratios of 94 and 100 were used. The top and bottom flanges were made with unequal widths for the two lapped purlins in order to provide proper sitting at the lapped section. A clearance of 2mm was provided in the bolt holes at the connection for easy installation. All bolts were tightened to 50 N·m torque.

The test results showed that the moment resistance and the flexural rigidity of lapped connections not only depend on the lap to span ratios but also on the lap to section depth ratios. The full flexural strength and full flexural stiffness of the continuous section might be achieved in the lapped connections when the lap to section depth ratios are equal or greater than 2.0 and 4.0 respectively. The common failure of the lapped Z sections was governed by the combined bending and shear at the critical section, which is always located at the end of lap of the connected section.

Chung and Ho (2005) proposed an analytical method to evaluate all the internal forces within the lapped connections and along the individual members based on the experiments they performed. The authors suggested that it was important to assess both the moment and the shear capacity at the critical cross-section at the end of lap of the lapped connections. The authors proposed that the shear capacity of the critical cross section could be improved by reducing the length of the shear panel due to the fairly localized shear buckling mode shape based on the test observation. Hence, due to the increased shear capacity, the moment capacity of the critical cross-section was reduced. Design rules were proposed based on checking the combined bending and shear at the critical cross-section at the end of lap. Moreover, design equations for calculating the maximum and minimum effective flexural rigidity of the lapped sections were also proposed.

Zhang and Tong (2007) conducted two series of tests on lapped CFS Z-shaped purlins to investigate the moment resistance and the flexural rigidity of lapped connections over the internal supports in multi-span purlin systems. Two connection configurations were adopted including web bolts plus

self-drilling screws at both flanges or at top flange only. One typical stiffened Z section with unequal top and bottom flange widths was used for all tests. The elliptical bolt holes with 16mm in vertical direction and 20mm in horizontal direction were employed at the connections for 12mm bolts to facilitate the on-site installation.

The results showed that the edge section of lapped connections is the most critical section of the lapped purlins, and the load-carrying capacity of lapped purlins was governed by the bending moment at the critical section. The self-drilling screws at bottom flange within the lapped connections have a small effect on the moment resistance, but no effect on the effective flexural rigidity of the lapped connections. The lap lengths of the connections did not have an obvious effect on the moment resistance for the tests in this study, but significantly influenced the effective flexural rigidity of the lapped connections.

Based on the results and observations from previous tests (Ho and Chung 2004, Zhang and Tong 2007), Dubina and Ungureanu (2010) carried out a numerical investigation on lapped CFS Z-purlins with bolted connections. The authors concluded that the purlins were semi-continuous at the junction between the single and lapped sections. The critical sections were also found to be at the edge of lap on individual sections, but the load-carrying capacity of lapped purlins was governed by the combined bending and web crippling due to the local transverse action induced by bolts in bearing and locking of flanges. The authors also concluded that for laterally unrestrained purlins, the lateral-torsional buckling strength should be checked at the edge of the lap, and might become the relevant design criteria.

ArcelorMittal Dofasco (Previously called Dofasco) (2008) conducted a series of tests on lapped CFS Z-shaped purlins with equal top and bottom flange widths. There were 6 tests on non-lapped purlins and 12 tests on lapped purlins for two different purlin depths with two different lap lengths. Each specimen consisted of two sets of identical lapped purlins with the same top and bottom flange width. Three identical specimens were tested for each arrangement. During the tests, it was observed that the compression flanges of the two lapped purlins appear to share the load unequally at the connection. The top purlin flange didn’t appear to carry load without bolting to the lower purlin flange. Therefore, angle braces were added at the top and bottom flanges of the purlins within the lapped connection to improve the stability. The test results showed that added braces within the lap enhanced the lapped connection. The lap lengths of the connection directly influenced the flexural strength and stiffness of

lapped purlins. Both the flexural strength and stiffness of the lapped purlins increase as the lap length increases.

Very recently, Pham, Davis and Emmett (2014) performed both experimental and numerical investigations on high strength lapped CFS Z-purlins with bolted connections subjected to combined bending and shear in two series. In one series of tests, straps were attached to the top flanges of lapped purlins to provide torsion/distortion restraint, which may have enhanced the lapped connection. In the other series of tests, straps were not used. One Z section with unequal top and bottom flange widths and various thicknesses was used for all tests and simulations.

The results showed that all section failures occurred just outside the end of laps and were governed by combined bending and shear at the critical sections. For tests without straps, significant cross-section distortion was observed at the end of lap, which led to the discontinuity of the lapped connections resulting in a large reduction of the flexural strength of lapped purlins. The author concluded that the failure mode was mainly due to the bending, and the current design rules of Direct Strength Method (DSM, will be discussed in Section 2.3) for CFS Z-sections subjected to combined bending and shear may not be applicable. Therefore, a simple design approach was proposed based on applying factors to lower the nominal flexural strength (either local buckling strength or distortional buckling strength) of the purlin at the critical section.

For tests with straps, the continuity of the lapped connection was enhanced and no distortion at the cross-section was observed. The flexural strength of the lapped purlins was significantly increased. Based on the test and numerical results, new linear interaction equations fitting all the results were proposed as an extension of the current Direct Strength Method design rules for checking CFS Z-sections subjected to combined bending and shear.

2.3 Design Considerations and Specification for CFS Z-section Flexural Members

In multi-span purlin roof systems, CFS Z-purlins are used to support the roofing sheets and to stiffen the whole roof structure. Thus, the purlins must be designed as flexural members to resist bending. Due to the high width-to-thickness ratios of the Z-sections, local buckling may occur at a lower stress level before the section reaches the yielding strength when subjected to bending. The local buckling strength (nominal section strength) of the section is a common governing design criterion, and has

taken into account the elastic critical buckling and post-buckling capacity. However, as the Z-sections are also easy to twist and deflect laterally, the moment resistance of the member may also be limited by lateral-torsional buckling if the lateral braces are not adequately provided. Furthermore, for Z-sections with edge stiffeners at compression flanges, distortional buckling could also be critical for design. In addition, due to the slenderness of the web, the shear, combined shear and bending, web crippling, and combined web crippling and bending must also be checked for the webs of the flexural members.

The current specification used throughout Canada, Mexico and the United States for designing CFS members is the North American Specification for the Design of Cold-Formed Steel Structural Members (CSA 2012). The specification includes three design approaches – Allowable Strength Design (ASD), Load and Resistance Factor Design (LRFD), and Limit States Design (LSD). The LSD is limited to use in Canada, while the ASD and LRFD are limited to use in the United States and Mexico. The specification provides well-defined procedures for the design of flexural cold-formed steel members. The sections of the North American Specification (CSA 2012) referenced for design are summarized in Table 2.1.

Table 2-1 Applicable Design Sections of the Specification (CSA 2012)

Design Considerations	**North American Specification Section Referenced (CSA S136-2012)**
Local buckling Strength	Section C3.1.1
Lateral-Torsional Buckling Strength	Section C3.1.2
Distortional Buckling Strength	Section C3.1.4
Shear	Section C3.2
Combined Bending and Shear	Section C3.3
Web Crippling	Section C3.4
Combined Bending and Web Crippling	Section C3.5

It should be noted that Direct Strength Method (DSM) is included in Appendix 1 of the North American Specification (CSA 2012). The method adopts the effective stress concept as the alternative to the traditional effective width concept. The gross properties of the sections are used for strength calculations. The DSM provides design provisions for determining local buckling strength, lateral-

torsional buckling strength, distortional buckling strength, shear, and combined shear and bending of CFS flexural members. However, some geometric and material limitations of the section need to be satisfied to derive accurate results.

The North American Specification (CSA 2012) also provides some provisions for lapped connection of nested CFS Z-sections as follows:

- For continuous span systems, the lap length at each interior support in each direction (distance from centre of support to end of lap) is not less than 1.5 times of the member depth.
- The round holes and short-slotted holes (slotted vertically) should be used when the hole occurs within the lap of lapped or nested Z-members.
- The short-slotted hole with dimensions 9/16 in. x 7/8 in. (14.3mm x 22.2mm) is only applicable for 1/2 in. (12.7mm) diameter bolts.

Chapter 3
Experimental Setup

3.1 General

The experimental investigation was conducted in the Structures Lab at University of Waterloo in two phases. As shown in Figure 1-1, the simplified analysis method was used for testing lapped purlins under one point load instead of carrying out full-scale uniform loaded tests on multi-span purlin systems. The test procedures were developed based on similar tests performed by ArcelorMittal Dofasco (2009) and by Ho and Chung (2004).

In the first phase, 36 one-point load tests were performed on lapped Z-shaped purlins with vertical slotted holes for three different purlin depths and thicknesses. Purlins with section depths of 8 inch (203mm) and 10 inch (254mm) were tested for 10 gauge (0.135 inch or 3.429mm), 13 gauge (0.090 inch or 2.286mm) and 16 gauge (0.060 inch or 1.524mm) thicknesses. The 12 inch (305mm) purlins were tested for 10 gauge (0.135 inch or 3.429mm), 12 gauge (0.105 inch or 2.667mm) and 14 gauge (0.075 inch or 1.905mm) thicknesses. For each section depth, a specified span was used, i.e. 10 ft (3.048m) for 8 inch (203mm) purlins, 15 ft (4.572m) for 10 inch (254mm) purlins, and 20 ft (6.096m) for 12 inch (305mm) purlins. Each combination of purlin depth and thickness was tested with two common lapped lengths --- the short lap length of 34 inch (0.864m) and the long lap length of 60 inch (1.524m).

In the second phase, 18 one-point load tests were conducted on 12 inch (305mm) Z-shaped purlins for the same selected member thicknesses and span as that of the first phase, including 6 tests of lapped purlins with vertical slotted holes, 6 tests of lapped purlins with round holes, and 6 tests of non-lapped purlins. For the tests with vertical slotted holes, a medium lap length of 48 inch (1.219m) was selected to make the results comparable to those of the first phase. For tests with round holes, a lap length of 48 inch (1.219m) was also used, so that the results are comparable to those for the same purlins with vertical slotted holes. The results of the confirmatory tests on non-lapped purlins were used as benchmarks for comparing the calculated flexural strength and the stiffness of the purlins.

All specimen assemblies were constructed with materials and methods according to the North American Specification for the Design of Cold-Formed Steel Structural Members (CSA S136 2012). All specimen materials were provided by Steelway Building Systems of Aylmer, Ontario, Canada.

Installation of cold formed steel purlins and the testing was performed entirely at the University of Waterloo except that a few 12-inch (305mm) purlins with round holes and 10 gauge (0.135 inch or 3.429mm) thickness were pre-assembled at Steelway Building Systems due to the difficulty of installing the bolts at the lapped section.

3.2 Test Specimen

3.2.1 Material Properties

All steel materials conformed to CSA G40.21 (CSA 2004) and ASTM A1011/A1011M (ASTM 2009) with 50ksi (345MPa) minimum yield strength. The mechanical properties of cold-formed steel Z-shape purlins were determined based on the standard tensile coupon tests as per ASTM standard E8 (ASTM 2011).

For the first phase, Steelway Building Systems provided virgin steel plates from the coils used for making the test specimens. For the second phase, each coupon specimen was cut from the web section of the cold-formed steel Z-shaped purlins where the longitudinal direction of the coupon was parallel to the longitudinal direction of the purlin. Four standard coupons were made from each plate as per ASTM standard A370 (ASTM 2012) by the University of Waterloo's machine shop. Coupons were dipped in paint remover and given the acid bath to remove the paint and the galvanized coating prior to the tensile test. The thickness and width of each coupon were measured using a digital micrometer and caliper respectively. All tests were performed at ambient temperature about 20°C by using an 810MTS frame with an MTS 634.12e-24 extensometer in a displacement control mode. Four properties of the material, Young's modulus, yield stress, tensile strength, and the final elongation were obtained according to ASTM standard E8 (ASTM 2011). The yield stress was determined by using the 0.2% offset method. The average mechanical properties of the test materials are shown in Table 3-1.

Table 3-1 Mechanical Properties

	Material Thickness[1]	Uncoated Thickness (inch)	Young's Modulus (ksi)	Yield Stress (ksi)	Tensile Strength (ksi)	Average Elongation (%)
Phase one	Ga. 10	0.132	29180	61.4	71.1	30%
	Ga. 12	0.102	29641	63.1	72.1	28%
	Ga. 13	0.090	29214	59.5	69.1	28%
	Ga. 14	0.081	30961	64.1	74.0	27%
	Ga. 16	0.058	29739	60.7	66.8	16%
Phase two	Ga. 10	0.133	29489	62.3	80.4	28%
	Ga. 12	0.106	31002	67.0	77.6	28%
	Ga. 14	0.075	30402	67.3	78.8	27%

Metric Conversion: 1 inch = 25.4 mm, 1 ksi = 6,895 kPa.

[1] Material thickness is in gauges, 10 ga. = 0.135 in. (3.429mm), 12 ga. = 0.105 in. (2.667mm), 13 ga. = 0.09 in. (2.286mm), 14 ga. = 0.075 inin. (1.905mm) and 16 ga. = 0.06 in. (1.524mm)

3.2.2 Section Properties

The geometry of the Z-shaped purlins is shown in Figure 3-1 and the geometric data and section properties are shown in Table 3-2. An Excel spreadsheet was developed to calculate the section properties. Effective section modulus and effective moment of inertia of the CFS Z-shaped purlins were calculated by using the effective width method according to the North American Specification for the Design of Cold-Formed Steel Structural Members (CSA 2012). The effective moment of inertia I_e and the effective section modulus S_e were calculated based on the extreme compression fiber, which is equal to the yield stress determined from the standard coupon test of the given material ($f = F_y$). All inner radii of the web to flange corners for tested Z shaped purlins were taken as 3/16" (4.76mm) as indicated in the material standard of Steelway Building Systems (2009). The corner was assumed to be fully effective when calculating the effective section properties.

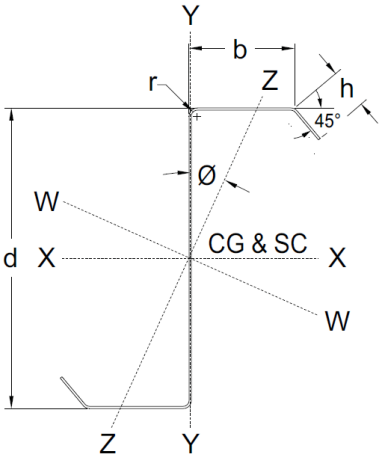

d = depth of section

b = flange width

h = length of lip

t = thickness of steel

r = inside bend radius, use 3/16" (4.763mm) for sections as per material standard of Steelway Building Systems

Figure 3-1 Z-shaped Purlin Geometry

Table 3-2 Dimensions and Section Properties

	Assembly Designation[1]	Depth (in.)	Flange Width (in.)	Length of Lip (in.)	Thickness (in.)	Gross Moment of Inertia, I_g (in.^{4})	Effective Moment of Inertia, I_e (in.^{4})	Effective Section Modulus, S_e (in.^{3})
Phase one	08Z10	8	2.80	1.08	0.132	19.46	19.45	4.86
	08Z13	8	2.80	1.08	0.090	13.56	12.75	3.06
	08Z16	8	2.80	1.08	0.058	8.88	7.76	1.77
	10Z10	10	3.02	1.18	0.132	34.85	34.84	6.97
	10Z13	10	3.02	1.18	0.090	24.20	22.41	4.28
	10Z16	10	3.02	1.18	0.058	15.82	12.84	2.23
	12Z10	12	3.14	1.18	0.132	54.90	54.15	8.95
	12Z12	12	3.14	1.18	0.102	42.92	39.91	6.37
	12Z14	12	3.14	1.18	0.081	34.36	24.42	3.70
Phase two	12Z10	12	3.14	1.18	0.133	55.30	54.56	9.02
	12Z12	12	3.14	1.18	0.106	44.53	41.71	6.69
	12Z14	12	3.14	1.18	0.075	31.89	24.60	3.63

Metric Conversion: 1 inch = 25.4 mm, 1 in.^{4} = 416,231 mm^4, 1 in.^{3} = 16,378mm^3.

[1] Assembly designation is adopted from the material standard of Steelway Building Systems. For example, 08Z10 represents the specimen for 8 inch (203mm) Z-shaped purlins with 10 gauge (0.135 inch or 3.429mm) thickness.

3.2.3 Connection Configuration and Hole Sizes of Bolts

The connection configuration is detailed in Figure 3-2. Six bolts connected the webs of lapped Z-shaped purlins. The four outer bolts, located 1 inch (25.4mm) inside the end of the lap and 2 inch (50.8mm) inward from the top and bottom flanges, were used to resist the flexural bending and shear. The two inner bolts at the centreline of the lap were used to connect the web cleat of the loading plate to resist lateral loads and to transfer the load directly into the purlin webs. This lapped configuration is commonly used in the North American metal building industry. The SAE J429 Grade 8.2 bolts with 1/2 inch (12.7mm) diameter and 150 ksi (1020MPa) specified minimum tensile strength were used for assembling all the specimens.

For all 42 tests on lapped purlins with vertical slotted connections, vertical slotted holes with dimensions of 9/16 inch (14.3mm) x 7/8 inch (22.2mm) were used in the lapped section to connect the webs of the Z sections. Standard holes with diameters of 9/16 inch (14.3mm) were used for bolts at end reaction supports and internal braces. In order to compare the effect of the vertical slotted holes with the effect of the round holes, 6 additional tests of 12-inch (305mm) purlins with round holes were performed in the second phase. The round holes with diameter of 5/8 inch (15.9mm) were used instead of the vertical slotted holes at the lapped section.

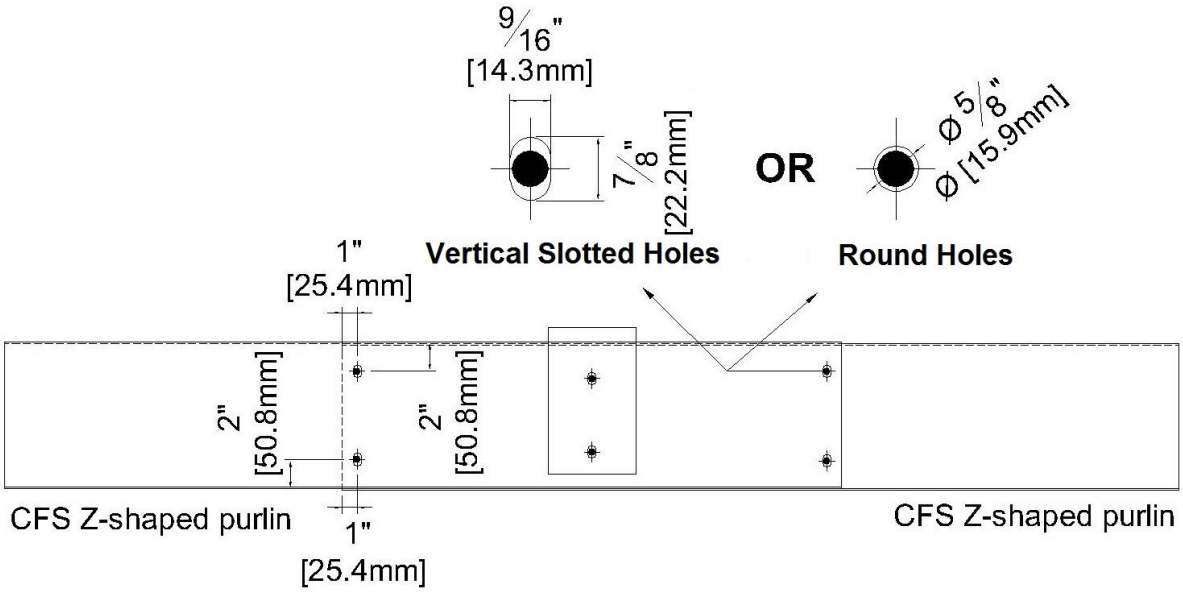

Figure 3-2 Connection Configuration and Bolt Holes

3.2.4 Specimen Assemblies

The test specimens were designated using the purlin depth, thickness (gauge) and lapped length. This assembly designation was adopted from the material standard of Steelway Building Systems (2009). The first two numbers indicate the section depth (inch) of the purlins, and the first letter "Z" represents the shape of the purlin. The second pair of digits indicates the steel thickness in gauge (ga.), for example 10 ga. = 0.135 inch (3.43mm), and the third pair of digits presents the lapped length (inch) of the connection. The last digit indicates the number of identical assemblies. For example, 08Z13-34-2 denotes the second test for 8-inch (203mm) Z-shaped purlins with 13 gauge (0.09 inch or 2.286mm) thickness at 34-inch (0.864m) length of lapped connections.

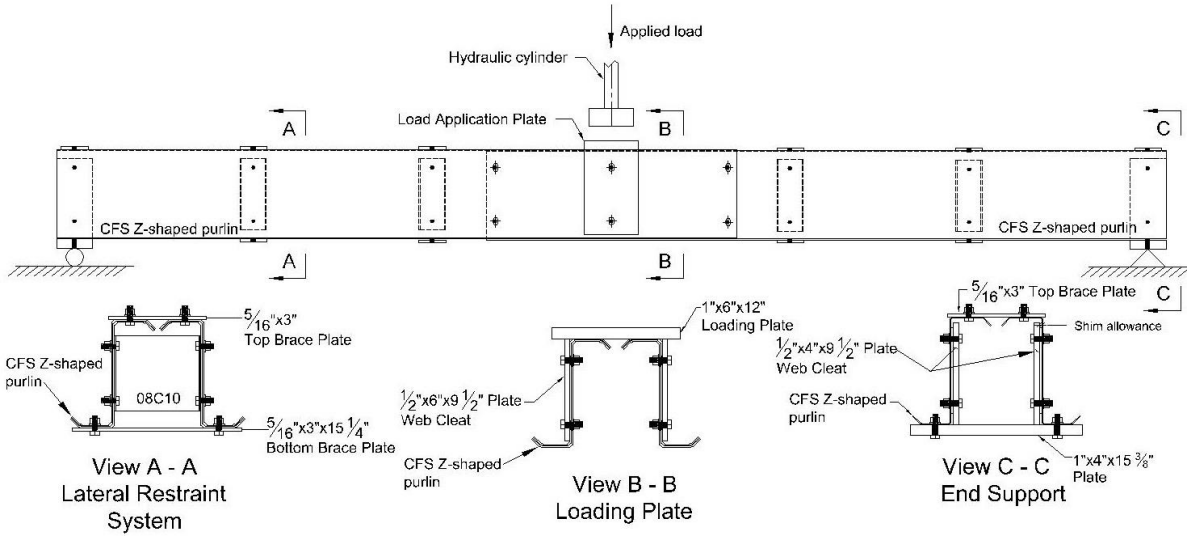

Figure 3-3 Test Specimen Assembly Details

Each test specimen consisted of two pairs of lapped CFS Z-purlins with top flanges facing inwards and a 1/2 inch (12.7mm) clearance between them. In order to prevent lateral-torsional bucking and instability, a lateral restraint system similar to those used by Ho and Chung (2004) was adopted, as shown in Figure 3-3. The lateral restraint system consisted of two 5/16 inch (7.94mm) bracing plates connected at both top and bottom flanges, and an internal brace connecting the webs of the two purlins. A vertically placed CFS 08C10 section, which is a C-shaped purlin with 8-inch (203mm) depth and 10-gauge (0.135 inch or 3.429mm) thickness, was used as the internal brace. Shim plates were provided to fill the gaps between the internal braces and the purlin webs. The lateral restraint

system was located at intervals of one-sixth of the span length to prevent tipping and lateral deflection of either flange in either direction at the intermediate braces. At loading point, two vertical plates were welded on the bearing plates as web cleats, and the purlins were connected at the cleat by two bolts in the web. The cleats at the loading plate simulated the connection over the rafter as shown in Detail 1 of Figure 1-1, and prevented lateral loads. At the end supports, web cleats were also used. Two bolts in the web and one bolt at the bottom flange connected the purlins at end supports. The end support design also prevents the lateral deformation and twisting during the tests. Connection drawings showing the details of the lateral braces, loading plate and end supports, and identifying the locations of lateral braces for each specimen span are included in Appendix A.

3.3 Specimen Test Setup

All specimens were set on two leveled support pedestals and tested by using an H shaped universal testing frame in the Structures Lab at the University of Waterloo. The specimens were simply supported with bearing plates at either end. As shown in Figure 3-4, a pinned support was simulated by using semicircular steel between the bearing plate and pedestal at one end, while the roller support consisted of a steel rod between two smooth steel surfaces at the other end.

At the loading section, the frame was equipped with a hydraulic actuator with a 35 kip (156 kN) maximum capacity and a linear variable differential transducer (LVDT). All specimens were loaded with a single point load applied at mid-span. A pivot plate was attached to the hydraulic cylinder, and it distributed load evenly on both sets of the purlins through the loading plate on the specimens as shown in Figure 3-4 (b). A MTS Flex Test SE controller controlled the hydraulic actuator and applied a constant rate of displacement of 0.24 inch (6.1mm) per minute to the specimens through the test.

Four linear motion transducers (LMT) were used to monitor and record the deflections of the specimens. Two LMTs were used at mid span and were attached to the bottom flange of each purlin. These LMTs were used to verify the load was evenly distributed on both sets of the purlins. The other two LMTs were attached to the middle of bottom brace located just outside the lapped section from each end as shown in Figure 3-4 (a) and (b). All data was collected and processed through LabVIEW 8.5, which is a data acquisition software developed by National Instruments (LabVIEW 2007).

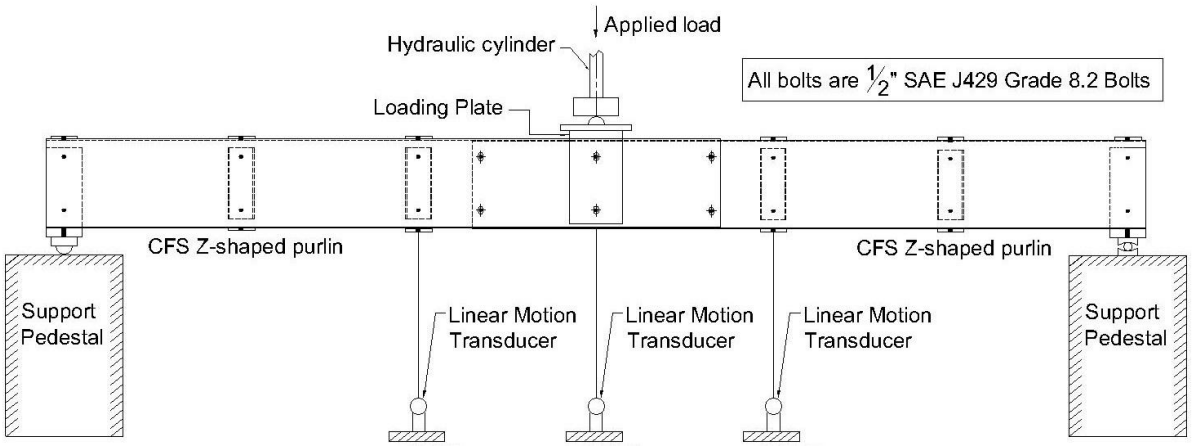

a. General Set-up of One Point Load Test

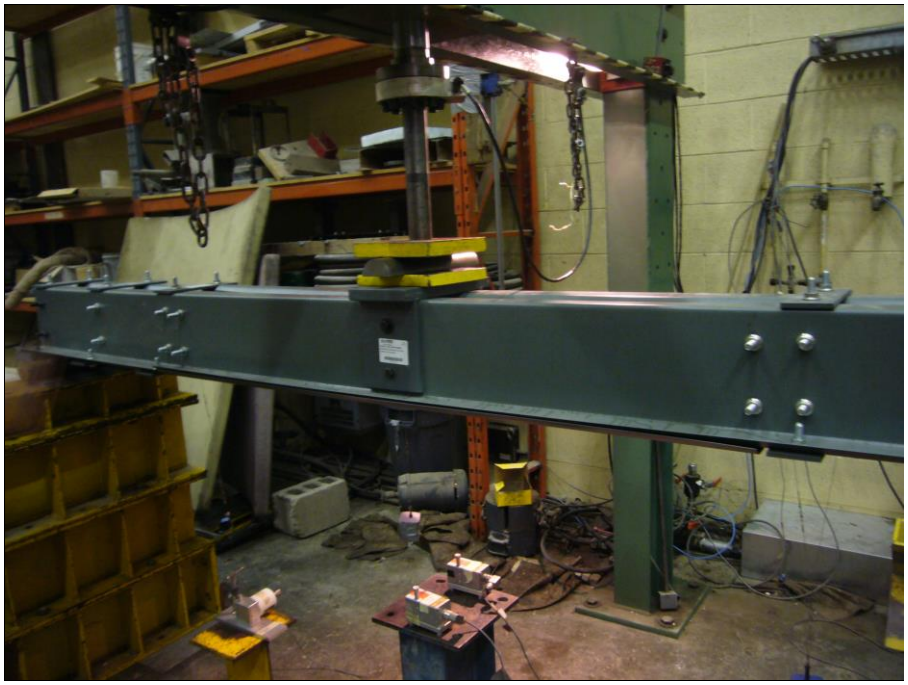

b. Actual Experiment

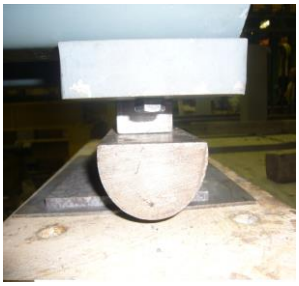

c. Pin Support

d. Roller Support

Figure 3-4 General Set-up of One Point Load Test and Actual Experiment

Chapter 4
Experimental Results and Analysis

4.1 General

54 laterally restrained one-point load tests were performed to investigate the structural performance of the lapped CFS Z-shaped purlins, including 6 tests on non-lapped purlins, 6 tests on the lapped purlins with round holes, and 42 tests on lapped purlins with vertical slotted holes. The flexural strength and deflection of the purlins in each test were examined in detail. The characteristics of the moment resistance and the flexural stiffness of the purlins were carefully calculated. The test results on non-lapped purlins were used to verify the flexural strength of the purlins from the calculations and to act as a baseline. The test results for lapped purlins with round holes were compared to the results for the same purlins with vertical slotted holes. An analysis of lapped purlins with vertical slotted holes was carried out based on the experimental investigation. The findings are summarized in this chapter.

4.2 Flexural Strength and Stiffness of Non-lapped Purlins

4.2.1 Flexural Strength of Non-lapped Purlins

For non-lapped purlins, the ultimate loads were determined directly from the tests. Since all the purlins were tested in pairs, the ultimate load (P_t) of a single section was half of the maximum applied load recorded at the failure point in each test. The flexural strength (M_t) of a single section was calculated by using equation (4.1) based on the ultimate load (P_t).

$$M_t = \frac{P_t L_t}{4} \tag{4.1}$$

Where P_t is the ultimate load at failure for a single purlin and L_t is the span of the purlin.

For calculating the nominal flexural strength (M_n), only the local buckling strength (M_{nl}) and the distortional buckling strength (M_{nd}) were considered as the lateral restraints used in the test setup efficiently prevented tipping and lateral deflection of either flange in either direction. Therefore, lateral torsional buckling did not occur and was not considered in determining the nominal flexural strength (M_n) of the purlins. The mechanical properties of the purlins measured from standard coupon tests were used to calculate the nominal flexural strength of the purlins.

4.2.1.1 Local Buckling Strength – Limit State Design

According to the North American Specification for the Design of Cold-Formed Steel Structural Members (CSA S136 2012), the local buckling strength (M_{nl}) of the purlins was calculated by using equation (4.2) on the basis of initiation of yielding of the effective section.

$$M_{nl} = S_e \cdot F_y \tag{4.2}$$

Where F_y is the yield stress of the steel and S_e is the elastic section modulus of the effective section calculated relative to extreme compression fiber at F_y.

4.2.1.2 Distortional Buckling Strength – Limit State Design

The distortional buckling strength (M_{nd}) of the purlins was calculated by using the method indicated in the clause C3.1.4 of CSA S136-2012 (CSA 2012), as follows.

$$For\ \lambda_d \leq 0.673: \quad M_{nd} = M_y \tag{4.3}$$

$$For\ \lambda_d > 0.673: \quad M_{nd} = \left(1 - 0.22\left(\frac{M_{crd}}{M_y}\right)^{0.5}\right)\left(\frac{M_{crd}}{M_y}\right)^{0.5} M_y \tag{4.4}$$

Where

$$\lambda_d = \sqrt{M_y / M_{crd}} \tag{4.5}$$

$$M_y = S_{fy} F_y \tag{4.6}$$

$$M_{crd} = S_f F_d \tag{4.7}$$

Where

S_{fy} Elastic section modulus of full unreduced cross-section relative to extreme fiber in first yielding

S_f Elastic section modulus of full unreduced cross-section relative to extreme compression fiber

F_d Elastic distortional buckling stress

$$F_d = \beta \frac{k_{\phi fe} + k_{\phi we} + k_{\phi}}{\tilde{k}_{\phi fg} + \tilde{k}_{\phi wg}} \tag{4.8}$$

$$\beta = 1.0 \leq 1 + 0.4(L/L_m)^{0.7}(1 + M_1/M_2)^{0.7} \leq 1.3 \quad (4.9)$$

L = min $\{L_m, L_{cr}\}$

$$L_{cr} = \left\{\frac{4\pi^4 h_o(1-\mu^2)}{t^3}\left(I_{xf}\left(x_{of} - h_{xf}\right)^2 + C_{wf} - \frac{{I_{xyf}}^2}{I_{yf}}\left(x_{of} - h_{xf}\right)^2\right) + \frac{\pi^4 {h_o}^4}{720}\right\}^{1/4} \quad (4.10)$$

L_m Distance between discrete restrains that restrict distortional buckling

M_1, M_2 Smaller and larger end moments, respectively, in the unbraced segment (L_m) of the beam

h_o Out-to-out web depth

μ Poisson's ratio of steel

I_{xf} x-axis moment of inertia of the flange

x_{of} x distance from the centroid of the flange to the shear centre of the flange

h_{xf} x distance from the centroid of the flange to the flange / web junction

C_{wf} Warping torsion constant of the flange

I_{xyf} Product of the moment of inertia of the flange

I_{yf} y-axis moment of inertia of the flange

$k_{\phi fe}$ = Elastic rotational stiffness provided by the flange to the flange/web juncture

$$= \left(\frac{\pi}{L}\right)^4 \left(EI_{xf}\left(x_{of} - h_{xf}\right)^2 + EC_{wf} - E\frac{{I_{xyf}}^2}{I_{yf}}\left(x_{of} - h_{xf}\right)^2\right) + \left(\frac{\pi}{L}\right)^2 GJ_f \quad (4.11)$$

Where

E Modulus of elasticity of steel

G Shear modulus of steel

J_f St. Venant torsion constant of the compression flange, plus edge stiffener about an x-y axis located at the centroid of the flange, with the x-axis measured positive to the right from the centroid, and the y-axis positive down from the centroid

$k_{\phi we}$ = Elastic rotational stiffness provided by the web to the flange/web juncture

$$= \frac{Et^3}{12(1-\mu^2)}\left(\frac{3}{h_o} + \left(\frac{\pi}{L}\right)^2 \frac{19h_o}{60} + \left(\frac{\pi}{L}\right)^4 \frac{{h_o}^3}{240}\right) \quad (4.12)$$

k_ϕ Rotational stiffness provided by a restraining element to the flange / web juncture of a member (zero if the compression flange is unrestrained)

$\tilde{k}_{\phi fg}$ = Geometric rotational stiffness demanded by the flange from the flange/web juncture

$$= \left(\frac{\pi}{L}\right)^2 \left[A_f \left(\left(x_{of} - h_{xf}\right)^2 \left(\frac{I_{xyf}}{I_{yf}}\right)^2 - 2y_{of}\left(x_{of} - h_{xf}\right)\left(\frac{I_{xyf}}{I_{yf}}\right) + {h_{xf}}^2 + {y_{of}}^2\right) + I_{xf} + I_{yf}\right] \quad (4.13)$$

Where

A_f Cross-sectional area of the compression flange plus edge stiffener about an x-y axis located at the centroid of the flange, with the x-axis measured positive to the right form the centroid, and the y-axis positive down from the centroid

y_{of} y distance from the centroid of the flange to the shear centre of the flange

$\tilde{k}_{\phi wg}$ = Geometric rotational stiffness demanded by the web from the flange/web juncture

$$= \frac{h_o t \pi^2}{13440}\left\{\frac{[45360(1-\xi_{web})+62160](\frac{L}{h_o})^2+448\pi^2+(\frac{h_o}{L})^2[53+3(1-\xi_{web})]\pi^4}{\pi^4+28\pi^2(\frac{L}{h_o})^2+420(\frac{L}{h_o})^4}\right\} \quad (4.14)$$

Where

$\xi_{web} = \frac{f_1 - f_2}{f_1}$, stress gradient in the web, where $f_1$and $f_2$are the stresses at the opposite ends of the web, (e.g., pure symmetrical bending, $f_1 = -f_2, \xi_{web} = 2$)

Distortional buckling only occurred and controlled when the unrestrained length (L_m) of the purlins was larger than the critical unbraced length for distortional buckling (L_{cr}) since the lateral torsional buckling was prevented by the lateral restraints. The unrestrained length (L_m) of the purlins was taken to be the distance between the adjacent lateral restraint systems, and the critical unbraced length for distortional buckling (L_{cr}) was calculated by using equation (4.10).

Rotational stiffness (k_ϕ) was used in calculating the distortional buckling strength (M_{nd}) to account for restraining elements (brace, panel, and sheathing) to the flange / web juncture as indicted in equation (4.8). For the test specimens, the lateral restrained system was discrete, and the compression flange was unrestrained and free to rotate between two adjacent braces. Therefore, k_ϕ was set to zero

for all calculations for the reason of conservative. In practice, the compression or the tension flange of the purlin is attached to continuous panels or sheathings. The actual value of k_ϕ needs to be determined by either testing or rational engineering analysis.

The distortional buckling strength (M_{nd}) of the purlins calculated using the equations (4.3) to (4.12) was compared to the distortional buckling strength of the purlins calculated by using the Direct Strength Method (DSM) from Appendix B, according to section 1.2.2.3 of CSA S136-2012 (CSA 2012). The results are summarized in Table B-1 in Appendix B. For the Direct Strength Method, the critical elastic distortional buckling moment (M_{crd}) was determined using the software CUFSM 4.05 (Li, Z., Schafer, B.W., 2010). This software employs the semi-analytical finite strip method to provide solutions for thin-walled members and has been successfully used by researchers and practicing engineers. The results show that the distortional buckling strength (M_{nd}) of the purlins calculated by using the two methods are very close. The average difference is only 3% for the test specimens. Therefore, the distortional buckling strength (M_{nd}) of the purlins calculated by using the method shown above is accurate and can be used as the benchmark to compare with the test results when the distortional buckling of the purlins occurred and controlled.

4.2.1.3 Comparison of the Calculated and the Tested Flexural Strength

The test results and the flexural strength of non-lapped purlins are summarized in Table 4-1. The ultimate load (P_t) for a single section of purlin was calculated. According to clause F1.1 in CSA S136-2012 (CSA 2012), the deviation of any individual test result from the average value obtained from all tests should not exceed ±15%. The deviations of the test results for the same specimens were all within ±4%. Therefore, the test results met the requirement, and the data can be used to compare with the calculated flexural strength (M_n). The tested flexural strength (M_t) for a single section was calculated by using equation (4.1) based on the average ultimate load (P_t) of the section in two identical tests.

From the observation of all six tests, the failure mode for non-lapped purlins was distortional buckling. The rotation of the flange at the flange/web junction occurred. The half-waves in compression flange were observed and are shown in the photograph in Figure 4-1. The half-wave occurred within the two adjacent bracings. The unrestrained length (L_m) of purlins, which is the distance between two adjacent bracings, and the calculated critical unbraced length of distortional buckling (L_{cr}), which is the half-wave length, are also listed in Table 4-1. The results show that for

all non-lapped 12-inch (305mm) purlins with three different thicknesses, the calculated half-wave lengths (L_{cr}) for distortional bucking was smaller than the bracing length. The calculated results are consistent with the observed test results. Therefore, the distortional buckling strength (M_{nd}) controls the flexural strength (M_n) for non-lapped 12-inch (305mm) purlins.

Table 4-1 Flexural Strength of Non-lapped Purlins

Non-lapped purlins[1]	Ultimate Load P_t (kip)				M_t (kip in)	L_m (in.)	L_{cr} (in.)	M_n (kip in)	$\frac{M_t}{M_n}$
	Test 1	Test 2	Avg.	Dev.					
12Z10	8.06	8.54	8.30	±2.90%	498	40	24	466	106%
12Z12	7.07	6.67	6.87	±2.90%	412	40	27	362	112%
12Z14	3.54	3.28	3.41	±3.81%	205	40	32	217	94%
								Average Difference	**8%**

Metric Conversion: 1 in. = 25.4mm, 1 kip = 4.448 kN, 1 kip in = 0.112kN m

[1] Purlin designation: for example, 12Z10 represents the specimen for 12-inch (305mm) Z-shaped purlins with 10-gauge (0.135 inch or 3.429mm) thickness.

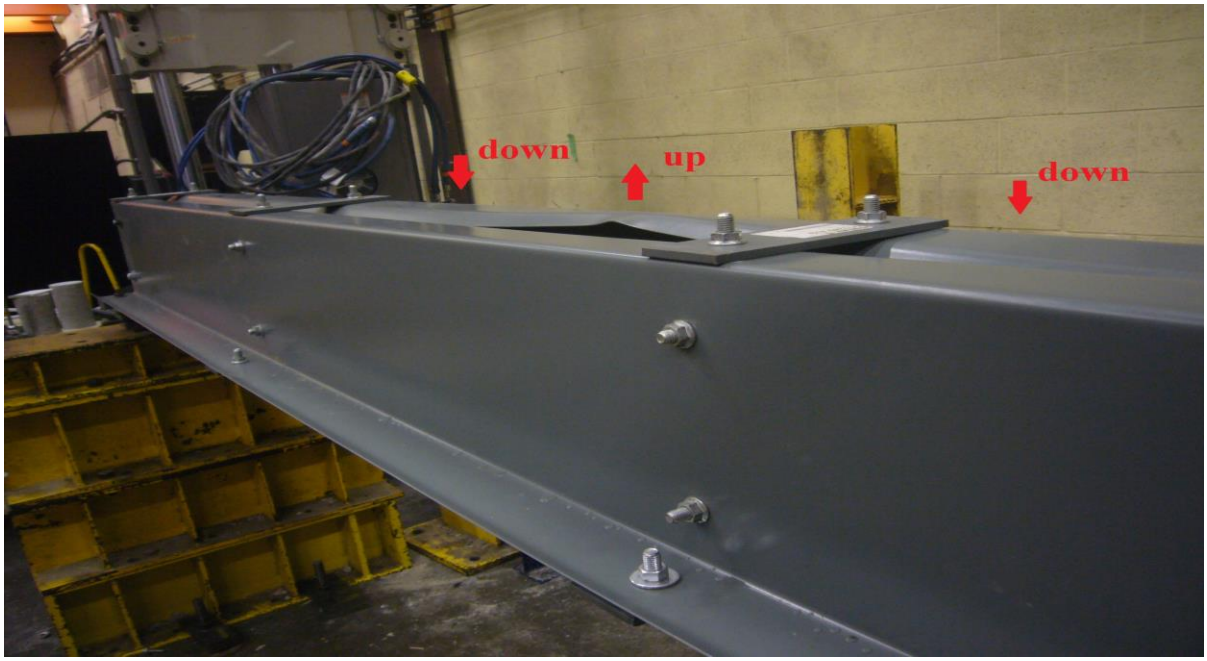

Figure 4-1 Photograph of Distortional Buckling of Compression Flange for Non-lapped Purlins

Table 4-1 shows that the tested flexural strengths are 6% to 12% higher than the calculated flexural strengths of non-lapped 12-inch (305mm) purlins with thicknesses of 10 gauge (0.135 inch or 3.429mm) and 12 gauge (0.105 inch or 2.667mm), but 6% lower than the calculated flexural strengths of non-lapped 12-inch (305mm) purlins with thickness of 14 gauge (0.075 inch or 1.905mm). The average difference is approximate 8% between the tested and the calculated flexural strengths of non-lapped purlins. This difference was considered low enough that the calculated flexural strength of non-lapped purlins could be used as the benchmark to compare with the tested flexural strengths of lapped purlins. The additional 8% difference may be considered on top of that comparison, and the comparison results are conservative.

4.2.2 Deformation / Stiffness of Non-lapped Purlins

The test results and the flexural stiffness of non-lapped purlins are summarized in Table 4-2. The tested vertical deflection (Δ_t) at mid-span was taken at 60% of the ultimate load of the non-lapped purlins. For serviceability analysis, 60% of the ultimate load was used as a practical approximation of the service load level (P_s). The tested stiffness (K_t) of non-lapped purlins was calculated by using equation (4.15). The mid-span vertical deflection and the flexural stiffness of the non-lapped purlins associated with 40% and 80% of the ultimate load were also obtained and are provided in Table C-1 and C-2 of Appendix C.

$$K_t = \frac{P_s}{\Delta_t} \tag{4.15}$$

where P_s is service load which taken at 60% of the ultimate load and Δ_t is the corresponding vertical deflection at the service load P_s.

For a simply supported beam with a concentrated load applied at mid-span, the flexural stiffness (K_d) for the serviceability design of non-lapped purlins was determined by using equation (4.16)

$$K_d = \frac{P_s}{\Delta_d} = \frac{48\,EI_e}{{l_t}^3} \tag{4.16}$$

where I_e is the effective moment of inertia computed at $f = 0.6\,F_y$, l_t is the total length of the specimen, and E is the modulus of elasticity of steel.

Table 4-2 Deformation and Flexural Stiffness of Non-lapped Purlins

Non-lapped purlins[1]	Deflection Δ_t (in.)				K_t (kip/in)	K_d (kip/in)	$\frac{K_t}{K_n}$
	Test 1	Test 2	Avg.	Deviation			
12Z10	0.900	0.896	0.898	±0.19%	5.19	5.66	92%
12Z12	0.862	0.845	0.853	±0.98%	4.24	4.79	89%
12Z14	0.721	0.731	0.726	±0.69%	3.04	3.26	93%
Metric Conversion: 1 in. = 25.4mm, 1 kip/in = 175 kN/m						**Average Difference**	**9%**

[1] Purlin designation: for example, 12Z10 represents the specimen for 12-inch (305mm) Z-shaped purlins with 10-gauge (0.135 inch or 3.429mm) thickness.

According to Table 4-2, the deviations calculated from the mid-span vertical deflections for identical specimens were within 1%. The test results are accurate and meet the requirement indicated in CSA S136-2012 (CSA 2012). The tested flexural stiffness (K_t) of a single section was calculated based on the average vertical deflection (Δ_t) of the purlins in two identical tests. The results show that the tested flexural stiffness of the 12-inch (305mm) non-lapped purlins is 7%-11% lower than its calculated flexural stiffness because the measured mid-span deflection was greater than the calculated mid-span deflection at the same service load level. Therefore, factors other than the flexural stresses also influence the overall mid-span deflection. Shear deformations may have an impact on the deflection of the specimens, which are typically neglected in the calculated deflection. The effect of shear deformation can result in the lower tested flexural stiffness compared to the calculated flexural stiffness for non-lapped purlins. The average difference is approximately 9%, which is considered low enough. Therefore, the calculated flexural strength of non-lapped purlins could be conservatively used as the benchmark to compare with the tested flexural strengths of lapped purlins.

4.3 Comparison of Lapped Purlins with Round Holes and Vertical Slotted Holes

4.3.1 Ultimate Load of Lapped Purlins with Round Holes and Vertical Slotted Holes

The test results are summarized in Table 4-3. The tested ultimate load was determined directly from the test output. Since all the lapped purlins were tested in pairs, the tested ultimate tested load (P_t) of a single section was calculated as half of the maximum applied load recorded at the failure point of each specimen. The deviations calculated from the two identical specimens were all within ±4%. The ultimate loads of non-lapped purlins were considered as baselines, and used to compare to the ultimate loads of lapped purlins with different types of holes at the lapped connection. The results

showed that the ultimate loads increased for lapped purlins with round holes and vertical slotted holes. The amount of increase was approximately 5% for 12-inch (305mm) lapped purlins at thicknesses of 10 gauge (0.135 inch or 3.429mm) and 12 gauge (0.105 inch or 2.667mm), and 13% for lapped purlins with 14 gauge (0.075 inch or 1.905mm) thickness. The increase in the ultimate loads is mainly due to the extra materials at the lapped section compared to the non-lapped purlins. For the same lapped purlin with the same lapped length, the materials reduction in the web of the section are minor for connections with vertical slotted holes compared to that of using round holes. Therefore, using round holes or vertical slotted holes at lapped connections does not have a significant impact on the ultimate load of lapped purlins as indicated by the data in Table 4-3.

Table 4-3 Ultimate Load of Lapped Purlins with Different Types of Holes

Test[1]	**Lapped length (in.)**	**Types of holes at connection**	**Ultimate load P_t (kip)**			**Dev.**	$\frac{P_{t-lapped}}{P_{t-non\ lapped}}$
			Test 1	**Test 2**	**Avg.**		
12Z10	Non-lapped	N/A	8.06	8.54	8.30	±2.90%	**100% (baseline)**
	48	Round holes	10.74	10.60	10.67	±0.66%	**129%**
	48	Vertical slotted holes	10.00	10.51	10.25	±2.47%	**124%**
12Z12	Non-lapped	N/A	7.07	6.67	6.87	±2.90%	**100% (baseline)**
	48	Round holes	7.84	8.19	8.01	±2.18%	**117%**
	48	Vertical slotted holes	7.54	7.86	7.70	±2.05%	**112%**
12Z14	Non-lapped	N/A	3.54	3.28	3.41	±3.81%	**100% (baseline)**
	48	Round holes	4.38	4.48	4.43	±1.08%	**130%**
	48	Vertical slotted holes	4.03	3.95	3.99	±1.05%	**117%**

Metric Conversion: 1 kip = 4.448 kN

[1] Test designation: for example, 12Z10 represents the specimen for 12-inch (305mm) Z-shaped purlins with 10-gauge (0.135 inch or 3.429mm) thickness.

4.3.2 Deformation / Stiffness of Lapped Purlins with Round or Vertical Slotted Holes

The test results and the flexural stiffness of lapped purlins are presented in Table 4-4. The tested vertical deflection (Δ_t) at mid-span was computed at the service load level (P_s), which is 60% of the ultimate load of the non-lapped purlins. The tested stiffness (K_t) of the lapped purlins was calculated by using equation (4.15). In addition, the mid-span vertical deflection and the stiffness of the lapped purlins associated with 40% and 80% of the ultimate load were also obtained and are provided in Table C-1 and C-2 of Appendix C.

The deviations calculated from two identical specimens were all within 2.5% for lapped purlins. The flexural stiffness of non-lapped purlins were considered as the baseline and used to compare to the stiffness of lapped purlins with different types of holes.

For 10-gauge (0.135 inch or 3.429mm) thickness, the stiffness of the lapped purlins with round holes was 111% of the stiffness of non-lapped purlins. For 12-gauge (0.105 inch or 2.667mm) and 14-gauge (0.075 inch or 1.905mm) thicknesses, the stiffness of the lapped purlins with round holes was 98% and 101% of the stiffness of non-lapped purlins respectively. The inconsistency could be due to the different installation processes for the 10-gauge purlins. When two purlins nest together, the holes at the same location on each purlin are offset by the thickness of purlin at the lapped section. With 5/8 inch (15.9mm) round holes, the maximum offset allowance for 1/2-inch (12.7mm) structural bolt is only 1/8 inch (3.175mm) at bolt holes, which is slightly smaller than the 10 gauge (0.135 inch or 3.429mm) thickness of the purlins. Therefore, the bolts at lapped connections for these purlins were pre-installed at Steelway Building Systems using proper tools. The bolt holes were reamed out to fit the 1/2 inch (12.7mm) bolts, and stud guns were used to install the bolts. For the same purlins with thicknesses of 12 gauge (0.105 inch or 2.667mm) and 14 gauge (0.075 inch or 1.905mm), the specimens were assembled at University of Waterloo since the maximum offset allowance at bolt holes were larger than the thicknesses of the purlins, and all bolts were snug tight. The over tightened bolts by using the stud gun at the connections could result in the increase in the stiffness for the 10-gauge (0.135 inch or 3.429mm) purlins. Overall, the stiffness of lapped purlins with round holes either increased or almost matched the full stiffness of non-lapped purlins.

For connections with vertical slotted holes, the stiffness of the lapped purlins was 6%-17% lower than the full stiffness of non-lapped purlins. The vertical slotted holes provided extra tolerance at bolt holes to facilitate the installation but considerably increased the connection flexibility. Therefore, the

presence of vertical slotted holes at lapped connections results in a major impact on the flexural stiffness of lapped purlins compared to that of round holes. The characteristics of flexural stiffness of the lapped purlins with vertical slotted connections are discussed in Section 4.4.3.

Table 4-4 Deformation and Flexural Stiffness of Lapped Purlins with Different Types of Holes

Test[1]	**Lapped length (in.)**	**Types of holes at connection**	P_s **(kip)**	**Deflection** Δ_t **(in.) at** P_s			**Dev.**	K_t **(kip/in)**	$\frac{K_{t-lapped}}{K_{t-non\ lapped}}$
				Test 1	**Test 2**	**Avg.**			
12Z10	Non-lapped	N/A	4.66	0.900	0.896	0.898	±2.90%	5.19	**100% (baseline)**
	48	Round holes		0.799	0.818	0.809	±0.66%	5.77	**111%**
	48	Vertical slotted holes		1.097	1.069	1.083	±2.47%	4.31	**83%**
12Z12	Non-lapped	N/A	3.62	0.862	0.845	0.853	±2.90%	4.24	**100% (baseline)**
	48	Round holes		0.884	0.865	0.874	±2.18%	4.14	**98%**
	48	Vertical slotted holes		0.987	0.918	0.952	±2.05%	3.80	**90%**
12Z14	Non-lapped	N/A	2.21	0.721	0.731	0.726	±3.81%	3.04	**100% (baseline)**
	48	Round holes		0.738	0.700	0.719	±1.08%	3.07	**101%**
	48	Vertical slotted holes		0.787	0.763	0.775	±1.05%	2.85	**94%**

Metric Conversion: 1 in. = 25.4mm, 1 kip = 4.448 kN, 1 kip/in = 175 kN/m

[1] Test designation: for example, 12Z10 represents the specimen for 12-inch (305mm) Z-shaped purlins with 10-gauge (0.135 inch or 3.429mm) thickness.

4.4 Test Results of Lapped Purlins with Vertical Slotted Holes

4.4.1 Observation of Failure

The section failure location of the lapped purlins in all tests was just outside the end of the lap caused by combined shear and bending. The top flange buckling was found to always initiate the failure as shown in the photograph in Figure 4-2. The top flange was subjected to compression stress due to the bending. The applied load dropped rapidly once the top flange buckled, then the failure extended to the webs. The shear buckling of the web section was also observed just outside the end of lapped connections. Significant cross-section distortion of the Z-section occurred at the end of the lap at large deformation. The failure mode is consistent with the test results for standard holes carried out by Ho and Chung (2004). In the research conducted by Dubina and Ungureanu (2010), it was suggested that the web crippling should be checked instead of the shear buckling of the web at the failure of the section. However, no web crippling was observed at the failure of the section for any test, only shear buckling. After examining the dissembled tested specimens, no bearing deformation was found at the bolt holes.

Figure 4-2 Photograph of Typical Failure Mode at the End of Lapped Connection

4.4.2 Flexural Strength of Lapped Purlins with Vertical Slotted Holes

For lapped purlins with slotted holes, the tested ultimate load (P_t) was determined for each specimen. The tested maximum flexural strength (M_{t-lap}) was evaluated at mid-span of the test specimen and compared to the calculated maximum flexural strength ($M_{n-non\ lap}$) of non-lapped purlins. All calculations were based on a single purlin. The mechanical properties obtained from standard coupon tests were used in the calculation of the maximum flexural strength ($M_{n-non\ lap}$) of non-lapped purlins. All data is summarized in Table 4-5. The lap length to section depth ratio (L_p/D) and the section depth to thickness ratio (D/t, the web slenderness ratio) are also included in Table 4-3. For all calculations, the lap length (L_p) of the connection was taken to be the distance between the centre of the outer bolts of the lapped section instead of the actual edge to edge distance.

Table 4-5 Test Strength Results - Lapped Purlins with Vertical Slotted Holes

Test[1]	L_p/D	D/t	P_t (kip)	M_{t-lap} (kip·in)	$M_{n-non\ lap}$ (kip·in)	$\frac{M_{t-lap}}{M_{n-non\ lap}}$
08Z10-34-1	4.00	59.26	12.91	387	298	**1.30**
08Z10-34-2	4.00	59.26	12.52	375	298	**1.26**
08Z10-60-1	7.25	59.26	16.78	503	298	**1.69**
08Z10-60-2	7.25	59.26	16.67	500	298	**1.68**
08Z13-34-1	4.00	88.89	7.77	233	182	**1.28**
08Z13-34-2	4.00	88.89	7.64	229	182	**1.26**
08Z13-60-1	7.25	88.89	9.72	292	182	**1.60**
08Z13-60-2	7.25	88.89	9.18	276	182	**1.51**
08Z16-34-1	4.00	133.33	4.24	127	108	**1.18**
08Z16-34-2	4.00	133.33	4.09	123	108	**1.14**
08Z16-60-1	7.25	133.33	4.31	129	108	**1.20**
08Z16-60-2	7.25	133.33	4.49	135	108	**1.25**
10Z10-34-1	3.20	74.07	10.80	486	428	**1.14**
10Z10-34-2	3.20	74.07	10.82	487	428	**1.14**
10Z10-60-1	5.80	74.07	12.69	571	428	**1.34**
10Z10-60-2	5.80	74.07	11.92	536	428	**1.25**

Metric Conversion: 1 kip = 4.448 kN, 1 kip·in = 0.112kN·m

[1] Test designation: For example, 08Z13-34-2 denotes the second test for 8-inch (203mm) Z-shaped purlins with 13 gauge (0.09 inch or 2.286mm) thickness at 34-inch (0.864m) length of lapped connections.

Table 4-5 cont. Test Strength Results - Lapped Purlins with Vertical Slotted holes

Test[1]	L_p/D	D/t	P_t (kip)	M_{t-lap} (kip·in)	$M_{n-non\ lap}$ (kip·in)	$\frac{M_{t-lap}}{M_{n-non\ lap}}$
10Z13-34-1	3.20	111.11	6.05	272	254	**1.07**
10Z13-34-2	3.20	111.11	5.58	251	254	**0.99**
10Z13-60-1	5.80	111.11	7.52	338	254	**1.33**
10Z13-60-2	5.80	111.11	7.39	333	254	**1.31**
10Z16-34-1	3.20	166.67	2.85	128	135	**0.95**
10Z16-34-2	3.20	166.67	2.77	125	135	**0.92**
10Z16-60-1	5.80	166.67	2.97	134	135	**0.99**
10Z16-60-2	5.80	166.67	3.25	146	135	**1.08**
12Z10-34-1	2.67	88.89	7.74	465	549	**0.85**
12Z10-34-2	2.67	88.89	7.90	474	549	**0.86**
12Z10-48-1	3.83	88.89	10.00	600	562	**1.07**
12Z10-48-2	3.83	88.89	10.51	630	562	**1.12**
12Z10-60-1	4.83	88.89	10.83	650	549	**1.18**
12Z10-60-2	4.83	88.89	10.99	660	549	**1.20**
12Z12-34-1	2.67	114.29	5.15	309	402	**0.77**
12Z12-34-2	2.67	114.29	5.36	322	402	**0.80**
12Z12-48-1	3.83	114.29	7.54	453	448	**1.01**
12Z12-48-2	3.83	114.29	7.86	472	448	**1.05**
12Z12-60-1	4.83	114.29	7.29	438	402	**1.09**
12Z12-60-2	4.83	114.29	7.56	454	402	**1.13**
12Z14-34-1	2.67	160.00	3.45	207	238	**0.87**
12Z14-34-2	2.67	160.00	3.63	218	238	**0.92**
12Z14-48-1	3.83	160.00	4.03	242	244	**0.99**
12Z14-48-2	3.83	160.00	3.95	237	244	**0.97**
12Z14-60-1	4.83	160.00	4.63	278	238	**1.17**
12Z14-60-2	4.83	160.00	5.06	303	238	**1.28**
					Mean	**1.15**
					Std. Dev	**0.22**
					COV	**0.19**

Metric Conversion: 1 kip = 4.448 kN,
1 kip·in = 0.112kN·m

[1] Test designation: for example, 08Z13-34-2 denotes the second test for 8-inch (203mm) Z-shaped purlins with 13 gauge (0.09 inch or 2.286mm) thickness at 34-inch (0.864m) length of lapped connections.

It can be observed from Table 4-5 that the moment resistance ratio ($M_{t-lap}/M_{n-non\ lap}$) lies between 0.77 and 1.69 while the lap length to section depth ratio (L_p/D) ranges from 2.67 to 7.25. As the lap length increases, the moment resistance ratio ($M_{t-lap}/M_{n-non\ lap}$) increases. For lapped purlins with vertical slotted holes, the moment resistance ratio is directly related to the lap length to section depth ratio (L_p/D). The findings are similar to the findings on the lapped purlins with standard holes by Ho and Chung (2004). Ho and Chung (2004) suggested that a unity moment resistance ratio may be achieved with a minimum lap length to section depth ratio of 2.0 for lapped purlins with standard holes. For the purpose of comparison, the moment resistance ratios ($M_{t-lap}/M_{n-non\ lap}$) vs. the lap length to section depth ratios (L_p/D) are shown in Figure 4-3. The best trend line of test data reaches the $M_{t-lap}/M_{n-non\ lap}$ ratio at 1.00, when the L_p/D ratio is approximately equal to 3.0. The benchmark used for the comparison is the calculated flexural strength of non-lapped purlins ($M_{n-non\ lap}$). As discussed in 4.2.1.3, the actual flexural strength could be 8% higher than the calculated flexural strength. By considering this additional 8% difference, the L_p/D ratio can be conservatively taken as 3.7, which is also shown in Figure 4-3. In summary, the full flexural strength of the continuous purlin can be achieved with a minimum lap length to section depth ratio of 3.0 for lapped purlins with vertical slotted holes. This result confirmed the design criteria given in CSA S136-2012 (CSA 2012).

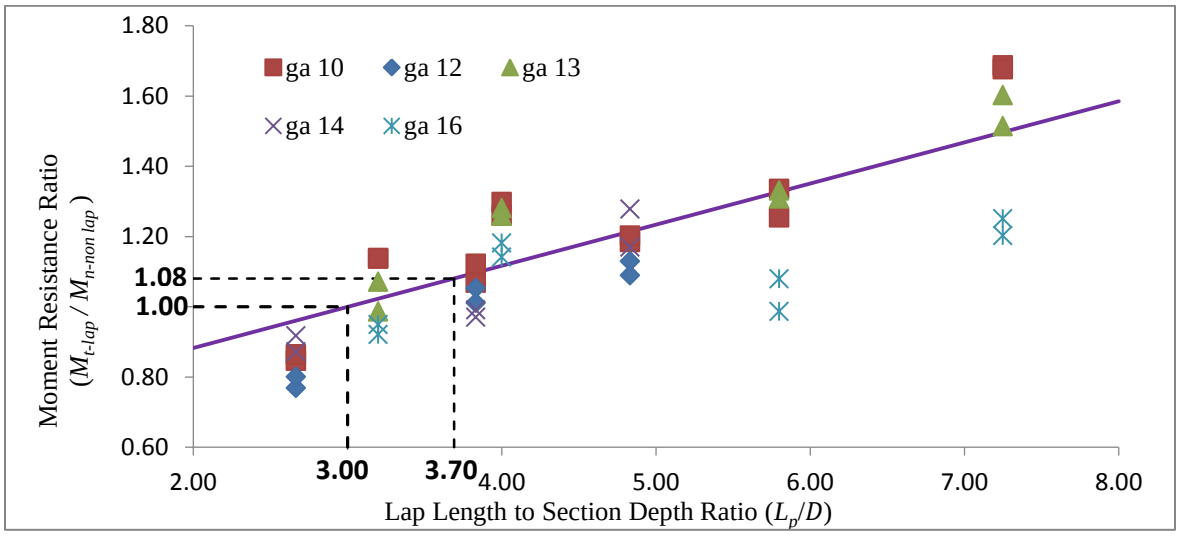

Figure 4-3 Moment Resistance Ratio vs. Lap Length to Section Depth Ratio

Figure 4-3 also shows that the moment resistance ratios ($M_{t-lap}/M_{n-non\ lap}$) vary for the same lap length to section depth ratio (L_p/D). For example, $M_{t-lap}/M_{n-non\ lap}$ ranges from 1.20 to 1.69 for the lapped purlins with the L_p/D ratio of 7.25, and the moment resistance ratios of lighter gauge purlins are always lower than that of thicker gauge purlins. The thickness of the section also influences the moment resistance of the lapped connections. Therefore, the section depth to thickness ratios (D/t, the web slenderness ratios) were compared to the moment resistance ratios ($M_{t-lap}/M_{n-non\ lap}$), and the results are shown in Figure 4-4.

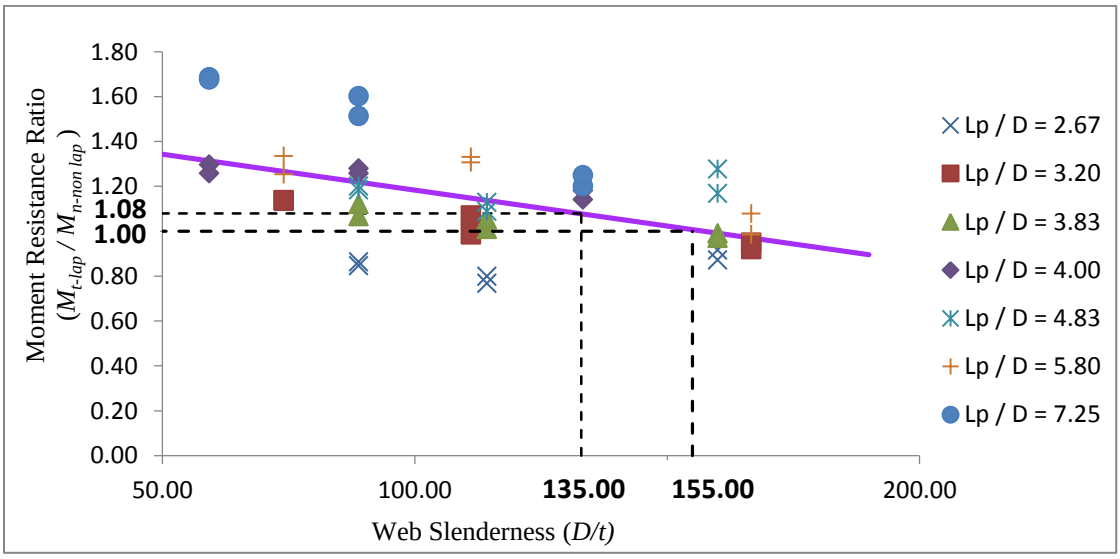

Figure 4-4 Moment Resistance Ratio vs. Web Slenderness Ratio

The results indicate that the lowest $M_{t-lap}/M_{n-non\ lap}$ ratios occurred for the lapped purlins with large web slenderness ratios even when the lap length exceeded 3.7 times of the section depth. The section with larger web slenderness is easier to buckle than the section with smaller web slenderness; this results in the reduction of the moment resistance of the lapped connection. As shown in Figure 4-4, the $M_{t-lap}/M_{n-non\ lap}$ ratios decrease as the web slenderness ratios increase. The best trend line of the test data reaches the $M_{t-lap}/M_{n-non\ lap}$ ratio at 1.00, when the L_p/D ratio is approximately equal to 155. As discussed in 4.2.1.3, by considering the additional 8% difference between the calculated and the actual flexural strength of non-lapped purlins, the D/t ratio can be conservatively taken as 135, which is also shown in Figure 4-4. In summary, the maximum section depth to

thickness ratio (D/t, the web slenderness ratio) of 155 should be met in order to achieve the unity moment resistance ratio for the lapped purlins with vertical slotted holes. For example, in Table 4-5, the 10-inch (254mm) purlins with 16-gauge (0.060 inch or 1.524mm) thickness and 12-inch (305mm) purlins with 14-guage (0.075 inch or 1.905mm) thickness don't satisfy the suggested requirement because the corresponding D/t ratios are 160 and 167.

For the comparison in this section, all moment resistances were the maximum moment evaluated at mid-span of the specimens. However, all section failures were found at the end of the lapped sections for lapped purlins with vertical slotted holes, which is similar to the test results of lapped purlins with standard holes obtained by Ho and Chung (2004). Therefore, the same analysis method proposed by Chung and Ho (2005) was used to determine the internal forces within the lapped connections and to check the combined bending and shear at the end of lapped section. The analysis results and the design recommendations are presented in Chapter 5.

4.4.3 Stiffness of Lapped Purlins with Vertical Slotted Holes

The effective flexural rigidity ratio α was adopted to evaluate the stiffness of the lapped connections with vertical slotted holes, which was first introduced for the lapped connections with standard holes by Ho and Chung (2004). The effective flexural rigidity ratio α was defined as the effective flexural rigidity of the lapped section over the flexural rigidity of the single section. The expression of determining the effective flexural rigidity ratio α is presented in Appendix D. The calculated effective flexural rigidity ratio, denoted by α_t, is summarized in Table 4-6. The tested flexural stiffness (K_{t-lap}) of lapped purlins with vertical slotted holes was also determined using equation (4.15). The results were compared to the calculated stiffness of non-lapped purlins ($K_{d-non\ lap}$), which was the benchmark and was determined using equation (4.16). Since the actual stiffness of the non-lapped purlins could be 9% lower than the calculated stiffness as discussed in 4.2.2, K_{t-lap} was also compared to the actual stiffness of non-lapped purlins ($K_{t-non\ lap}$), which is taken as the $\mathbf{0.91} * K_{d-non\ lap}$ for reference. It should be noted that the stiffness shown in Table 4-6 was determined at 60% of the ultimate load of the non-lapped purlins. The stiffness of lapped purlins associated with 40%, 80%, and 100% of the ultimate load as well as the complete deflection results were also obtained and are provided in Table C-3, C-4, C-5 and C-6 of Appendix C. All results were based on a single set of purlin for direct comparison. The mechanical properties obtained from standard coupon tests were used in the calculations.

Table 4-6 Test Stiffness Results - Lapped Purlins with Vertical Slotted holes

Test[1]	L_p/D	L_p/t	α_t	K_{t-lap} (kip/in)	$K_{d-non\ lap}$ (kip/in)	$\frac{K_{t-lap}}{K_{d-non\ lap}}$	$\frac{K_{t-lap}}{K_{t-non\ lap}}$
08Z10-34-01	4.00	237	0.388	8.07	15.76	**51%**	56%
08Z10-34-02	4.00	237	0.430	8.74	15.76	**55%**	61%
08Z10-60-01	7.25	430	0.725	11.88	15.76	**75%**	83%
08Z10-60-02	7.25	430	0.707	11.61	15.76	**74%**	81%
08Z13-34-01	4.00	356	0.523	7.09	11.00	**64%**	71%
08Z13-34-02	4.00	356	0.270	4.17	11.00	**38%**	42%
08Z13-60-01	7.25	644	0.641	7.42	11.00	**67%**	74%
08Z13-60-02	7.25	644	0.628	7.28	11.00	**66%**	73%
08Z16-34-01	4.00	533	0.356	3.32	6.96	**48%**	52%
08Z16-34-02	4.00	533	0.536	4.57	6.96	**66%**	72%
08Z16-60-01	7.25	967	0.915	6.45	6.96	**93%**	102%
08Z16-60-02	7.25	967	1.150	7.85	6.96	**113%**	124%
10Z10-34-01	3.20	237	0.320	4.30	8.37	**51%**	56%
10Z10-34-02	3.20	237	0.340	4.49	8.37	**54%**	59%
10Z10-60-01	5.80	430	0.884	7.68	8.37	**92%**	101%
10Z10-60-02	5.80	430	0.673	6.27	8.37	**75%**	82%
10Z13-34-01	3.20	356	0.317	2.97	5.82	**51%**	56%
10Z13-34-02	3.20	356	0.408	3.54	5.82	**61%**	67%
10Z13-60-01	5.80	644	0.856	5.21	5.82	**90%**	99%
10Z13-60-02	5.80	644	1.057	6.04	5.82	**104%**	114%
10Z16-34-01	3.20	533	0.510	2.49	3.56	**70%**	77%
10Z16-34-02	3.20	533	0.615	2.78	3.56	**78%**	86%
10Z16-60-01	5.80	967	1.212	4.04	3.56	**114%**	125%
10Z16-60-02	5.80	967	0.941	3.41	3.56	**96%**	105%
12Z10-34-01	2.67	237	0.294	3.03	5.56	**54%**	60%
12Z10-34-02	2.67	237	0.317	3.17	5.56	**57%**	63%
12Z10-48-01	3.83	341	0.579	4.22	5.66	**74%**	82%
12Z10-48-02	3.83	341	0.612	4.36	5.66	**77%**	85%
12Z10-60-01	4.83	430	0.715	4.54	5.56	**82%**	90%
12Z10-60-02	4.83	430	0.782	4.81	5.56	**86%**	95%

Metric Conversion: 1 kip/in = 175 kN/m

[1] Test designation: for example, 08Z13-34-2 denotes the second test for 8-inch (203mm) Z-shaped purlins with 13 gauge (0.09 inch or 2.286mm) thickness at 34-inch (0.864m) length of lapped connections.

Table 4-6 cont. Test Stiffness Results - Lapped Purlins with Vertical Slotted holes

Test[1]	L_p/D	L_p/t	α_t	K_{t-lap} (kip/in)	$K_{d-non\ lap}$ (kip/in)	$\frac{K_{t-lap}}{K_{d-non\ lap}}$	$\frac{K_{t-lap}}{K_{t-non\ lap}}$
12Z12-34-01	2.67	305	0.367	2.76	4.42	**62%**	69%
12Z12-34-02	2.67	305	0.297	2.42	4.42	**55%**	60%
12Z12-48-01	3.83	438	0.608	3.67	4.79	**77%**	84%
12Z12-48-02	3.83	438	0.686	3.94	4.79	**82%**	90%
12Z12-60-01	4.83	552	0.928	4.23	4.42	**96%**	105%
12Z12-60-02	4.83	552	0.794	3.85	4.42	**87%**	96%
12Z14-34-01	2.67	427	0.340	2.18	3.66	**60%**	65%
12Z14-34-02	2.67	427	0.369	2.29	3.66	**63%**	69%
12Z14-48-01	3.83	613	0.730	2.78	3.26	**85%**	94%
12Z14-48-02	3.83	613	0.772	2.86	3.26	**88%**	96%
12Z14-60-01	4.83	773	0.769	3.13	3.66	**86%**	94%
12Z14-60-02	4.83	773	0.723	3.01	3.66	**82%**	90%
					Mean	**74%**	81%
					Std. Dev	**0.18**	0.20
					COV	**0.24**	0.24

Metric Conversion: 1 kip/in = 175 kN/m

[1] Test designation: for example, 08Z13-34-2 denotes the second test for 8-inch (203mm) Z-shaped purlins with 13 gauge (0.09 inch or 2.286mm) thickness at 34-inch (0.864m) length of lapped connections.

It can be observed from Table 4-6 that the effective flexural rigidity ratio (α_t) is directly proportional to the stiffness ratio ($K_{t-lap}/K_{d-non\ lap}$ or $K_{t-lap}/K_{t-non\ lap}$). The values of α_t vary between 0.27 and 1.21 while the lap length to section depth ratios range from 2.67 to 7.25. As the lap length increases, the flexural rigidity ratio (α_t) increases. For lapped purlins with vertical slotted holes, the flexural rigidity ratio is directly proportional to the lap length to section depth ratio (L_p/D). The findings are similar to the findings on lapped purlins with standard holes obtained by Ho and Chung (2004). Ho and Chung (2004) suggested that the full stiffness of non-lapped purlins may be achieved with a minimum lap length to section depth ratio of 4.0 for lapped purlins with standard holes. For the purpose of comparison, the effective flexural rigidity ratio (α_t) vs. lap length to section depth ratio (L_p/D) are plotted in Figure 4-5.

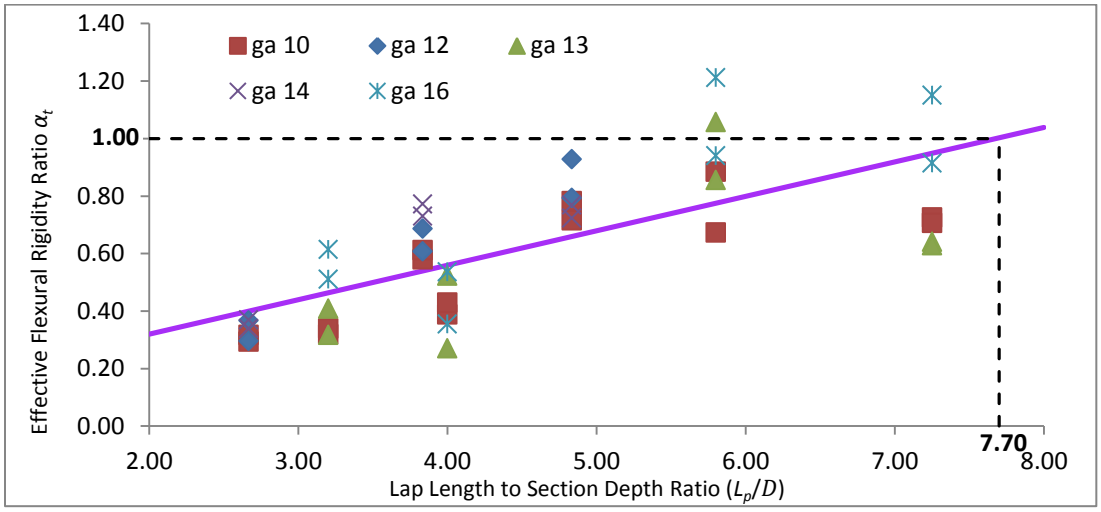

Figure 4-5 Effective Flexural Rigidity Ratio vs. Lap Length to Section Depth Ratio

According to Figure 4-5, along the best trend line of test data, the α_t value reaches 1.0 when the L_p/D ratio is approximately equal to 7.70. In other words, the full stiffness of non-lapped purlins can be achieved with a minimum lap length to section depth ratio of 7.70 for lapped purlins with vertical slotted holes. The minimum lap length to section depth ratio is significantly increased, and is almost 2.6 times of the suggested ratio of 3.0 indicated in the CSA S136-2012 (CSA 2012). The stiffness of the lapped purlins is substantially reduced when the vertical slotted connections are used. The vertical slotted holes provide the extra installation tolerance at the connections while increasing the flexibility of the connection. The large increased flexibility forms the significant connection rotation when the purlins are loaded. The connection rotation causes the larger deformation of the lapped purlins compared to non-lapped purlins. Therefore, the stiffness improvement is very limited when the vertical slotted holes are used at lapped connections. In order to study the reduced stiffness of lapped connections, the mid-span load-deflection curve for each specimen was plotted and is shown in Appendix F. Two typical shapes of load-deflection curve were found and are shown in Figure 4-6.

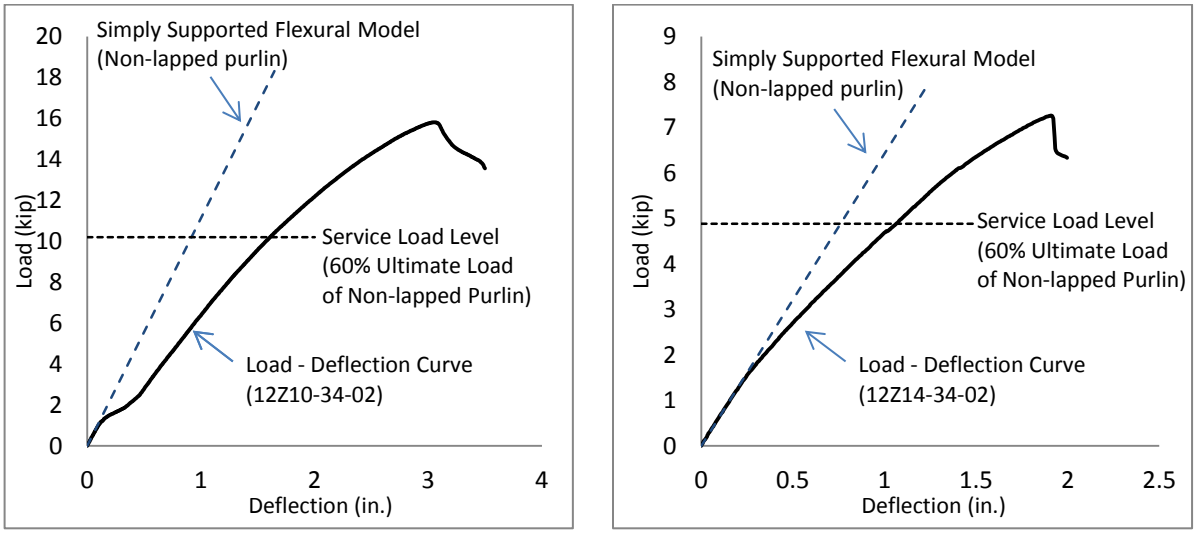

a) Thick Gauge Purlin

b) Light Gauge Purlin

Figure 4-6 Typical Load - Deflection Curves

The results are compared to the simply supported flexural deformation curve of non-lapped purlins, created based on equation (4.16). The slope of the load-deflection curve represents the stiffness of the lapped purlins. At the early stage of loading, the stiffness of the lapped purlins is the same as that of non-lapped purlins. As the applied load increases, the stiffness of the lapped purlins decreases. This result is consistent with the observed connection rotation and cross-section distortion at the edge of the lap. As shown in Figure 4-6 (a), a sudden drop in the slope occurred for thick gauge lapped purlins. However, shown in Figure 4-6 (b), the slope decreases slowly for light gauge purlins. The plateau of the load-deflection curve for the thick gauge purlins is caused by the initial slip at the lapped connections. When two purlins lap together, they cannot nest properly if the sections of the two purlins are identical as shown in Figure 4-7 (a). There is always a gap between the two Z-sections. The vertical slotted holes at the same location on each purlin are offset and provide the extra tolerance at the connections compared to the round holes. When the loading applied, the load is transferred through the bolts at the connections and the two top flanges. The load pulls the upper purlin down until the two vertical slotted holes align with each other and bear together as shown in Figure 4-7 (b). The gap between two lapped purlins is related to the thickness and stiffness of the Z-sections. For thick gauge purlins, the thickness is large and the flanges are stiff. The two purlins are forced to fit to each other, so the gap is large and the initial slip is significant and shows as the plateau

of the load-deflection curve. For light gauge purlins, the thickness is small and the flanges are flexible. The two purlins fit properly, so the gap is minor and the initial slip is negligible.

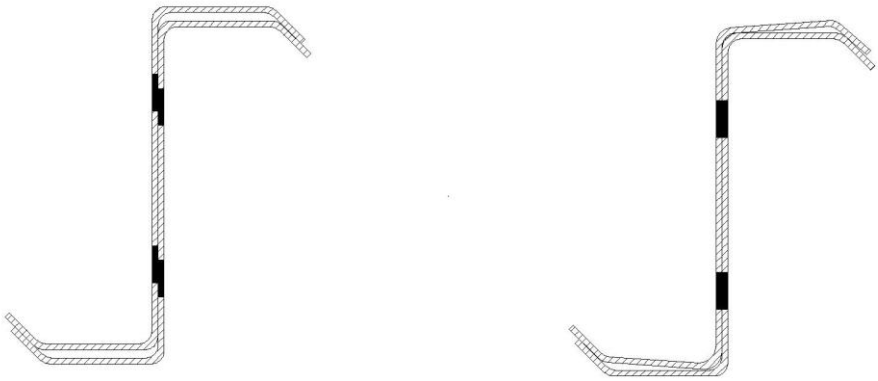

a) Unloaded shape b) Loaded shape

Figure 4-7 Initial Gap of Lapped Section

Therefore, the thickness of the section also influences the stiffness of lapped connection. The lap length to thickness ratios (L_p/t) were compared to the effective flexural rigidity ratios (α_t) and the results are shown in Figure 4-8. The results indicate that for a certain lap length to section depth ratio the flexural rigidity ratio (α_t) increases as the lap length to thickness ratio (L_p/t) increases. For lapped purlins with vertical slotted holes, the flexural rigidity ratio is directly related to the lap length to thickness ratio (L_p/t). This result is consistent with the findings from the load-deflection curve. For slender purlins with large L_p/t ratio, the two purlins fit properly at the lap and the connection rotation is minor compared to the stiff purlins with low L_p/t ratio. Along the best trend line of the test data, the α_t value reaches 1.0 when the L_p/t ratio is approximately equal to 935. Thus, it suggests that the minimum lap length to thickness ratio (L_p/t) of 935 should be met in order to achieve the unity effective flexural rigidity ratio for lapped purlins with vertical slotted holes.

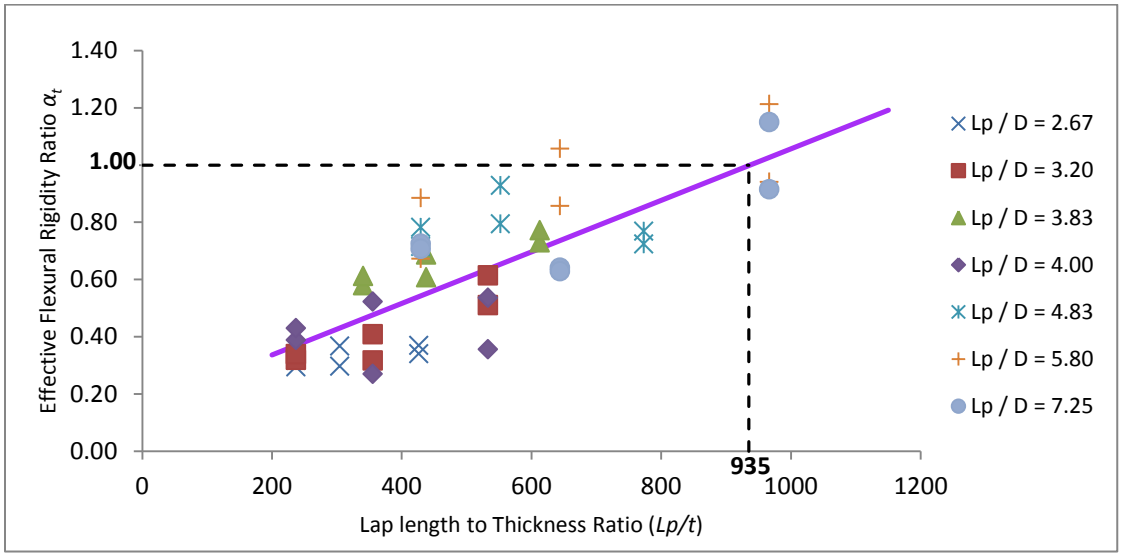

Figure 4-8 Effective Flexural Rigidity Ratio vs. Lap Length to Thickness Ratio

Consequently, the stiffness improvement is very limited when the vertical slotted holes are used at the lapped connections. In order to achieve the full stiffness of non-lapped purlins, a large lap length needs to be used. The flexural rigidity ratio not only depends on the lap length to section depth ratio, but also on the lap length to thickness ratio. A regression analysis was conducted, and a prediction equation of determining the flexural rigidity ratio for lapped purlins with vertical slotted holes is proposed in Chapter 5.

Chapter 5
Proposed Design Procedures

5.1 Proposed Design Rules for Combined Bending and Shear

5.1.1 Internal Forces at the Lapped Connections

From the test observations, all section failures were located at the end of the lapped sections for lapped purlins with vertical slotted holes. A static analysis was performed to determine all the internal forces at the lap connections under applied loads. The analysis used the method proposed by Ho and Chung (2005) on the lapped purlins with standard holes with the following assumptions.

- The centre of the bolt group is the centre of connection rotation.
- The magnitudes of shear force F_b at bolt holes are related to the distances *r*, which is the distance from the centre of the bolt hole to the centre of the connection rotation.
- The directions of shear force F_b at bolt holes are determined from the moment equilibrium consideration of the lapped connections.

The bending moment diagrams and shear force diagrams for each piece of lapped purlin as well as the expressions of the internal forces are shown in Figure E-1 in Appendix E. The corresponding shear forces (V_1, V_2, V_3) and moments (M_1, M_2, M_3) within the lapped connections were calculated according to the measured maximum applied load (P_t) from the tests, and all results are summarized in Table 5-1. Similar findings on lapped purlins with standard holes (Ho and Chung 2005) were also discovered from these tests on the lapped purlins with vertical slotted holes.

1. The critical section is found at the end of lap, which is the cross-section of the purlin containing the vertical slotted holes.
2. The moment (M_1) just outside the critical section at the end of lap is always found to be the largest moment along the individual length of purlin. The moment (M_2) just inside the critical section at the end of lap is slightly less than M_1. The moment (M_3) at the mid-span of the test specimen, which is distributed on the individual piece, is found to be relatively less than M_1 and M_2.

3. The shear force (V_2) just inside the critical section is related to the lap length. For connections with small lap length to section depth ratio (L_p/D), the shear force V_2 is considerably larger than the shear force (V_1), which is just outside the critical section. As the lap length increases, the magnitude of the shear force V_2 decreases. When the lap length to section depth ratio (L_p/D) of the connections is equal to or greater than 4.8, the magnitude of shear force V_2 becomes equal to or smaller than V_1.
4. The shear force V_3 at the mid-span of the test specimen is found to be the largest shear force along the member.

Therefore, the combined bending and shear should be checked near the critical section at the end of lap. Theoretically, the shear buckling strength of the section at the mid-span of the test specimen should be compared with the maximum shear force V_3. However, the webs of two nested purlins are bolted together and connected to the web cleats of the loading plate at this location. When one web intends to buckle, the other web and the cleat may act against it and prevent it from buckling. The shear buckling is never observed at the mid-span of the specimen during the tests. Furthermore, the corresponding moment M_3 is relatively small, and the combined bending and shear failures were not observed at this location. Therefore, instead of checking the combined bending and shear, only the shear yielding at the cross-section with vertical slotted holes at the mid-span of the specimen should be checked, as well as the bearing strength at the vertical slotted holes.

Table 5-1 Summary of Internal Forces with Lapped Connections

Test[1]	P_t (kip)	V_1 (kip)	V_2 (kip)	V_3 (kip)	M_1 (kip·in)	M_2 (kip·in)	M_3 (kip·in)
08Z10-34-1	12.91	6.45	-5.46	11.91	284	281	194
08Z10-34-2	12.52	6.26	-5.30	11.55	275	272	188
08Z10-60-1	16.78	8.39	-0.25	8.64	260	259	252
08Z10-60-2	16.67	8.33	-0.25	8.58	258	257	250
08Z13-34-1	7.77	3.88	-3.29	7.17	171	169	117
08Z13-34-2	7.64	3.82	-3.23	7.05	168	166	115

Metric Conversion: 1 kip = 4.448 kN, 1 kip·in = 0.112kN·m

[1] Test designation: for example, 08Z13-34-2 denotes the second test for 8-inch (203mm) Z-shaped purlins with 13 gauge (0.09 inch or 2.286mm) thickness at 34-inch (0.864m) length of lapped connections.

Table 5-1 cont. Summary of Internal Forces with Lapped Connections

Test[1]	P_t (kip)	V_1 (kip)	V_2 (kip)	V_3 (kip)	M_1 (kip·in)	M_2 (kip·in)	M_3 (kip·in)
08Z13-60-1	9.72	4.86	-0.14	5.01	151	150	146
08Z13-60-2	9.18	4.59	-0.14	4.73	142	142	138
08Z16-34-1	4.24	2.12	-1.79	3.91	93	92	64
08Z16-34-2	4.09	2.05	-1.73	3.78	90	89	61
08Z16-60-1	4.31	2.16	-0.06	2.22	67	67	65
08Z16-60-2	4.49	2.24	-0.07	2.31	70	69	67
10Z10-34-1	10.80	5.40	-9.27	14.67	399	391	243
10Z10-34-2	10.82	5.41	-9.29	14.70	400	392	243
10Z10-60-1	12.69	6.35	-3.40	9.74	387	384	286
10Z10-60-2	11.92	5.96	-3.19	9.15	364	361	268
10Z13-34-1	6.05	3.03	-5.19	8.22	224	219	136
10Z13-34-2	5.58	2.79	-4.79	7.57	206	202	125
10Z13-60-1	7.52	3.76	-2.01	5.77	229	228	169
10Z13-60-2	7.39	3.70	-1.98	5.67	225	224	166
10Z16-34-1	2.85	1.43	-2.45	3.88	106	103	64
10Z16-34-2	2.77	1.38	-2.38	3.76	102	100	62
10Z16-60-1	2.97	1.48	-0.79	2.28	91	90	67
10Z16-60-2	3.25	1.62	-0.87	2.49	99	98	73
12Z10-34-1	7.74	3.87	-9.79	13.66	403	389	232
12Z10-34-2	7.90	3.95	-9.99	13.94	411	397	237
12Z10-48-1	10.00	5.00	-7.66	12.66	485	476	300
12Z10-48-2	10.51	5.25	-8.05	13.30	510	500	315
12Z10-60-1	10.83	5.42	-5.58	11.00	493	487	325
12Z10-60-2	10.99	5.50	-5.66	11.16	500	494	330
12Z12-34-1	5.15	2.57	-6.51	9.09	268	259	154
12Z12-34-2	5.36	2.68	-6.78	9.46	279	269	161
12Z12-48-1	7.54	3.77	-5.78	9.55	366	359	226
12Z12-48-2	7.86	3.93	-6.02	9.95	381	374	236
12Z12-60-1	7.29	3.65	-3.76	7.40	332	328	219
12Z12-60-2	7.56	3.78	-3.90	7.68	344	340	227
12Z14-34-1	3.45	1.73	-4.36	6.09	179	173	104
12Z14-34-2	3.63	1.82	-4.59	6.41	189	182	109
12Z14-48-1	4.03	2.01	-3.09	5.10	195	192	121
12Z14-48-2	3.95	1.97	-3.02	4.99	191	188	118
12Z14-60-1	4.63	2.31	-2.38	4.70	211	208	139
12Z14-60-2	5.06	2.53	-2.61	5.13	230	227	152

Metric Conversion: 1 kip = 4.448 kN, 1 kip·in = 0.112kN·m

[1] Test designation: for example, 08Z13-34-2 denotes the second test for 8-inch (203mm) Z-shaped purlins with 13 gauge (0.09 inch or 2.286mm) thickness at 34-inch (0.864m) length of lapped connections.

5.1.2 Design Checks for Shear Strength, Bearing Strength and Combined Bending and Shear

The shear strength of a CFS Z-section is governed by either yielding or buckling, which is calculated as per clause C3.2.1 of CSA S136-2012 (CSA 2012).

For shear yielding, the nominal shear strength (V_{ny}) is determined by

$$V_{ny} = 0.60F_y h_n t \tag{5.1}$$

where h_n is the net section depth of flat portion of web for section with web holes, t is the web thickness, and F_y is the design yield stress.

For shear buckling, the nominal shear strength (V_n) can be evaluated as

$$V_n = A_w F_v \tag{5.2}$$

where $A_w = h_g t$, the gross area of web element, h_g is the depth of flat portion of web, t is web thickness, and F_v is the nominal shear stress.

For $\sqrt{Ek_v/F_y} < h_g/t \leq 1.51\sqrt{Ek_v/F_y}$, $\quad F_v = \frac{0.60\sqrt{Ek_v/F_y}}{(h_g/t)}$

For $h_g/t > 1.51\sqrt{Ek_v/F_y}$, $\quad F_v = \frac{\pi^2 Ek_v}{12(1-\mu^2)(h_g/t)^2}$

where $\mu = 0.3$ is the Poisson's ratio and k_v is the shear buckling coefficient for webs with restraint elements.

$$k_v = 5.34 + \frac{4.00}{(a/h_g)^2}$$

where a is the clear distance between transverse stiffeners of reinforced web elements, which is conservatively taken as the distance from the web cleat of loading plate at the mid-span of the specimen to the first adjacent internal brace.

The bearing strength of a CFS Z-section web at the bolt holes was calculated by using the method in the clause E3.3.1 of CSA S136-2012 (CSA 2012), as follows.

$$P_n = C m_f d_b t F_u \tag{5.3}$$

where d_b is the nominal bolt diameter, t is the web thickness, F_u is the tensile strength

C is the bearing factor which is taken as 3.0 since $d/t < 10$ for all specimens

m_f is the modification factor for type of bearing connection which is conservatively taken as 1.00 since washers under bolts head and nuts are both used for all specimens.

As previously discussed, the calculated shear yielding strength (V_{ny}) at the cross-section with vertical slotted holes and the bearing strength (P_n) at the bolts holes were both compared to the largest shear force V_3 from the tests, and the results are summarized in Table 5-2. According to Table 5-2, the maximum V_3/V_{ny} ratio is 0.44 and the maximum V_3/P_n ratio is 0.52. It can be concluded that the shear force at mid-span did not reach the shear yielding strength of the section or the bearing strength at bolt holes. Therefore, the cross-section at mid-span is not critical in terms of shear. This agrees with the test observations where the shear failures never occurred at the mid-span and the bearing deformation was not observed at bolt holes.

Table 5-2 Summary of Several Design Checks

Tests[1]	$\frac{V_3}{V_{ny}}$	$\frac{V_3}{P_n}$	M_{nl} (kip in)	M_{nd} (kip in)	V_n (kip)	$\frac{M_t}{M_{nl}}$	$\frac{M_t}{M_{nd}}$	$\frac{V_t}{V_n}$
08Z10-34-1	0.44	0.42	298	274	33.93	0.95	1.03	0.19
08Z10-34-2	0.42	0.41	298	274	33.93	0.92	1.00	0.18
08Z10-60-1	0.32	0.31	298	274	32.97	0.87	0.95	0.25
08Z10-60-2	0.31	0.30	298	274	32.97	0.87	0.94	0.25
08Z13-34-1	0.39	0.38	182	163	15.24	0.94	1.05	0.25
08Z13-34-2	0.39	0.38	182	163	15.24	0.92	1.03	0.25
08Z13-60-1	0.27	0.27	182	163	14.37	0.83	0.93	0.34
08Z13-60-2	0.26	0.25	182	163	14.37	0.78	0.87	0.32
08Z16-34-1	0.32	0.34	108	97	4.12	0.87	0.97	0.51
08Z16-34-2	0.31	0.32	108	97	4.12	0.84	0.93	0.50

Metric Conversion: 1 kip = 4.448 kN, 1 kip in = 0.112kN m

[1] Test designation: for example, 08Z13-34-2 denotes the second test for 8-inch (203mm) Z-shaped purlins with 13 gauge (0.09 inch or 2.286mm) thickness at 34-inch (0.864m) length of lapped connections.

Table 5-2 cont. Summary of Design Checks

Tests[1]	$\frac{V_3}{V_{ny}}$	$\frac{V_3}{P_n}$	M_{nl} (kip in)	M_{nd} (kip in)	V_n (kip)	$\frac{M_t}{M_{nl}}$	$\frac{M_t}{M_{nd}}$	$\frac{V_t}{V_n}$
08Z16-60-1	0.18	0.19	108	97	3.88	0.62	0.69	0.56
08Z16-60-2	0.19	0.20	108	97	3.88	0.65	0.72	0.58
10Z10-34-1	0.40	0.52	428	368	33.49	0.91	1.06	0.28
10Z10-34-2	0.40	0.52	428	368	33.49	0.92	1.06	0.28
10Z10-60-1	0.26	0.35	428	368	33.24	0.91	1.05	0.19
10Z10-60-2	0.25	0.32	428	368	33.24	0.85	0.99	0.18
10Z13-34-1	0.33	0.44	254	214	11.69	0.86	1.02	0.44
10Z13-34-2	0.31	0.41	254	214	11.69	0.79	0.94	0.41
10Z13-60-1	0.23	0.31	254	214	11.51	0.90	1.07	0.33
10Z13-60-2	0.23	0.30	254	214	11.51	0.89	1.05	0.32
10Z16-34-1	0.24	0.33	135	119	3.17	0.76	0.87	0.77
10Z16-34-2	0.23	0.32	135	119	3.17	0.74	0.84	0.75
10Z16-60-1	0.14	0.20	135	119	3.12	0.67	0.76	0.48
10Z16-60-2	0.15	0.21	135	119	3.12	0.73	0.83	0.52
12Z10-48-1	0.26	0.39	562	466	31.26	0.85	1.04	0.24
12Z10-48-2	0.28	0.41	562	466	31.26	0.89	1.09	0.26
12Z10-60-1	0.24	0.39	549	456	30.24	0.90	1.08	0.18
12Z10-60-2	0.24	0.40	549	456	30.24	0.91	1.10	0.18
12Z12-34-1	0.24	0.41	402	325	14.11	0.64	0.80	0.46
12Z12-34-2	0.25	0.43	402	325	14.11	0.67	0.83	0.48
12Z12-48-1	0.23	0.39	448	362	16.57	0.80	0.99	0.35
12Z12-48-2	0.24	0.40	448	362	16.57	0.84	1.03	0.36
12Z12-60-1	0.20	0.34	402	325	14.11	0.83	1.02	0.26
12Z12-60-2	0.21	0.35	402	325	14.11	0.86	1.06	0.27
12Z14-34-1	0.20	0.34	238	212	7.36	0.73	0.82	0.59
12Z14-34-2	0.21	0.36	238	212	7.36	0.77	0.86	0.62
12Z14-48-1	0.17	0.29	244	217	5.73	0.79	0.89	0.54
12Z14-48-2	0.17	0.28	244	217	5.73	0.77	0.87	0.53
12Z14-60-1	0.16	0.26	238	212	7.36	0.89	0.99	0.31
12Z14-60-2	0.17	0.29	238	212	7.36	0.97	1.09	0.34

Metric Conversion: 1 kip = 4.448 kN, 1 kip in = 0.112kN m

[1] Test designation: for example, 08Z13-34-2 denotes the second test for 8-inch (203mm) Z-shaped purlins with 13 gauge (0.09 inch or 2.286mm) thickness at 34-inch (0.864m) length of lapped connections.

For checking the critical section subjected to combined bending and shear, the following interaction equation indicated in the clause C3.3.2 of CSA S136-2012 (CSA 2012) was used.

$$\sqrt{\left(\frac{\bar{M}}{M_n}\right)^2 + \left(\frac{\bar{V}}{V_n}\right)^2} \leq 1.0 \tag{5.4}$$

Where $\bar{M}$ is the test moment M_t (either M_1 or M_2), M_n is the nominal flexural strength, $\bar{V}$ is the test shear forces V_t (either V_1 or V_2), and V_n is the nominal shear strength.

It should be noted that the nominal flexural strength (M_n) is based on the local buckling strength (M_{nl}) calculated by using equation (4.2). The nominal shear strength (V_n) at the critical section is always governed by the shear buckling strength for all test specimens; therefore, the gross area of the web section was used to determine V_n through equation (5.2). $\bar{M}$ and $\bar{V}$ are the critical pair of moment, M_t, and shear, V_t, obtained from the tests near the critical section. The corresponding pair of (M_t/M_n) and (V_t/V_n) ratios are summarized in Table 5-2, and are plotted in Figure 5-1 together with the interaction equation (5.4).

According to Figure 5-1, most of the test results are located below the interaction curve (equation (5.4)). Most of the (V_t/V_n) ratios are smaller than 0.6 whereas the (M_t/M_n) ratios range from 0.6 to 1, which indicates that shear has less effect than bending.

As shown in Figure 4-7, when two identical purlins lap together, the purlins cannot nest properly. The cross-section distortions are initiated once the loading is applied and forces the two purlins to fit to each other at the lapped section. The loading also causes the top flange of the upper purlin to immediately bear down to the top flange of the lower purlin. The bearing stress acting on the top flange of lower purlin is concentrated at the edge of the lapped section due to the connection rotation between the two purlins. It initiates the premature buckling of the top flange, and induces the shear buckling of the web of the lower purlin at the end of lap. Thus, the capacity of the lapped Z-shaped purlins is reduced. This is consistent with the observations that all the failures occurred in the lower purlins just outside the end of the lapped connection. Hence, new interaction equations are proposed in section 5.1.3 for checking the CFS-Z shaped purlins with vertical slotted connections subjected to combined bending and shear.

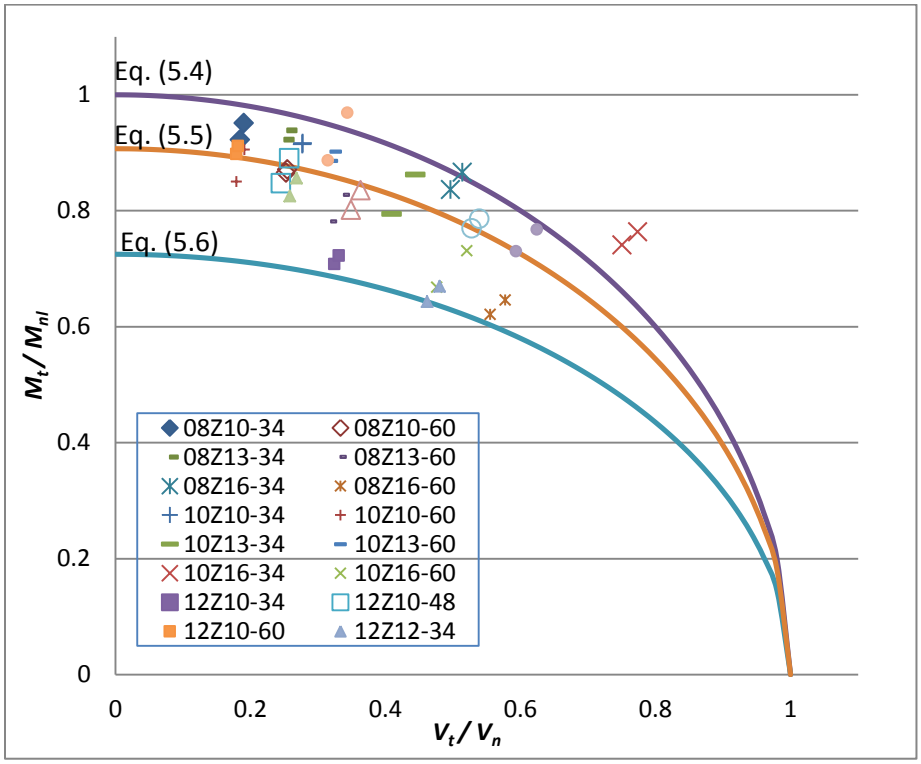

Figure 5-1 Interaction between (M_t/M_{nl}) and (V_t/V_n)

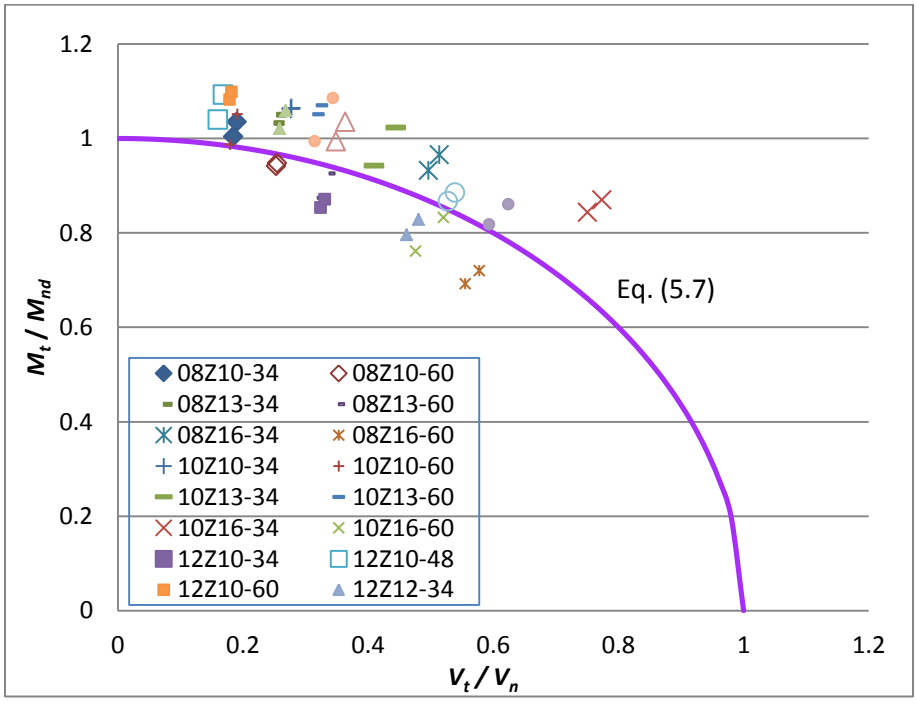

Figure 5-2 Interaction between (M_t/M_{nd}) and (V_t/V_n)

5.1.3 Proposed Interaction Equations for Checking Combined Bending and Shear

As previously discussed, the flexural capacity of the lapped Z-shaped purlin is reduced due to the presence of vertical slotted holes at the connections. Hence, two interaction equations are proposed to evaluate the member strength at the critical location based on the nominal section strength (M_{nl}) and given below:

Based on the best fit design curve:

$$\sqrt{\left(\frac{\bar{M}}{0.907M_{nl}}\right)^2+\left(\frac{\bar{V}}{V_n}\right)^2} \leq 1.0 \tag{5.5}$$

Based on the conservative design curve:

$$\sqrt{\left(\frac{\bar{M}}{0.725M_{nl}}\right)^2+\left(\frac{\bar{V}}{V_n}\right)^2} \leq 1.0 \tag{5.6}$$

Both interaction equations are plotted in Figure 5-1. Equation (5.5) is based on the best-fit curve, which fits all the test data. Equation (5.6) is more conservative and is derived using lower bound of the test data. The maximum design load (P_d) of the lapped purlins was calculated by using the two proposed equations and compared to the maximum applied load (P_t) obtained from the tests. The results are summarized in Table 5-3.

For the best-fit design, the average P_t/P_d ratio is 1.00 with a standard deviation of 0.078 and a coefficient of variance of 0.078. For the conservative design, the average P_t/P_d ratio is 1.21, with a standard deviation and coefficient of variance of 0.099 and 0.082, respectively.

Alternatively, instead of using the nominal section strength (M_{nl}), the member strength of lapped purlin can be checked with the interaction equation in term of the distortional buckling strength (M_{nd}), as shown below.

$$\sqrt{\left(\frac{\bar{M}}{M_{nd}}\right)^2+\left(\frac{\bar{V}}{V_n}\right)^2} \leq 1.0 \tag{5.7}$$

The interaction between the critical ratios (M_t/M_{nd}) and (V_t/V_n) are plotted in Figure 5-2 together with the interaction equation (5.7). The maximum design load (P_d) of the lapped purlin calculated based on equation (5.7) was compared to the maximum applied load (P_t) obtained from the tests as shown

in Table 5-3. For this alternative design approach, the average P_t/P_d ratio is 1.08, with a standard deviation of 0.074 and a coefficient of variance of 0.069.

The relationships between the test load (P_t) and the calculated design load (P_d) are plotted in Figures 5-3, 5-4 and 5-5 for all three proposed design equations. The solid line represents the ideal solution where P_t equals P_d. The two dash lines are the boundaries indicating the 15% difference from the ideal solution. For the points above the solid line, the design loads are underestimated, whereas for the points below the solid line, the design loads are overestimated.

The results indicate that equations (5.5) and (5.7) provide accurate design solutions, whereas equation (5.6) underestimates the design load and always provides more conservative solutions. In practice, distortional buckling does not play a significant role in the regions of high moment gradient where the combined bending and shear occurs (CSA, 2012). The nominal section strength (M_{nl}) should be used in the interaction equation. Consequently, in order to obtain an accurate and practical solution, the best-fit design equation (5.5) is recommended for checking CFS-Z shaped purlins with vertical slotted connections subjected to combined bending and shear.

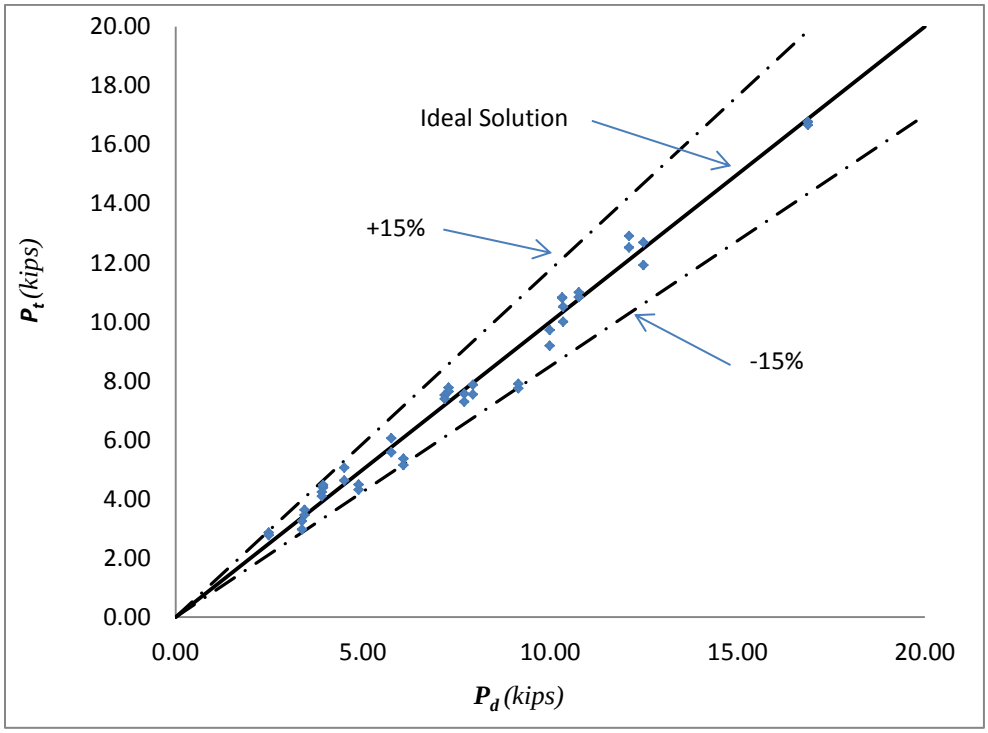

Figure 5-3 Results Comparison between Test P_t and Best Fit Design P_d (Eq. 5.5)

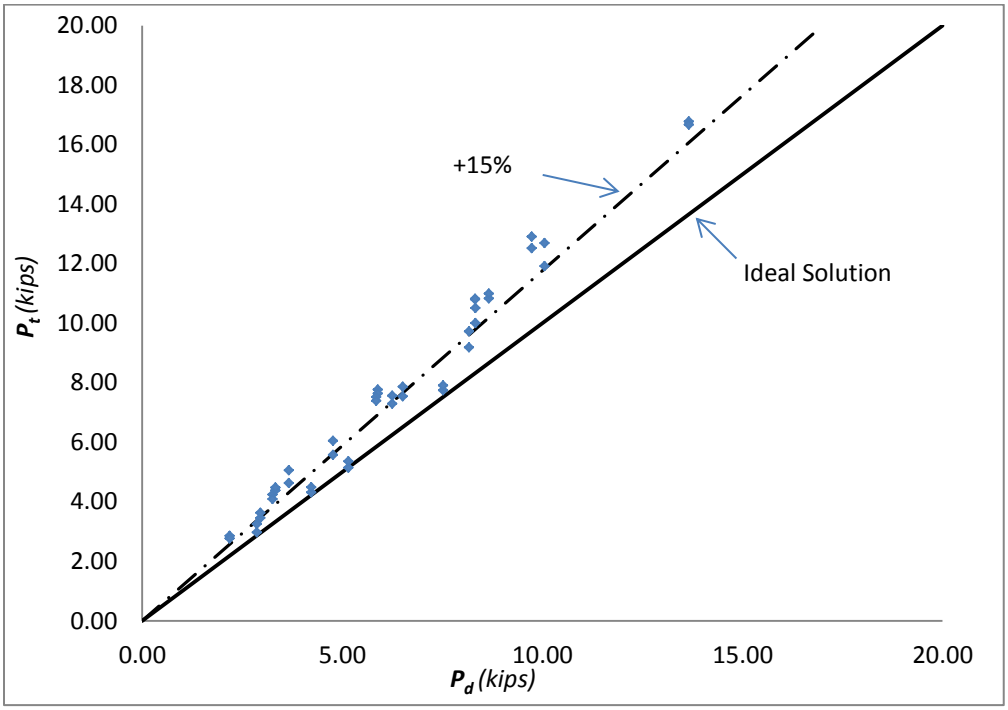

Figure 5-4 Results Comparison between Test P_t and Conservative Design P_d (Eq. 5.6)

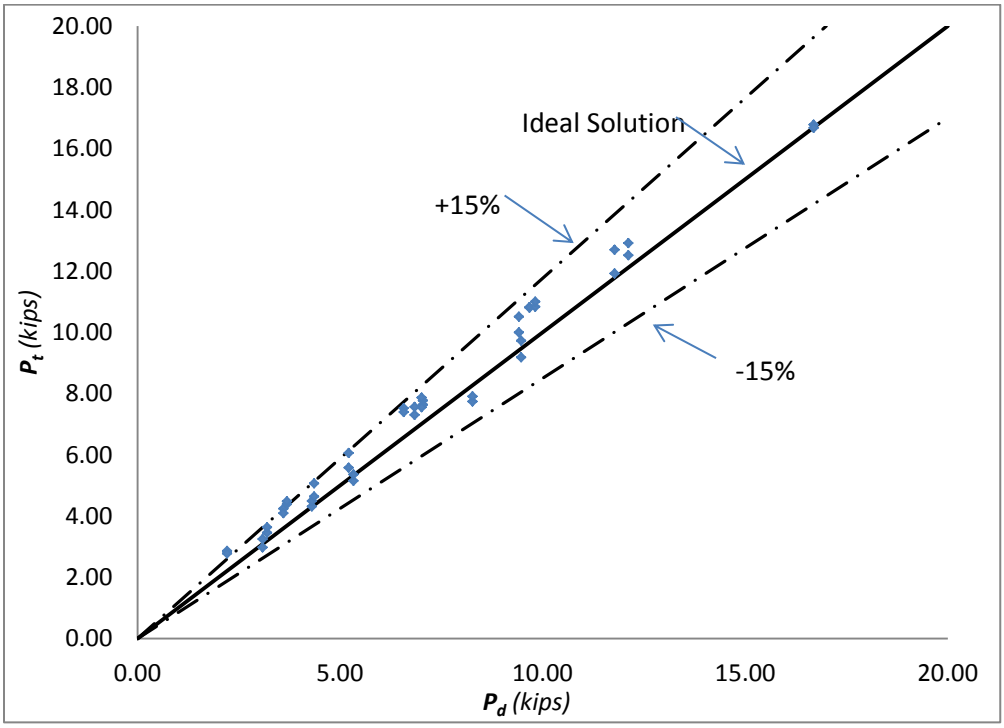

Figure 5-5 Results Comparison between Test P_t and Alternative Design P_d (Eq. 5.7)

Table 5-3 Summary of Back Calculated Design Load

Tests[1]	P_t (kip)	$\sqrt{\left(\frac{\bar{M}}{0.907M_{nl}}\right)^2+\left(\frac{\bar{V}}{V_n}\right)^2} \le 1.0$ Eq. (5.5)		$\sqrt{\left(\frac{\bar{M}}{0.725M_{nl}}\right)^2+\left(\frac{\bar{V}}{V_n}\right)^2} \le 1.0$ Eq. (5.6)		$\sqrt{\left(\frac{\bar{M}}{M_{nd}}\right)^2+\left(\frac{\bar{V}}{V_n}\right)^2} \le 1.0$ Eq. (5.7)	
		P_d (kip)	$\frac{P_t}{P_d}$	P_d (kip)	$\frac{P_t}{P_d}$	P_d (kip)	$\frac{P_t}{P_d}$
08Z10-34-1	12.91	12.11	1.07	9.73	1.33	12.12	1.06
08Z10-34-2	12.52	12.11	1.03	9.73	1.29	12.12	1.03
08Z10-60-1	16.78	16.88	0.99	13.66	1.23	16.70	1.00
08Z10-60-2	16.67	16.88	0.99	13.66	1.22	16.70	1.00
08Z13-34-1	7.77	7.29	1.07	5.89	1.32	7.05	1.10
08Z13-34-2	7.64	7.29	1.05	5.89	1.30	7.05	1.08
08Z13-60-1	9.72	9.99	0.97	8.17	1.19	9.48	1.03
08Z13-60-2	9.18	9.99	0.92	8.17	1.12	9.48	0.97
08Z16-34-1	4.24	3.91	1.08	3.26	1.30	3.61	1.17
08Z16-34-2	4.09	3.91	1.05	3.26	1.26	3.61	1.13
08Z16-60-1	4.31	4.89	0.88	4.23	1.02	4.31	1.00
08Z16-60-2	4.49	4.89	0.92	4.23	1.06	4.31	1.04
10Z10-34-1	10.80	10.32	1.05	8.32	1.30	9.68	1.12
10Z10-34-2	10.82	10.32	1.05	8.32	1.30	9.68	1.12
10Z10-60-1	12.69	12.49	1.02	10.05	1.26	11.78	1.08
10Z10-60-2	11.92	12.49	0.95	10.05	1.19	11.78	1.01
10Z13-34-1	6.05	5.77	1.05	4.77	1.27	5.22	1.16
10Z13-34-2	5.58	5.77	0.97	4.77	1.17	5.22	1.07
10Z13-60-1	7.52	7.19	1.05	5.85	1.29	6.58	1.14
10Z13-60-2	7.39	7.19	1.03	5.85	1.26	6.58	1.12
10Z16-34-1	2.85	2.50	1.14	2.18	1.31	2.22	1.29
10Z16-34-2	2.77	2.50	1.11	2.18	1.27	2.22	1.25
10Z16-60-1	2.97	3.38	0.88	2.86	1.04	3.10	0.96
10Z16-60-2	3.25	3.38	0.96	2.86	1.14	3.10	1.05

Metric Conversion: 1 kip = 4.448 kN

[1] Test designation: for example, 08Z13-34-2 denotes the second test for 8-inch (203mm) Z-shaped purlins with 13 gauge (0.09 inch or 2.286mm) thickness at 34-inch (0.864m) length of lapped connections.

Table 5-3 cont. Summary of Back Calculated Design Load

Tests[1]	P_t (kip)	$\sqrt{\left(\frac{\bar{M}}{0.907M_{nl}}\right)^2+\left(\frac{\bar{V}}{V_n}\right)^2} \le 1.0$ Eq. (5.5)		$\sqrt{\left(\frac{\bar{M}}{0.725M_{nl}}\right)^2+\left(\frac{\bar{V}}{V_n}\right)^2} \le 1.0$ Eq. (5.6)		$\sqrt{\left(\frac{\bar{M}}{M_{nd}}\right)^2+\left(\frac{\bar{V}}{V_n}\right)^2} \le 1.0$ Eq. (5.7)	
		P_d (kip)	$\frac{P_t}{P_d}$	P_d (kip)	$\frac{P_t}{P_d}$	P_d (kip)	$\frac{P_t}{P_d}$
12Z10-34-1	7.74	9.16	0.85	7.52	1.03	8.27	0.94
12Z10-34-2	7.90	9.16	0.86	7.52	1.05	8.27	0.95
12Z10-48-1	10.00	10.35	0.97	8.32	1.20	9.42	1.06
12Z10-48-2	10.51	10.35	1.01	8.32	1.26	9.42	1.12
12Z10-60-1	10.83	10.77	1.01	8.66	1.25	9.83	1.10
12Z10-60-2	10.99	10.77	1.02	8.66	1.27	9.83	1.12
12Z12-34-1	5.15	6.08	0.85	5.15	1.00	5.34	0.96
12Z12-34-2	5.36	6.08	0.88	5.15	1.04	5.34	1.00
12Z12-48-1	7.54	7.94	0.95	6.51	1.16	7.02	1.08
12Z12-48-2	7.86	7.94	0.99	6.51	1.21	7.02	1.12
12Z12-60-1	7.29	7.71	0.95	6.25	1.17	6.85	1.07
12Z12-60-2	7.56	7.71	0.98	6.25	1.21	6.85	1.11
12Z14-34-1	3.45	3.45	1.00	2.95	1.17	3.21	1.08
12Z14-34-2	3.63	3.45	1.05	2.95	1.23	3.21	1.13
12Z14-48-1	4.38	3.95	1.11	3.33	1.32	3.70	1.09
12Z14-48-2	4.48	3.95	1.13	3.33	1.35	3.70	1.07
12Z14-60-1	4.63	4.51	1.03	3.67	1.26	4.36	1.06
12Z14-60-2	5.06	4.51	1.12	3.67	1.38	4.36	1.16
		Mean	1.00	Mean	1.21	Mean	1.08
		Std. Dev.	0.078	Std. Dev.	0.099	Std. Dev.	0.074
		COV	0.078	COV	0.082	COV	0.069

Metric Conversion: 1 kip = 4.448 kN

[1] Test designation: for example, 08Z13-34-2 denotes the second test for 8-inch (203mm) Z-shaped purlins with 13 gauge (0.09 inch or 2.286mm) thickness at 34-inch (0.864m) length of lapped connections.

5.2 Proposed Design Equation for Evaluating the Effective Flexural Rigidity Ratio

The mid-span deflections obtained from one-point load tests of the lapped purlins with vertical slotted holes were found to be larger than that of the lapped purlins with standard holes. The increase in the mid-span deflection is mainly caused by the increased rotations at the connections due to the presence of vertical slotted holes. The effective flexural rigidity ratio (α) (Ho and Chung 2005), defined as the flexural rigidity at the lapped section over the continued section, was used to evaluate the stiffness of the lapped connections. Once α is determined, the stiffness of the connection can be determined. Thus, the vertical deflection can be calculated for a given service load level. Therefore, α is a key parameter for estimating the vertical deflection of the lapped purlins.

As discussed in section 4.4.3, the effective flexural rigidity ratio (α) was found to be directly related to the lap length to section depth ratio (L_p/D) and the lap length to thickness ratio (L_p/t). Therefore, equation (5.8) for evaluating the effective flexural rigidity α is proposed based on these two parameters and shown below.

$$\alpha = 0.0115\left(\frac{L_p}{D}\right)^{0.597}\left(\frac{L_p}{t}\right)^{0.496} \tag{5.8}$$

where L_p is the lap length of the two connected CFS Z-sections, D is the section depth of the CFS Z-section, and t is the thickness of the CFS Z-section.

The empirical equation (5.8) was determined based on a regression analysis conducted by using MATLAB (MATLAB, 2009). The curve fitting coefficients were determined based on the mid-span deflections from 42 one-point load tests on the lapped CFS Z-shaped purlins with vertical slotted holes conducted in this investigation. Parametric studies were also performed. The section depth to thickness ratio (D/t) and the lap length to span ratio (L_p/L_t) were found to not have significant impacts on the flexural rigidity ratio. Therefore, neither ratio was included in the empirical equation. The predicted flexural rigidity ratio, denoted as α_d, was calculated directly from equation (5.8), then the predicted mid-span deflection (Δ_d) was calculated based on α_d by using equation (D.1) in Appendix D. The results were compared to the measured deflection (Δ_t) and are summarized in Table 5-4. It should be noted that the average value of two identical tests was used for the comparison, and all deflections were conducted at service load level, which is 60% of the ultimate load of non-lapped purlins.

Table 5-4 Predicted Effective Flexural Rigidity Ratio and Deflection

Test[1]	α_t	α_d	Δ_t(in.)	Δ_d(in.)	$\frac{\alpha_t}{\alpha_d}$	$\frac{\Delta_t}{\Delta_d}$
08Z10-34	0.408	0.396	0.702	0.719	1.030	0.977
08Z10-60	0.716	0.759	0.502	0.476	0.943	1.054
08Z13-34	0.356	0.485	0.694	0.544	0.735	1.274
08Z13-60	0.635	0.928	0.495	0.353	0.684	1.403
08Z16-34	0.428	0.593	0.595	0.466	0.722	1.278
08Z16-60	1.019	1.135	0.323	0.295	0.898	1.096
10Z10-34	0.329	0.347	1.218	1.175	0.949	1.037
10Z10-60	0.764	0.664	0.776	0.862	1.150	0.900
10Z13-34	0.357	0.424	1.050	0.934	0.841	1.124
10Z13-60	0.946	0.812	0.606	0.676	1.165	0.897
10Z16-34	0.558	0.519	0.730	0.762	1.075	0.958
10Z16-60	1.059	0.993	0.519	0.542	1.066	0.957
12Z10-34	0.305	0.311	1.645	1.624	0.980	1.013
12Z10-48	0.596	0.463	1.189	1.394	1.287	0.853
12Z10-60	0.747	0.596	1.091	1.267	1.254	0.861
12Z12-34	0.328	0.352	1.597	1.528	0.931	1.045
12Z12-48	0.645	0.524	1.081	1.226	1.230	0.882
12Z12-60	0.856	0.675	1.020	1.184	1.268	0.861
12Z14-34	0.354	0.416	1.092	0.993	0.850	1.099
12Z14-48	0.751	0.619	0.866	0.966	1.212	0.897
12Z14-60	0.745	0.798	0.796	0.763	0.935	1.043
				Mean	1.010	1.024
				Std. Dev.	0.187	0.151
				COV	0.185	0.147

Correlation (α_t, α_d):	0.866
Correlation (Δ_t, Δ_d):	0.961

Metric Conversion: 1 in. = 25.4mm,

[1] Test designation: for example, 08Z13-34 denotes the test for 8-inch (203mm) Z-shaped purlins with 13 gauge (0.09 inch or 2.286mm) thickness at 34-inch (0.864m) length of lapped connections.

The α_t/α_d and Δ_t/Δ_d ratios are used to compare the test results and the predicted results. The average α_t/α_d ratio is 1.010, with a standard deviation of 0.187 and a coefficient of variance of 0.185. The average Δ_t/Δ_d ratio is 1.024, with a standard deviation of 0.151 and coefficient of variance of 0.147. The results show that both the predicted α_d and Δ_d are close to the test results. Even though that the correlation coefficient of α_t and α_d is 0.866, the correlation coefficient of Δ_t and Δ_d is 0.961.

The relationship between the test and predicted deflection is plotted in Figure 5-6. The solid line represents the ideal solution where the predicted deflection is the same as the measured deflection. The two dashed lines are the boundaries indicating the 15% difference from the ideal solution. For the points above the solid line, the predicted values are less than the test results, implying that the deflections are underestimated. For the points below the solid line, the predicted values are larger than the test results, implying that the deflections are overestimated. The results show that most of the data is within the 15% of the ideal solution, except for a few points that are very close to the boundary lines. Consequently, the flexural rigidity ratio (α) could be directly obtained from the proposed equation (5.8) and used in determining the stiffness and the deflection of the lapped purlins with vertical slotted holes at the service load level (60% of the ultimate load).

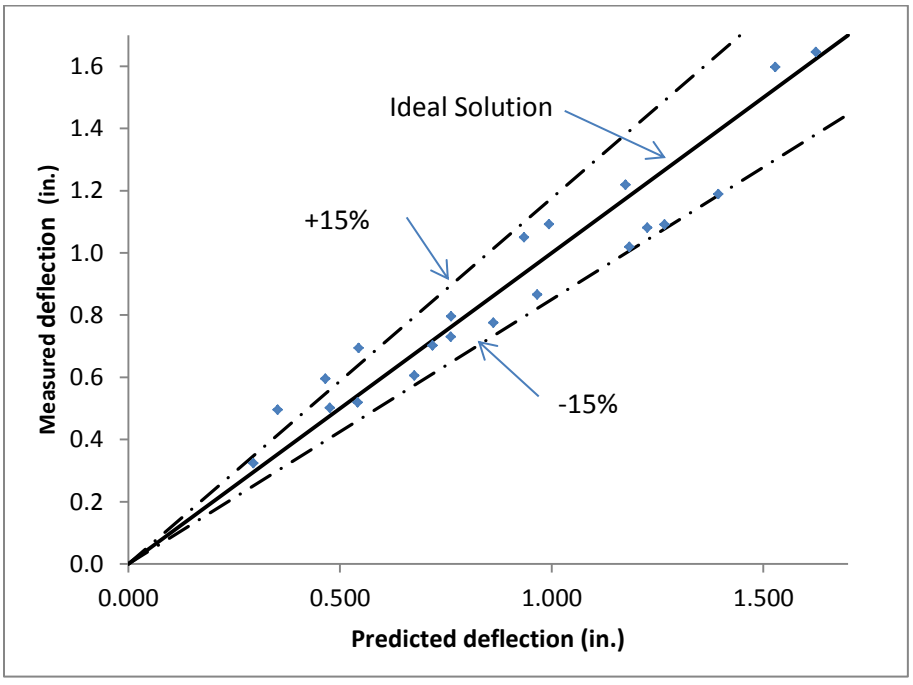

Figure 5-6 Comparison of the predicted and the measured deflection

Chapter 6
Conclusion and Recommendations

In order to investigate the structural performance of the lapped connections with vertical slotted holes, 54 laterally restrained one-point load tests were performed on CFS Z-shaped purlins, including six tests on non-lapped purlins, six tests on the lapped purlins with round holes at connections, and 42 tests on the lapped purlins with vertical slotted holes at connections. The flexural strength and the deflection of the purlins in each test were examined in detail. The characteristics of moment resistance and flexural stiffness of the purlins were calculated. Based on the test results and the analysis, the following conclusions were reached.

For the flexural strength of lapped purlins:

- The section failure in all tests occurred just outside the end of the lapped connection due to combined shear and bending.
- The sections within the lap are not critical in terms of the shear and the combined shear and bending due to the mutual restraint of the connected webs and the restraint of the rafter connection. The shear yielding at the cross-section with vertical slotted holes and the bearing deformation at the bolts holes were not observed.
- The overall load carrying capacity of Z-shaped purlins is enhanced by the lapped connection. Using the round holes or vertical slotted holes at the lapped connections does not have a significant impact on the enhancement of the load carrying capacity.
- The moment resistance of the lapped purlins with vertical slotted connections is dependent on the ratio of lap length to purlin depth. In order to achieve the full flexural strength of continuous purlins, the lap length of the connections should be at least 3.0 times of the purlin depth. The suggested minimum lap length to section depth ratio of 3.0 indicated in CSA S136-2012 (CSA 2012) was verified. The moment resistance of the lapped purlins is also dependent on the ratio of lap length to purlin depth. The maximum purlin depth to purlin web thickness ratio should be limited to 155 when designing the lapped connection with slotted holes. For the reason of being conservative, the minimum lap length to purlin depth ratio and the maximum purlin depth to purlin web thickness ratio may also be considered as 3.7 and 135 respectively.

- The critical section of the failure is found at the end of lap on the lower member of the two lapped purlins. The flexural strength of the critical section is reduced due to the initial cross-section distortion and the concentrated bearing stress from the upper purlins at the edge of the slotted connection. The traditional interaction equation (5.4) for checking the section subjected to combined bending and shear may not be applicable for the CFS-Z shaped purlins with vertical slotted connections. Therefore, new interaction equations are proposed. Among the three proposed equations, the best-fit design equation (5.5) fits all the test results and provides the most accurate design solutions, and it is recommended for checking the section capacity of CFS-Z shaped purlins with vertical slotted connections subjected to combined bending and shear.

For the flexural stiffness of lapped purlins:

- The presence of vertical slotted holes at lapped connections results in a substantial increase in the connection flexibility. Consequently, the presence of vertical slotted holes considerably reduces the flexural stiffness of lapped purlins in contrast to that of round holes.
- The effective flexural rigidity ratio, a parameter introduced to account for the effect of the slotted connections on the purlin stiffness, is related to the ratio of lap length to purlin depth and the ratio of lap length to purlin web thickness. In order to achieve the full flexural stiffness of continuous purlins, the lap length of the connection should be at least 7.7 times the purlin depth, and the lap length to purlin thickness ratio should be equal to or greater than 935.
- A design equation is proposed for determining the flexural rigidity ratio of lapped purlins with slotted connections. The flexural rigidity ratio is used to calculate the stiffness of the lapped purlins as well as the vertical deflection at the service load level (60% of the ultimate load).

6.1 Recommendations for Future Research

Based on the findings of this study, the following recommendations for future work are proposed:

1. Additional tests should be performed on non-lapped purlins. The test results should be used as baselines instead of the theoretical values for comparing with the structural behaviour of lapped purlins with vertical slotted holes.

2. A finite element analysis model should be developed to efficiently simulate the structural behaviour of lapped purlins with slotted connections. The numerical investigations could be verified by experimental tests. The proposed model should characterize the moment resistance and the flexural stiffness of the slotted connection, and describe how the joint provides purlin continuity.

3. Additional investigations should be carried out on lapped purlins under other types of loadings such as uniform distributed loads to compare with and to verify the findings from one-point load tests and the proposed design recommendations.

4. The findings from the simplified analysis method under one point load tests should be further calibrated and the proposed design recommendations should be adopted to evaluate the structural performances of multi-span purlin systems subjected to uniform distributed load.

Bibliography

AISI. (2012). *North American Specification for the Design of Cold-Formed Steel Structural Members AISI S100-2012*. Washington, D.C.: American Iron and Steel Institute.

ArcelorMittal. (2008). *12 Inch & 8 Inch Z Lapped Purlins Load versus Deflection Testing*. Hamilton, Ontario: ArcelorMittal – Dofasco.

ASTM. (2012). *Standard Test Methods and Definitions for Mechanical Testing of Steel Products (A370)*. West Conshohocken, P.A.: American Society for Testing and Materials.

ASTM. (2011). *Standard Test Methods for Tension Testing of Metallic Materials.* West Conshohocken, P.A.: American Society for Testing and Materials.

ASTM. (2009). *Standard Specification for Steel, Sheet and Strip, Hot-Rolled, Carbon, Structural, High-Strength Low-Alloy, High-Strength Low-Alloy with Improved Formability, and Ultra-High Strength (A1011/A1011M)*. West Conshohocken, P.A.: American Society for Testing and Materials.

Chung, K. F., & Ho, H. C. (2005). Analysis and design of lapped connections between cold-formed steel Z sections. Thin-Walled Structures, 43(7), 1071-1090.

CSA. (2012). *North American Specification for the Design of Cold-Formed Steel Structural Members S136-12*. Mississauga, Ontario: Canadian Standards Association.

CSA. (2004). *General Requirements for Rolled or Welded Structural Quality Steel CSA G40.20/21*. Mississauga, Ontario: Canadian Standards Association.

Dubina, D., & Ungureanu, V. (2010). *Behaviour of multi-span cold-formed Z-purlins with bolted lapped connections*. Thin-Walled Structures, 48(10-11), 866-871.

Ho, H. C., & Chung, K. F. (2004). *Experimental investigation into the structural behaviour of lapped connections between cold-formed steel Z sections*. Thin-Walled Structures, 42(7), 1013-1033.

Ho, H. C., & Chung, K. F. (2006). *Analytical prediction on deformation characteristics of lapped connections between cold-formed steel Z sections*. Thin-Walled Structures, 44(1), 115-130.

Ho, H. C., & Chung, K. F. (2006). *Structural behavior of lapped cold-formed steel Z sections with generic bolted configurations*. Thin-Walled Structures, 44(4), 466-480.

LabVIEW (2010). *Laboratory Virtual Instrument Engineering 2010*. Austin, Texas, USA: National Instruments Corporation.

Li, Z., Schafer, B.W. (2010) *"Buckling analysis of cold-formed steel members with general boundary conditions using CUFSM: conventional and constrained finite strip methods."* Proceedings of the 20th Int;l. Spec. Conf. on Cold-Formed Steel Structures, St. Louis, MO. November, 2010.

MATLAB, (2009). *Matrix Laboratory R2009b*, Natick, Massachusetts, USA: The MathWorks, Inc.

Pham, C. H., Davis, A. F., & Emmett, B. R. (2014). *Numerical investigation of cold-formed lapped Z purlins under combined bending and shear*. Journal of Constructional Steel Research, 95, 116-125

Steelway Building Systems (2009). *Steelway Building Systems Material Standard*, Aylmer, ON, Canada: Steelway Building Systems.

Zhang, L., & Tong, G. (2008). *Moment resistance and flexural rigidity of lapped connections in multi-span cold-formed Z purlin systems*. Thin-Walled Structures, 46(5), 551-560.

Appendix A
Test Specimen Drawings

University of Waterloo

PROJECT Lapped Z-purlin connections SKETCH SK001

Made by J.Liu Checked by L. Xu Date June 27, 2012 Page 1 of 5

The Canadian Cold-Formed Steel Research Group

8 inch CFS Z-purlin lapped connection

34" lap & 60 " lap

0

½" SAE J429 Grade 2 Bolts

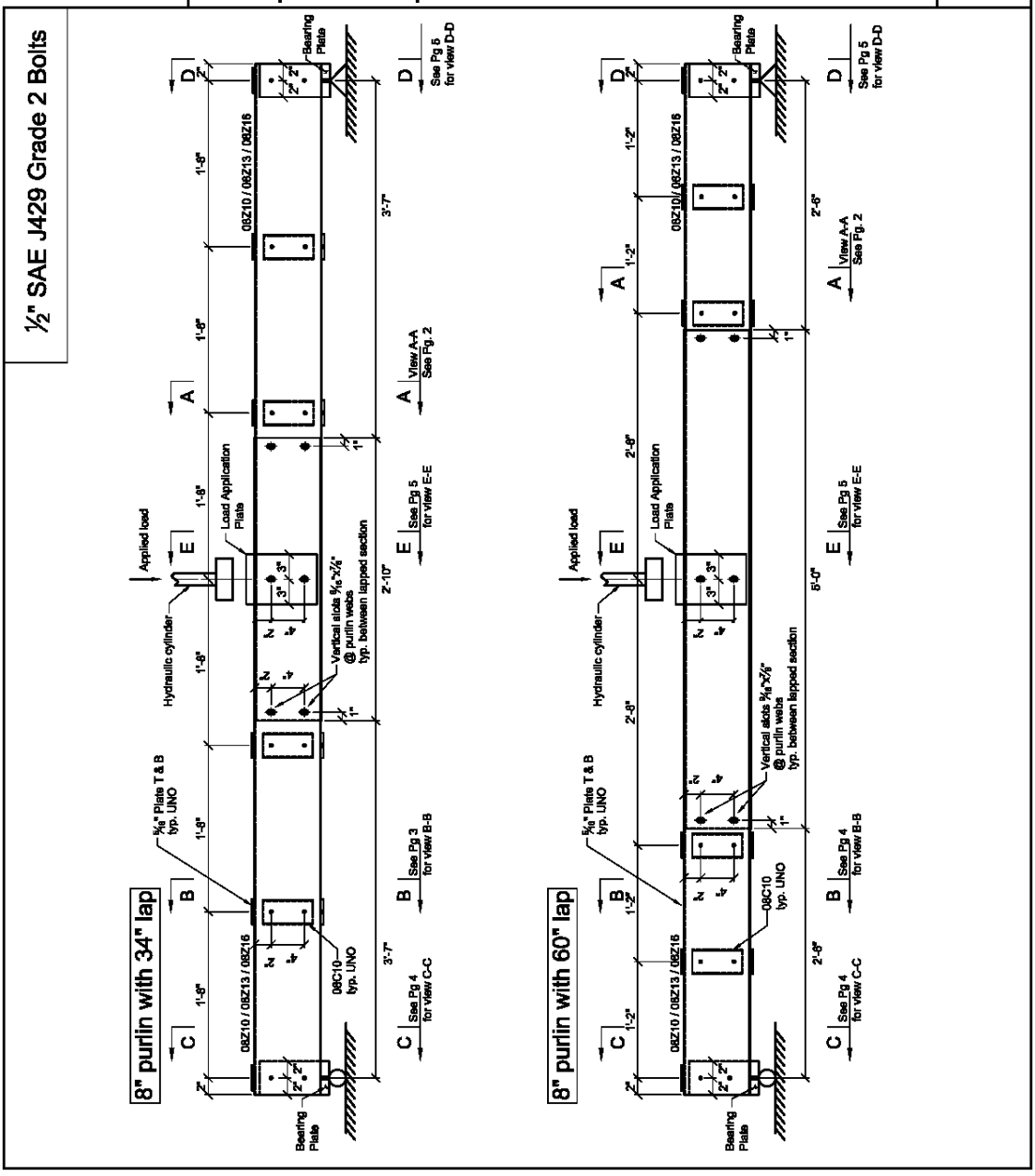

University of Waterloo

The Canadian Cold-Formed Steel Research Group

PROJECT Lapped Z-purlin connections SKETCH SK001

Made by J.Liu Checked by L. Xu Date June 27, 2012 Page 2 of 5

View A - A

0

½" SAE J429 Grade 2 Bolts

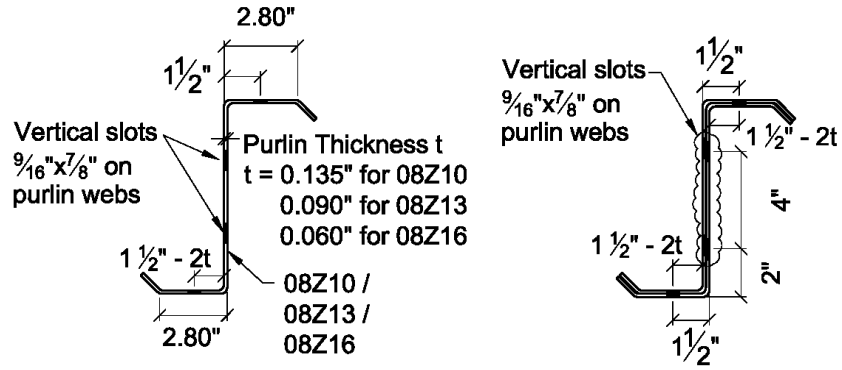

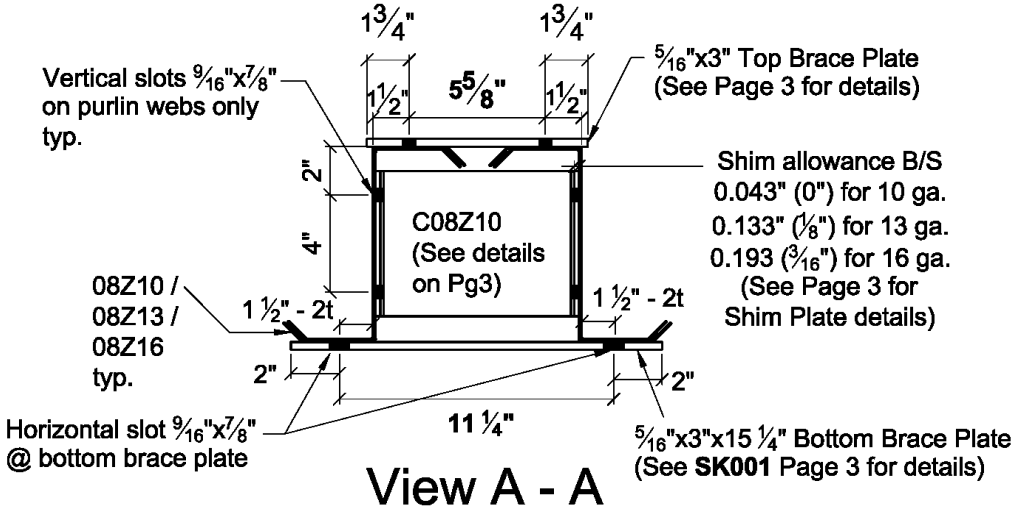

View A - A

University of Waterloo

The Canadian Cold-Formed Steel Research Group

PROJECT Lapped Z-purlin connections SKETCH SK001

Made by J.Liu Checked by L. Xu Date June 27, 2012 Page 3 of 5

Misc. details

0

½" SAE J429 Grade 2 Bolts

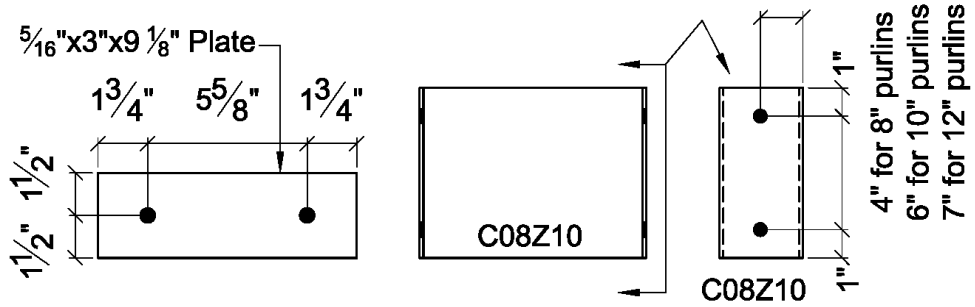

Top Brace Plate Details

Internal Brace Details

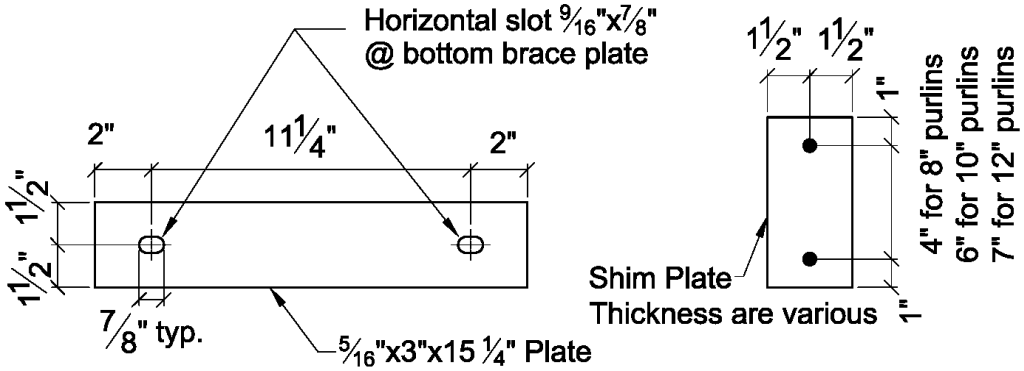

Bottom Brace Plate Details

Shim Plate Details

University of Waterloo

The Canadian Cold-Formed Steel Research Group

PROJECT Lapped Z-purlin connections SKETCH SK001

Made by J.Liu Checked by L. Xu Date June 27, 2012 Page 4 of 5

View B - B, view C - C

0

½" SAE J429 Grade 2 Bolts

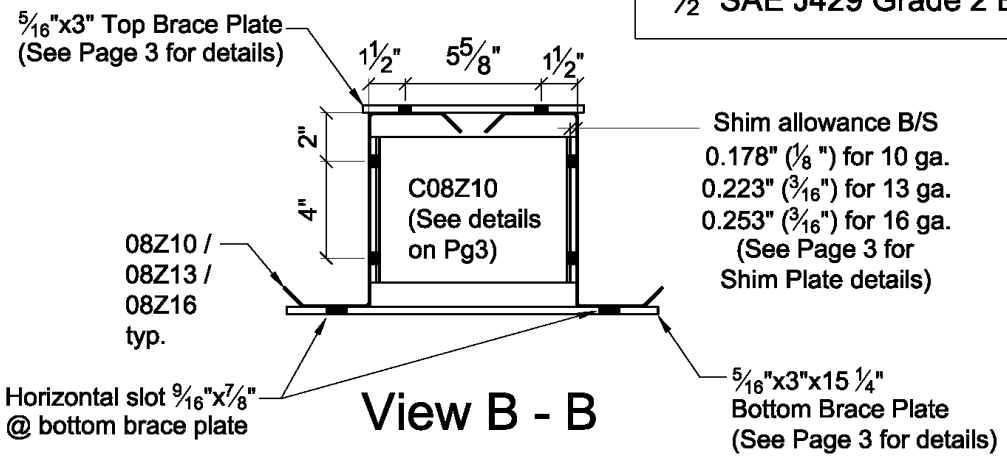

View B - B

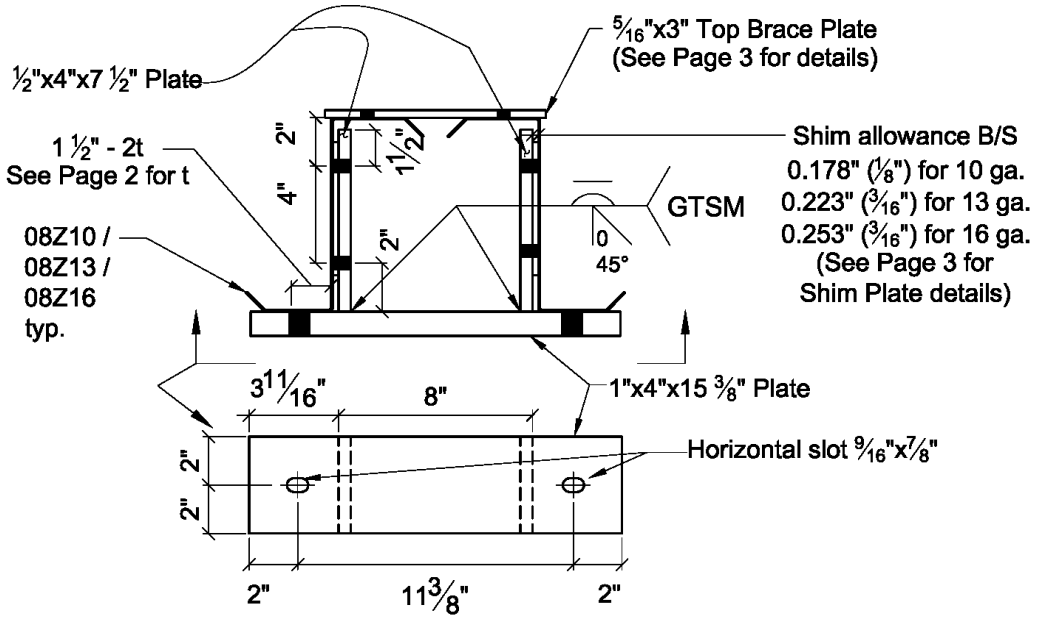

View C - C

University of Waterloo

The Canadian Cold-Formed Steel Research Group

PROJECT Lapped Z-purlin connections SKETCH SK001

Made by J.Liu Checked by L. Xu Date June 27, 2012 Page 5 of 5

View D - D, view E - E

0

½" SAE J429 Grade 2 Bolts

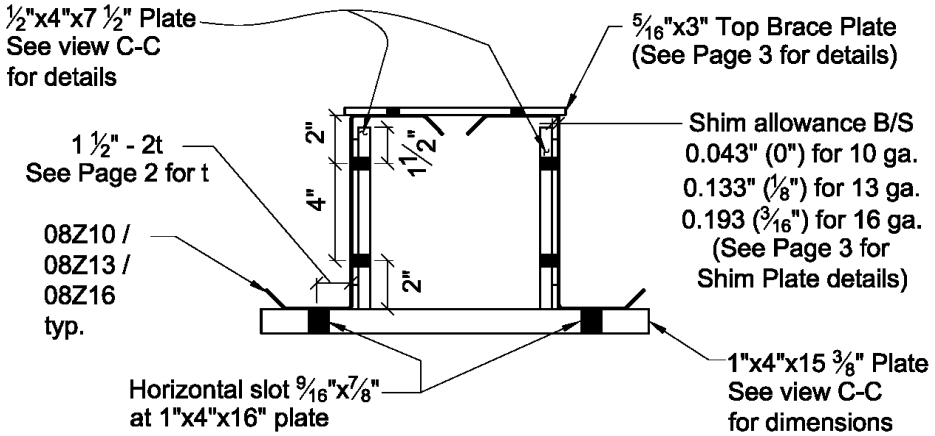

View D - D

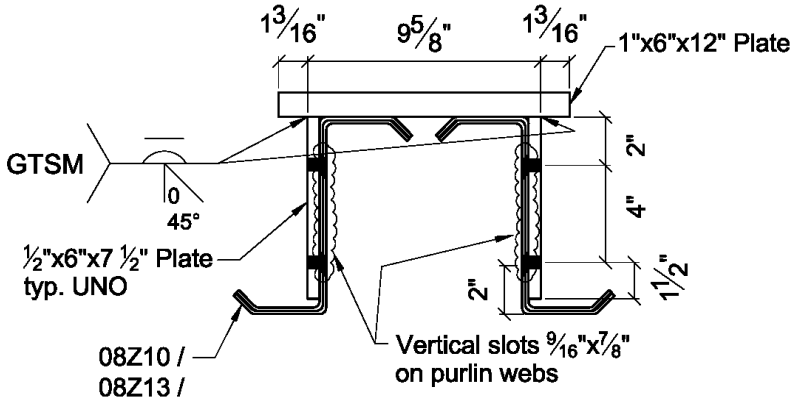

View E - E

University of Waterloo

The Canadian Cold-Formed Steel Research Group

PROJECT Lapped Z-purlin connections SKETCH SK002

Made by J.Liu Checked by L. Xu Date June 27, 2012 Page 1 of 4

10 inch CFS Z-purlin lapped connection

34" lap & 60 " lap

0

½" SAE J429 Grade 2 Bolts

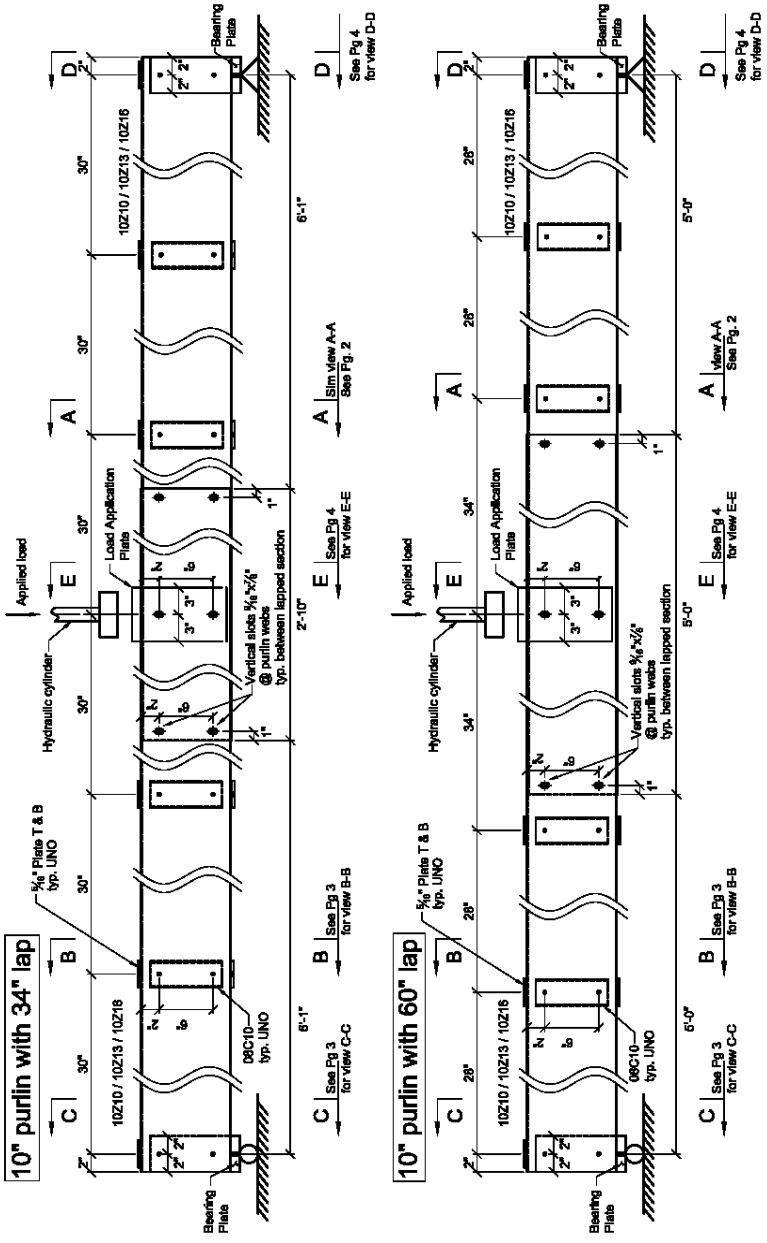

University of Waterloo

The Canadian Cold-Formed Steel Research Group

PROJECT Lapped Z-purlin connections SKETCH SK002

Made by J.Liu Checked by L. Xu Date June 27, 2012 Page 2 of 4

View A - A

0

½" SAE J429 Grade 2 Bolts

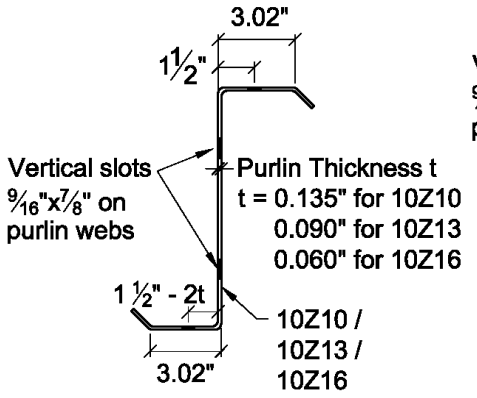

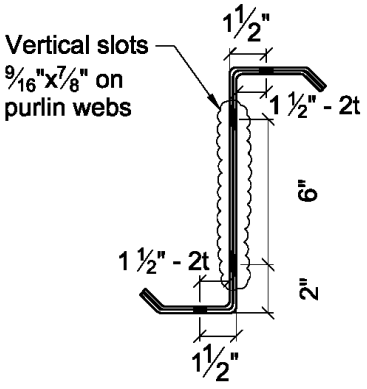

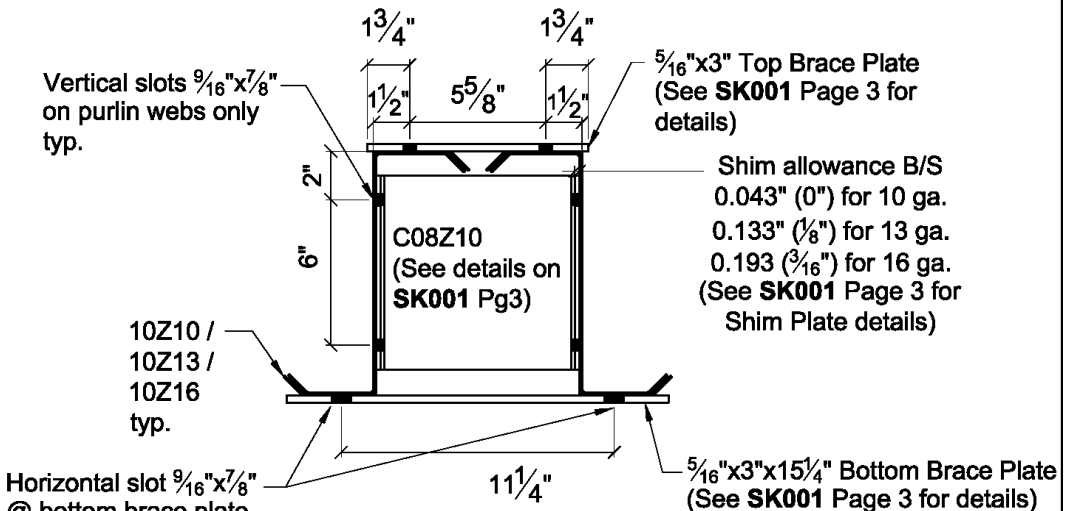

View A - A

University of Waterloo

The Canadian Cold-Formed Steel Research Group

PROJECT Lapped Z-purlin connections SKETCH SK002

Made by J.Liu Checked by L. Xu Date June 27, 2012 Page 3 of 4

View B - B, view C - C

0

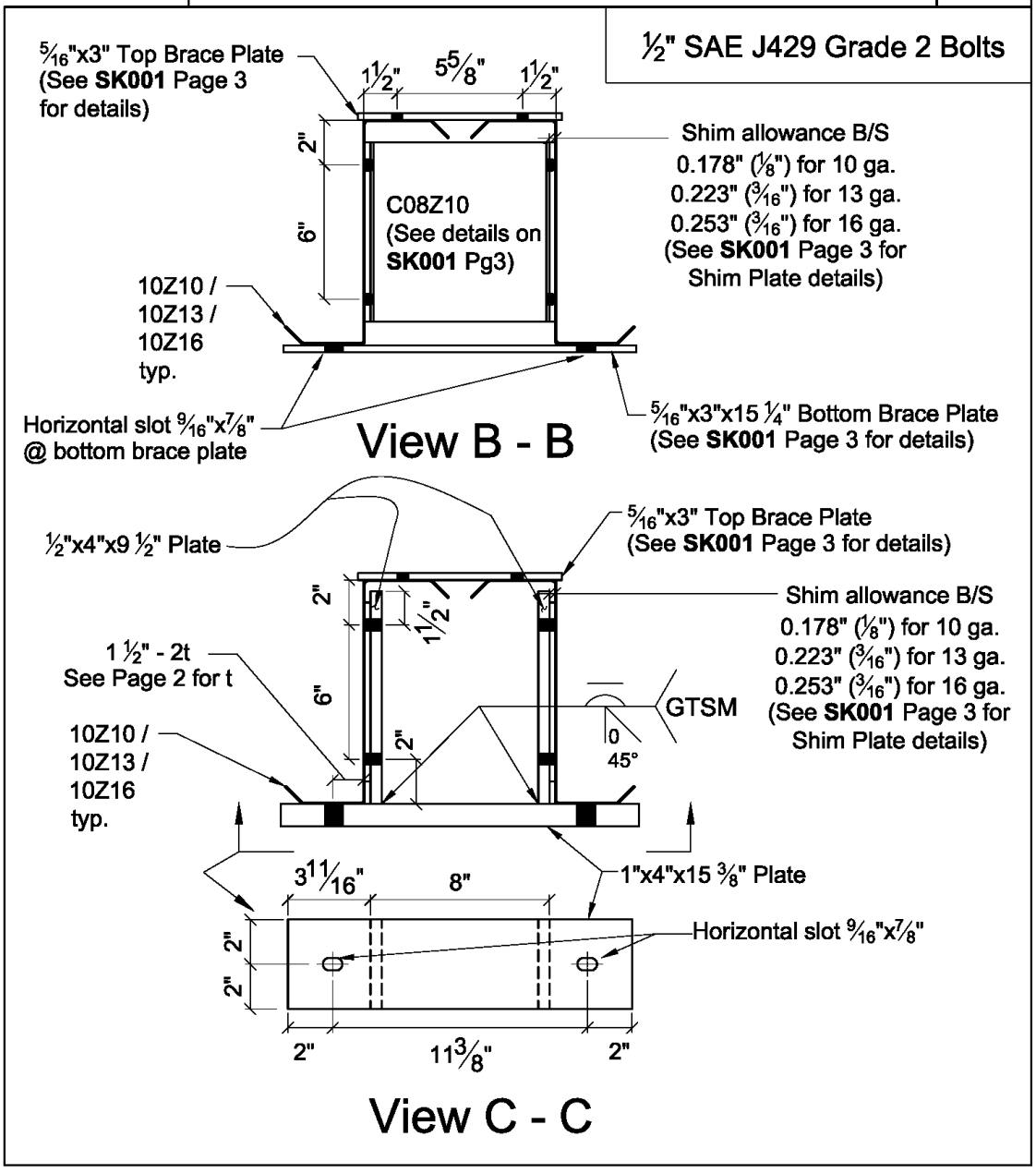

University of Waterloo

The Canadian Cold-Formed Steel Research Group

PROJECT Lapped Z-purlin connections SKETCH SK002

Made by J.Liu Checked by L. Xu Date June 27, 2012 Page 4 of 4

View D - D, view E - E

0

½" SAE J429 Grade 2 Bolts

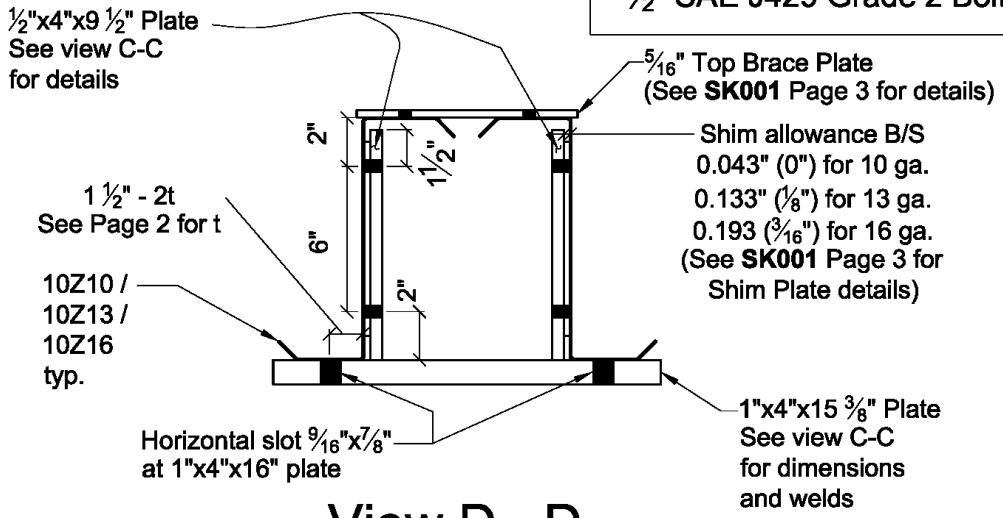

View D - D

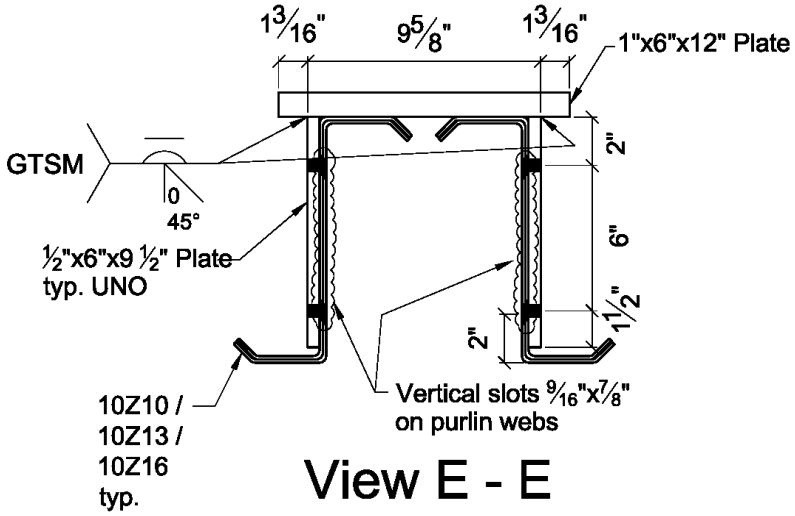

View E - E

University of Waterloo

PROJECT Lapped Z-purlin connections SKETCH SK003

Made by J.Liu Checked by L. Xu Date June 27, 2012 Page 1 of 4

The Canadian Cold-Formed Steel Research Group

12 inch CFS Z-purlin lapped connection

34" lap & 60 " lap

0

½" SAE J429 Grade 2 Bolts

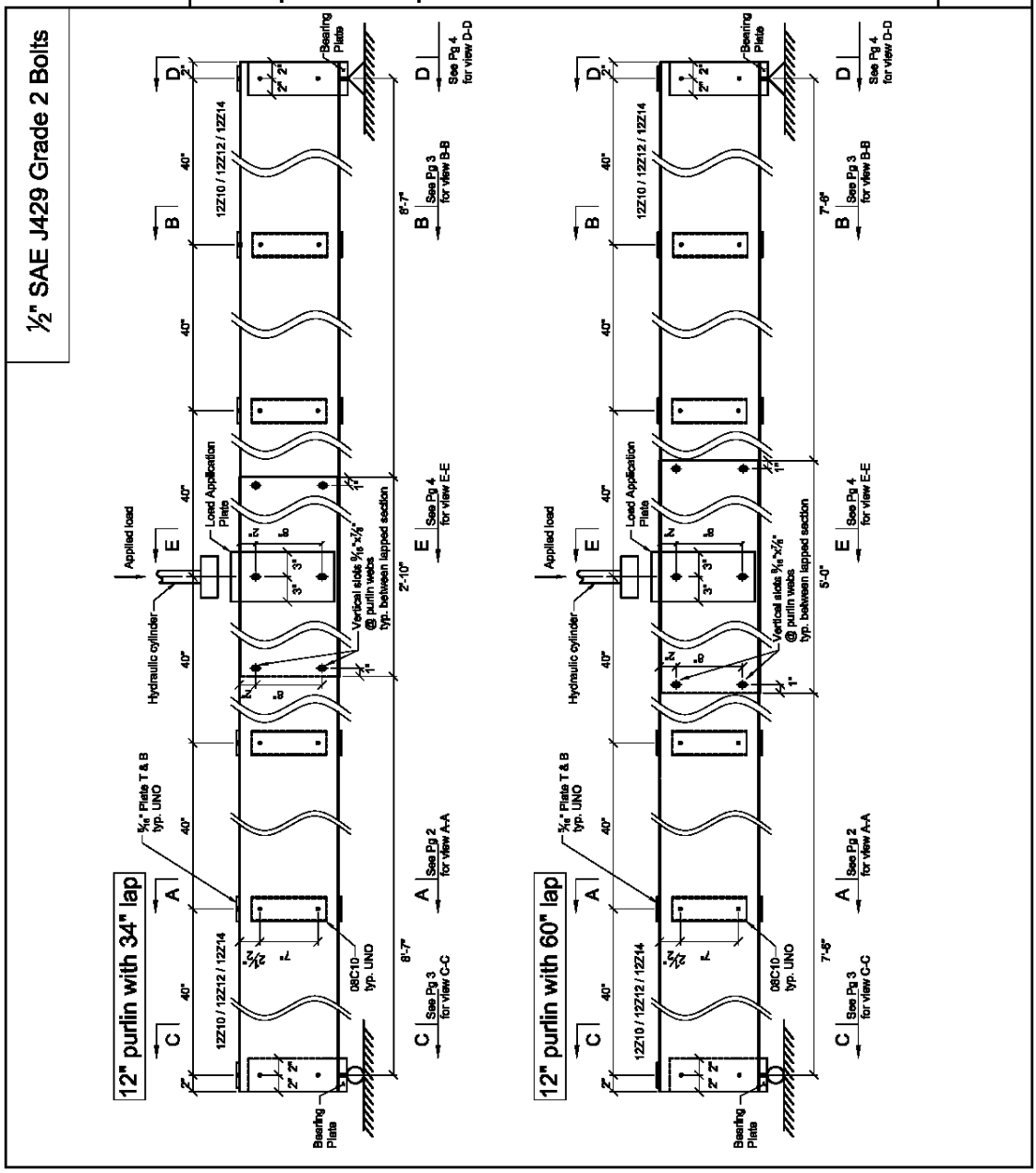

University of Waterloo

The Canadian Cold-Formed Steel Research Group

PROJECT Lapped Z-purlin connections SKETCH SK003

Made by J.Liu Checked by L. Xu Date June 27, 2012 Page 2 of 4

View A - A

0

½" SAE J429 Grade 2 Bolts

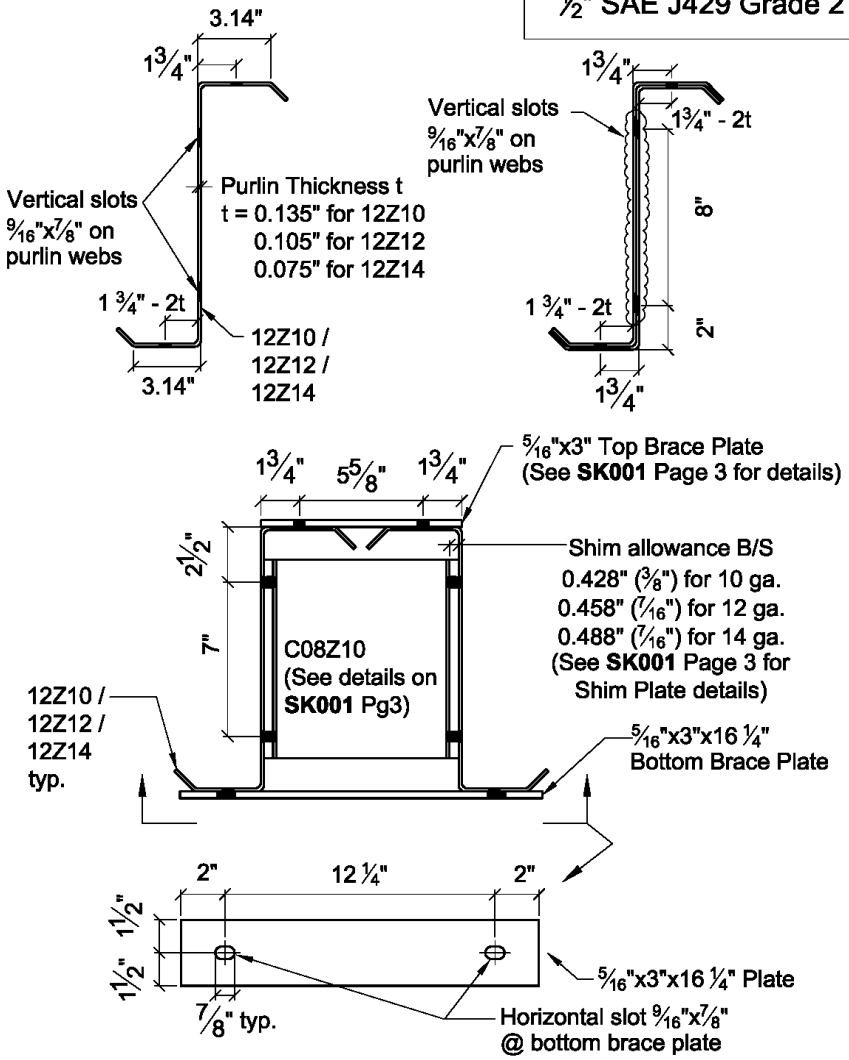

View A - A

University of Waterloo

The Canadian Cold-Formed Steel Research Group

PROJECT Lapped Z-purlin connections SKETCH SK003

Made by J.Liu Checked by L. Xu Date June 27, 2012 Page 3 of 4

View B - B, view C - C

0

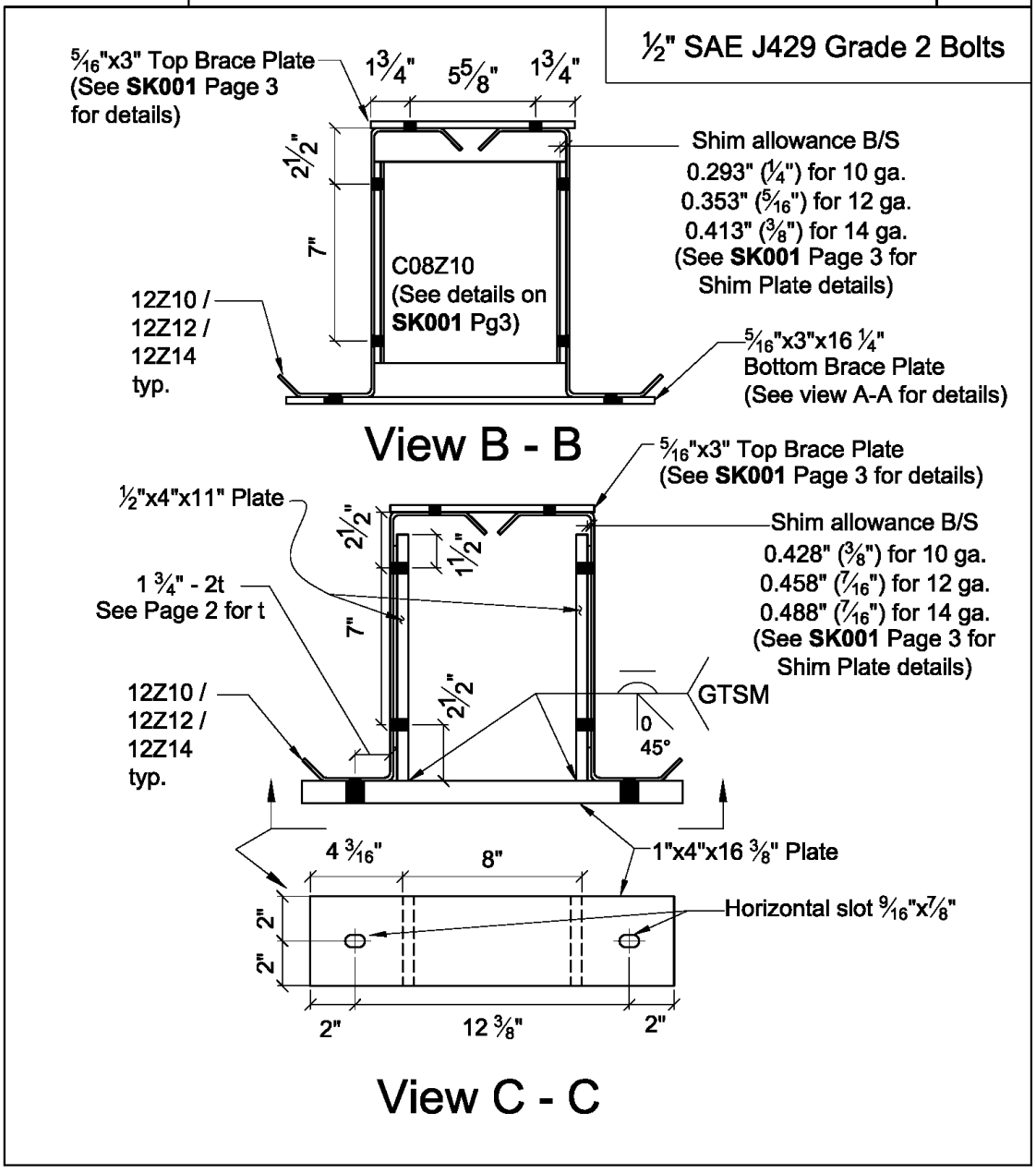

University of Waterloo

The Canadian Cold-Formed Steel Research Group

PROJECT Lapped Z-purlin connections SKETCH SK003

Made by J.Liu Checked by L. Xu Date June 27, 2012 Page 4 of 4

View D - D, view E - E

0

½" SAE J429 Grade 2 Bolts

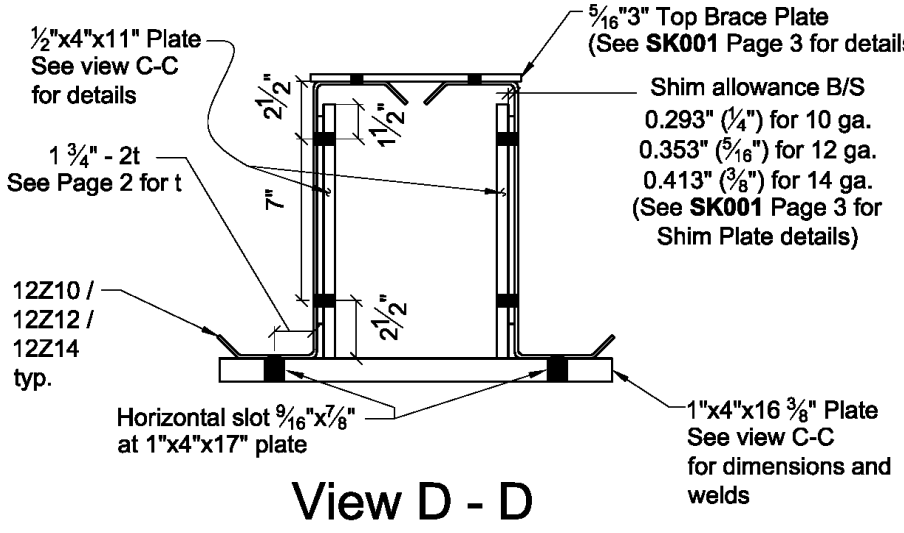

View D - D

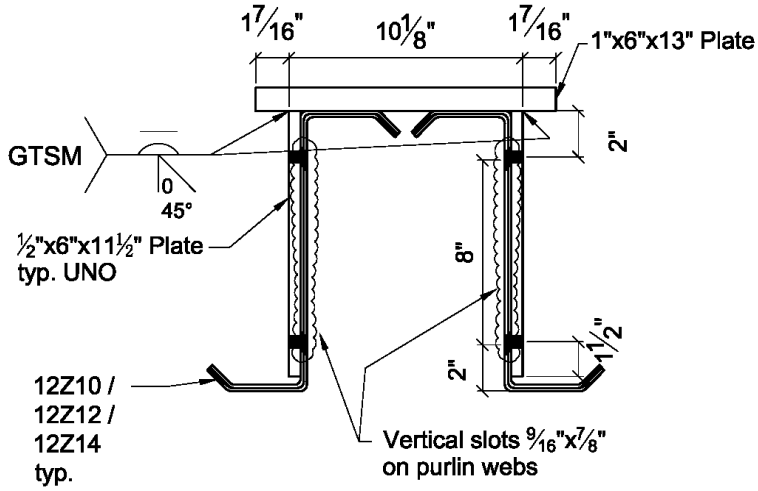

View E - E

University of Waterloo

PROJECT Lapped Z-purlin connections SKETCH SK005

Made by J.Liu Checked by L. Xu Date June 06, 2013 Page 1 of 4

The Canadian Cold-Formed Steel Research Group

12 inch CFS Z-purlin lapped connection

48" lap & no lap

0

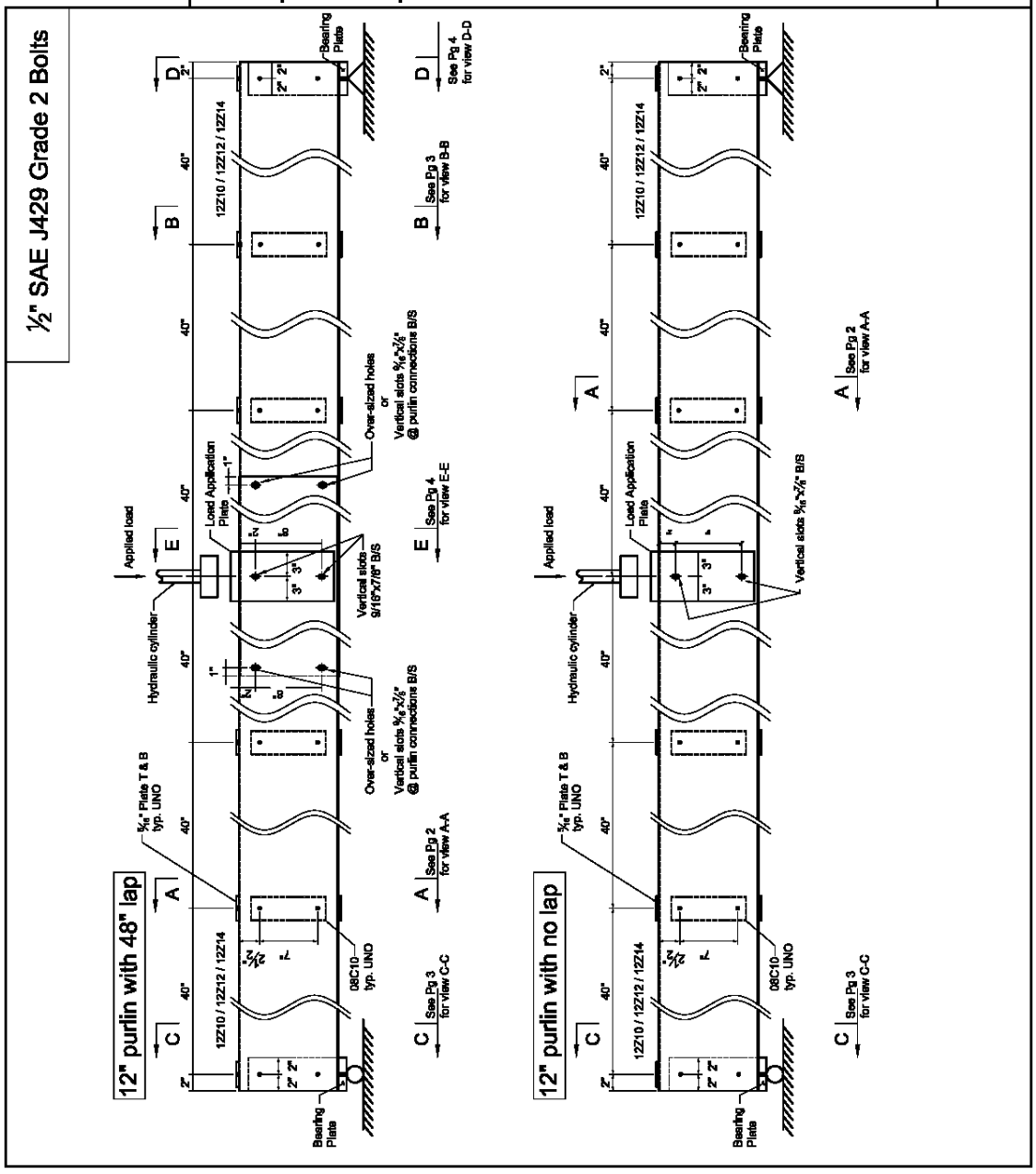

University of Waterloo

The Canadian Cold-Formed Steel Research Group

PROJECT Lapped Z-purlin connections SKETCH SK005

Made by J.Liu Checked by L. Xu Date June 06, 2013 Page 2 of 4

View A - A

0

½" SAE J429 Grade 2 Bolts

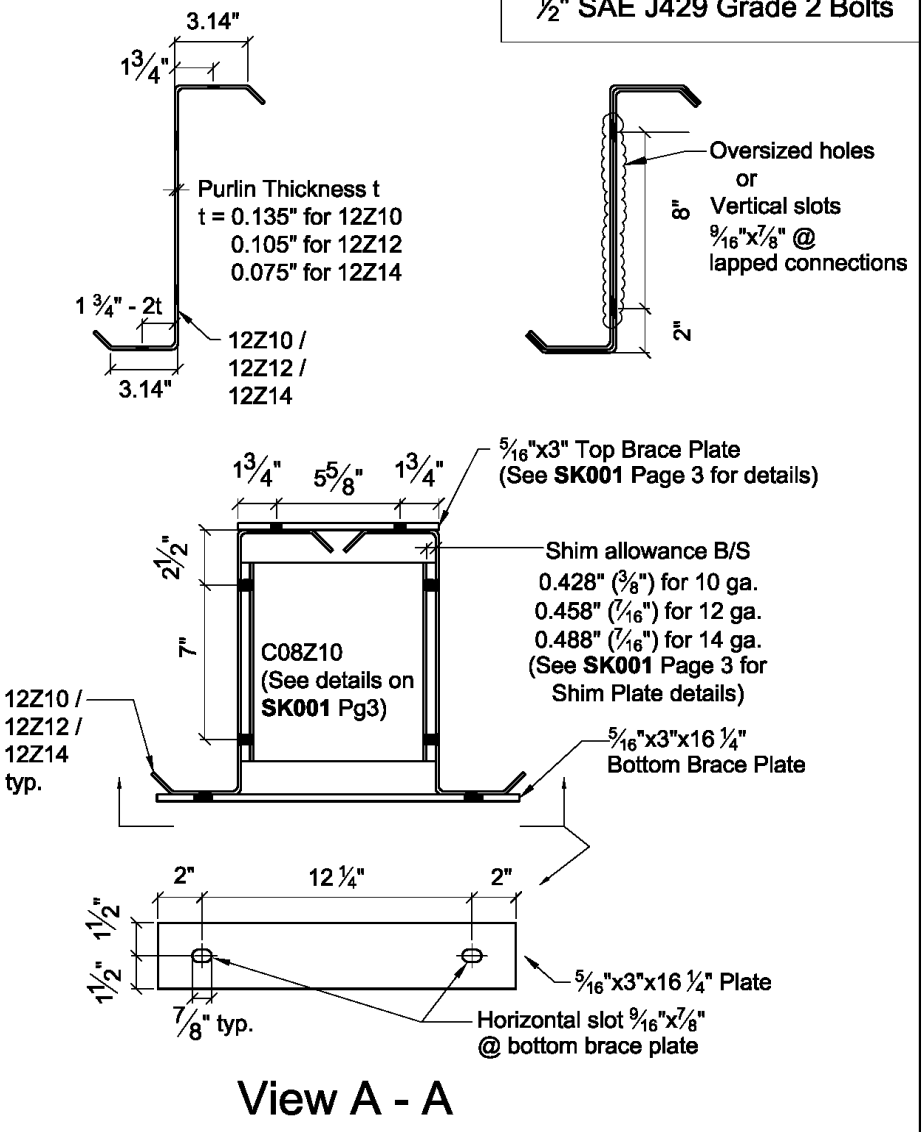

View A - A

University of Waterloo

The Canadian Cold-Formed Steel Research Group

PROJECT Lapped Z-purlin connections SKETCH SK005

Made by J.Liu Checked by L. Xu Date June 06, 2013 Page 3 of 4

View B - B, view C - C

0

½" SAE J429 Grade 2 Bolts

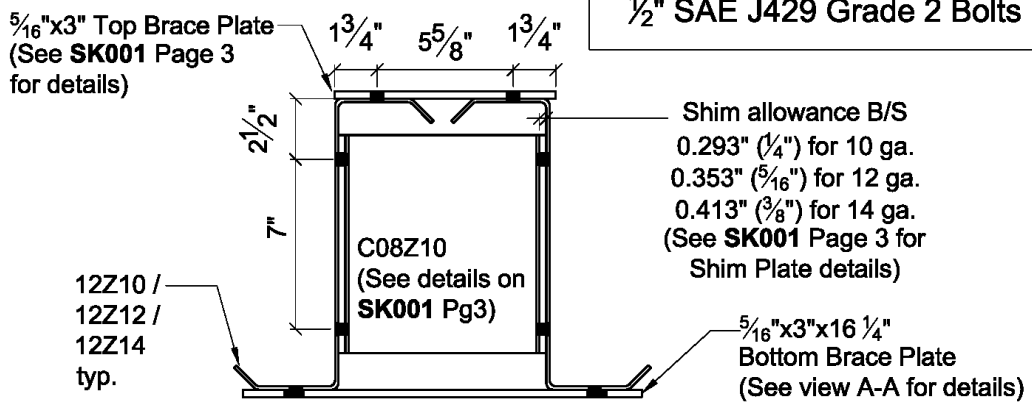

View B - B

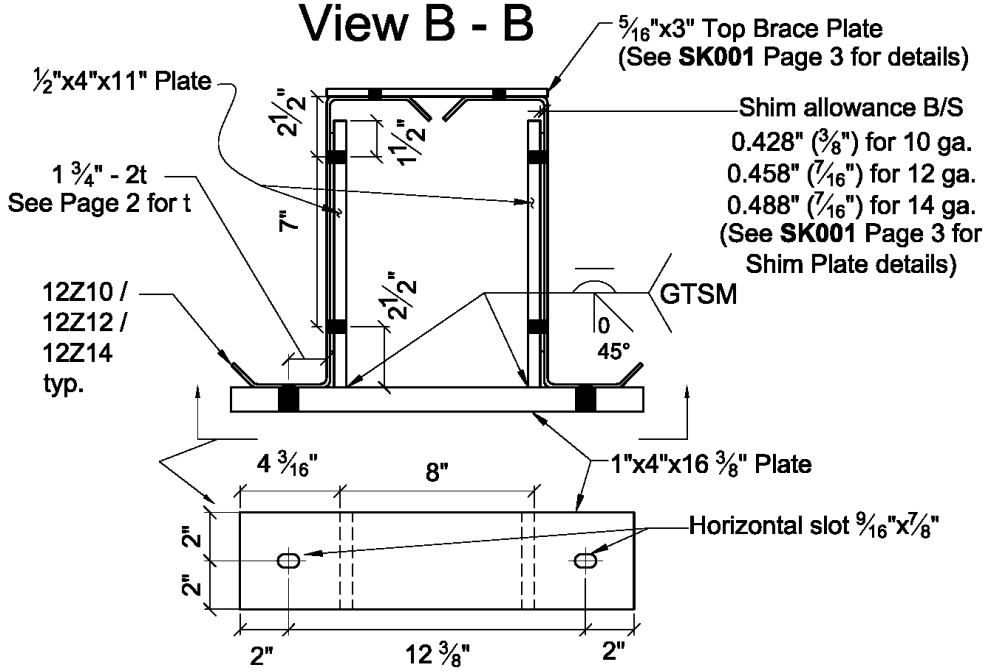

View C - C

University of Waterloo

The Canadian Cold-Formed Steel Research Group

PROJECT Lapped Z-purlin connections SKETCH SK005

Made by J.Liu Checked by L. Xu Date June 06, 2013 Page 4 of 4

View D - D, view E - E

0

½" SAE J429 Grade 2 Bolts

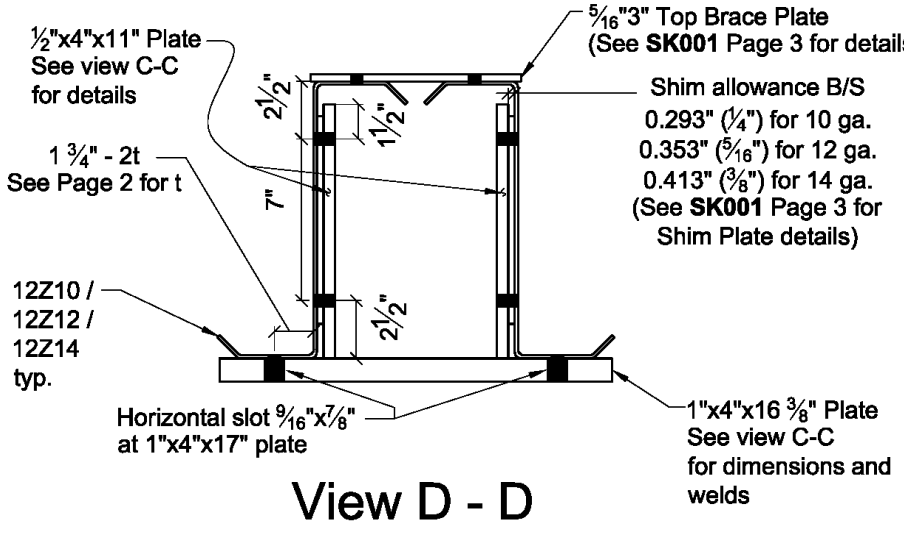

View D - D

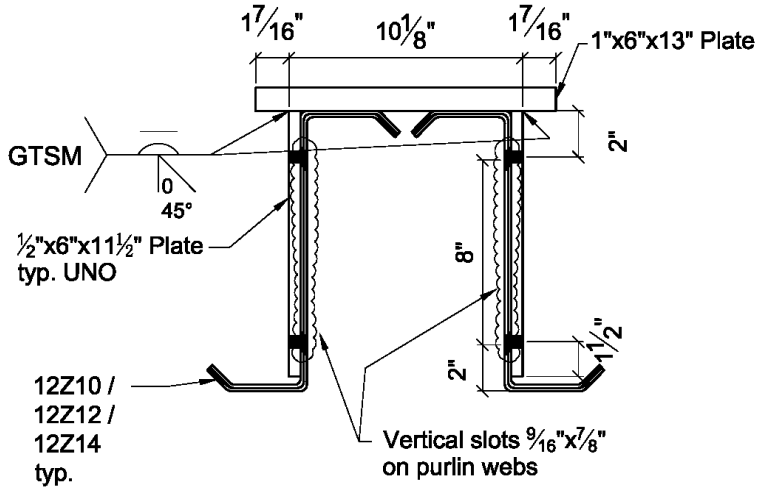

View E - E

Appendix B Distortional Buckling Strength (DSM)

The distortional buckling strength (M_{nd}) was calculated by using the Direct Strength Method (DSM) indicated in Appendix 1, Section 1.2.2.3 of CSA S136-2012 as follows.

$$For\ \lambda_d \leq 0.673: \quad M_{nd} = M_y \tag{B. 1}$$

$$For\ \lambda_d > 0.673: \quad M_{nd} = \left(1 - 0.22\left(\frac{M_{crd}}{M_y}\right)^{0.5}\right)\left(\frac{M_{crd}}{M_y}\right)^{0.5} M_y \tag{B. 2}$$

Where

$$\lambda_d = \sqrt{M_y / M_{crd}} \tag{B. 3}$$

$$M_y = S_{fy} F_y \tag{B. 4}$$

M_{crd} Critical elastic distortional buckling moment, determined by using software CUFSM 4.05 (Li and Schafer 2010)

S_{fy} Elastic section modulus of full unreduced cross-section relative to extreme fiber in first yielding

Table B-1 Comparison of Distortional Buckling Strength

Test[1]	**M_{nd} (kip in) C3.1.4 CSA S136-2012**	**M_{nd} (kip in) Direct Strength Method**	**Difference**
08Z10	274	281	2%
08Z13	163	157	3%
08Z16	97	90	6%
10Z10	368	379	3%
10Z13	214	210	2%
10Z16	119	120	1%
12Z10	466	477	2%
12Z12	362	354	2%
12Z14	217	218	1%
Metric Conversion: 1 kip in = 0.112kN m		Average	**3%**

[1] Test designation: for example, 12Z10 represents the specimen for 12 inch (305mm) Z-shaped purlins with 10 gauge (0.135 inch or 3.429mm) thickness.

Appendix C

Test Data of Mid-span Deflection and Flexural Stiffness

Comparison of Lapped Purlins with Round Holes and Vertical Slotted Holes

Table C-1 Deformation and Flexural Stiffness Obtained at 40% of the Ultimate Load of Non-lapped Purlins

Test[1]	Lapped length (in.)	Types of holes at connection	$P_{40\%}$ (kip)	Deflection Δ_t (in.) at $P_{40\%}$			Dev.	K_t (kip/in)	$\frac{K_{lap}}{K_{non-lap}}$
				Test 1	Test 2	Avg.			
12Z10	Non-lapped	N/A	3.11	0.597	0.598	0.598	±0.11%	5.20	**100% (baseline)**
	48	Round holes		0.514	0.522	0.518	±0.78%	6.00	**115%**
	48	Vertical slotted holes		0.686	0.631	0.658	±4.19%	4.72	**91%**
12Z12	Non-lapped	N/A	2.41	0.583	0.565	0.574	±1.50%	4.20	**100% (baseline)**
	48	Round holes		0.586	0.577	0.581	±0.77%	4.15	**99%**
	48	Vertical slotted holes		0.678	0.609	0.644	±5.35%	3.75	**89%**
12Z14	Non-lapped	N/A	1.47	0.481	0.486	0.484	±0.49%	3.04	**100% (baseline)**
	48	Round holes		0.482	0.452	0.467	±3.21%	3.15	**104%**
	48	Vertical slotted holes		0.497	0.494	0.495	±0.36%	2.97	**98%**

Metric Conversion: 1 in. = 25.4mm, 1 kip = 4.448 kN, 1 kip/in = 175 kN/m

[1] Test designation: for example, 12Z10 represents the specimen for 12 inch (305mm) Z-shaped purlins with 10 gauge (0.135 inch or 3.429mm) thickness.

Table C-2 Deformation and Flexural Stiffness Obtained at 80% of the Ultimate Load of Non-lapped Purlins

Test[1]	Lapped length (in.)	Types of holes at connection	$P_{80\%}$ (kip)	Deflection Δ_t (in.) at $P_{80\%}$			Dev.	K_t (kip/in)	$\frac{K_{lap}}{K_{non-lap}}$
				Test 1	Test 2	Avg.			
12Z10	Non-lapped	N/A	6.22	1.217	1.216	1.217	±0.08%	5.11	**100%(baseline)**
	48	Round holes		1.106	1.145	1.125	±1.75%	5.53	**108%**
	48	Vertical slotted holes		1.511	1.438	1.475	±2.45%	4.22	**82%**
12Z12	Non-lapped	N/A	4.82	1.142	1.127	1.135	±0.67%	4.25	**100%(baseline)**
	48	Round holes		1.193	1.173	1.183	±0.81%	4.08	**96%**
	48	Vertical slotted holes		1.320	1.230	1.275	±3.55%	3.78	**89%**
12Z14	Non-lapped	N/A	2.94	0.979	1.005	0.992	±1.32%	2.97	**100%(baseline)**
	48	Round holes		1.035	0.965	1.000	±3.51%	2.94	**99%**
	48	Vertical slotted holes		1.086	1.061	1.073	±1.19%	2.74	**92%**

Metric Conversion: 1 in. = 25.4mm, 1 kip = 4.448 kN, 1 kip/in = 175 kN/m

[1] Test designation: for example, 12Z10 represents the specimen for 12 inch (305mm) Z-shaped purlins with 10 gauge (0.135 inch or 3.429mm) thickness.

Table C-3 Deflection and Flexural Stiffness Results of Lapped Purlins with Vertical Slotted Holes at 40% of the Ultimate Load of Non-lapped Purlins

Test[1]	Lapped length (in.)	$P_{40\%}$ (kip)	Deflection Δ (in) at $P_{40\%}$			Dev.	K_{t-lap} (kip/in)	$K_{d-non\ lap}$ (kip/in)	$\frac{K_{t-lap}}{K_{d-non\ lap}}$	$\frac{K_{t-lap}}{K_{t-non\ lap}}$
			Test 1	Test 2	Avg.					
08Z10	34	3.93	0.546	0.488	0.517	±5.62%	7.60	15.76	**48%**	**53%**
	60	3.93	0.345	0.370	0.357	±3.63%	10.99	15.76	**70%**	**77%**
08Z13	34	2.43	0.311	0.686	0.498	±37.66%	4.87	11.00	**44%**	**49%**
	60	2.43	0.266	0.353	0.310	±13.98%	7.84	11.00	**71%**	**78%**
08Z16	34	1.53	0.527	0.349	0.438	±20.35%	3.49	7.24	**48%**	**53%**
	60	1.53	0.201	0.198	0.199	±0.84%	7.66	7.24	**106%**	**116%**
10Z10	34	3.57	0.918	0.865	0.892	±2.95%	4.00	8.37	**48%**	**53%**
	60	3.57	0.459	0.627	0.543	±15.52%	6.57	8.37	**79%**	**86%**
10Z13	34	2.26	0.760	0.599	0.679	±11.86%	3.33	5.82	**57%**	**63%**
	60	2.26	0.439	0.302	0.370	±18.55%	6.10	5.82	**105%**	**115%**
10Z16	34	1.28	0.433	0.388	0.410	±5.56%	3.12	3.76	**83%**	**91%**
	60	1.28	0.283	0.353	0.318	±11.00%	4.02	3.76	**107%**	**118%**
12Z10	34	3.40	1.155	1.057	1.106	±4.41%	3.07	5.56	**55%**	**61%**
	48	3.40	0.756	0.708	0.732	±3.25%	4.64	5.66	**82%**	**90%**
	60	3.40	0.786	0.735	0.761	±3.38%	4.47	5.56	**80%**	**88%**
12Z12	34	2.74	0.904	1.112	1.008	±10.35%	2.72	4.42	**62%**	**68%**
	48	2.74	0.759	0.694	0.727	±4.47%	3.77	4.79	**79%**	**86%**
	60	2.74	0.610	0.712	0.661	±7.75%	4.15	4.42	**94%**	**103%**
12Z14	34	1.63	0.723	0.633	0.678	±6.62%	2.40	3.69	**65%**	**71%**
	48	1.63	0.557	0.549	0.553	±0.74%	2.94	3.36	**87%**	**96%**
	60	1.63	0.461	0.472	0.467	±1.26%	3.49	3.69	**94%**	**104%**

Metric Conversion: 1 in. = 25.4mm, 1 kip = 4.448 kN, 1 kip/in = 175 kN/m

[1] Test designation: for example, 12Z10 represents the specimen for 12 inch (305mm) Z-shaped purlins with 10 gauge (0.135 inch or 3.429mm) thickness.

Table C-4 Deflection and Flexural Stiffness Results of Lapped Purlins with Vertical Slotted Holes at 60% of the Ultimate Load of Non-lapped Purlins

Test[1]	Lapped length (in.)	$P_{60\%}$ (kip)	Deflection Δ (in) at $P_{60\%}$			Dev.	K_{t-lap} (kip/in)	$K_{d-non\ lap}$ (kip/in)	$\frac{K_{t-lap}}{K_{d-non\ lap}}$	$\frac{K_{t-lap}}{K_{t-non\ lap}}$
			Test 1	Test 2	Avg.					
08Z10	34	5.89	0.730	0.674	0.702	±3.97%	8.39	15.76	**53%**	**58%**
	60	5.89	0.496	0.508	0.502	±1.15%	11.75	15.76	**75%**	**82%**
08Z13	34	3.64	0.514	0.873	0.694	±25.91%	5.25	11.00	**48%**	**52%**
	60	3.64	0.491	0.500	0.495	±0.91%	7.35	11.00	**67%**	**73%**
08Z16	34	2.29	0.690	0.501	0.595	±15.86%	3.85	6.96	**55%**	**61%**
	60	2.29	0.355	0.292	0.323	±9.78%	7.08	6.96	**102%**	**112%**
10Z10	34	5.35	1.245	1.192	1.218	±2.16%	4.39	8.37	**53%**	**58%**
	60	5.35	0.697	0.854	0.776	±10.10%	6.90	8.37	**82%**	**91%**
10Z13	34	3.39	1.142	0.958	1.050	±8.74%	3.23	5.82	**56%**	**61%**
	60	3.39	0.650	0.561	0.606	±7.36%	5.60	5.82	**96%**	**106%**
10Z16	34	1.92	0.770	0.690	0.730	±5.47%	2.63	3.56	**74%**	**81%**
	60	1.92	0.475	0.563	0.519	±8.54%	3.70	3.56	**104%**	**114%**
12Z10	34	5.09	1.684	1.607	1.645	±2.35%	3.10	5.56	**56%**	**61%**
	48	5.09	1.208	1.169	1.189	±1.66%	4.29	5.66	**76%**	**83%**
	60	5.09	1.122	1.060	1.091	±2.84%	4.67	5.56	**84%**	**92%**
12Z12	34	4.11	1.492	1.702	1.597	±6.58%	2.57	4.42	**58%**	**64%**
	48	4.11	1.119	1.043	1.081	±3.54%	3.80	4.79	**79%**	**87%**
	60	4.11	0.972	1.067	1.020	±4.69%	4.03	4.42	**91%**	**100%**
12Z14	34	2.44	1.119	1.065	1.092	±2.51%	2.23	3.66	**61%**	**67%**
	48	2.44	0.879	0.853	0.866	±1.54%	2.82	3.26	**86%**	**95%**
	60	2.44	0.780	0.811	0.796	±1.94%	3.07	3.66	**84%**	**92%**

Metric Conversion: 1 in. = 25.4mm, 1 kip = 4.448 kN, 1 kip/in = 175 kN/m

[1] Test designation: for example, 12Z10 represents the specimen for 12 inch (305mm) Z-shaped purlins with 10 gauge (0.135 inch or 3.429mm) thickness.

Table C-5 Deflection and Flexural Stiffness Results of Lapped Purlins with Vertical Slotted Holes Obtained at 80% of the Ultimate Load of Non-lapped Purlins

Test[1]	Lapped length (in.)	$P_{80\%}$ (kip)	Deflection Δ (in) at $P_{80\%}$			Dev.	K_{t-lap} (kip/in)	$K_{d-non\ lap}$ (kip/in)	$\frac{K_{t-lap}}{K_{d-non\ lap}}$	$\frac{K_{t-lap}}{K_{t-non\ lap}}$
			Test 1	Test 2	Avg.					
08Z10	34	7.86	0.919	0.873	0.896	±2.54%	8.77	15.76	**56%**	**61%**
	60	7.86	0.643	0.648	0.645	±0.39%	12.17	15.76	**77%**	**85%**
08Z13	34	4.86	0.753	1.050	0.902	±16.43%	5.39	10.95	**49%**	**54%**
	60	4.86	0.677	0.650	0.663	±2.03%	7.32	10.95	**67%**	**73%**
08Z16	34	3.05	0.862	0.660	0.761	±13.24%	4.01	6.96	**58%**	**63%**
	60	3.05	0.506	0.396	0.451	±12.19%	6.77	6.96	**97%**	**107%**
10Z10	34	7.14	1.621	1.576	1.599	±1.41%	4.46	8.37	**53%**	**59%**
	60	7.14	0.961	1.132	1.047	±8.18%	6.82	8.37	**81%**	**90%**
10Z13	34	4.52	1.543	1.415	1.479	±4.32%	3.06	5.67	**54%**	**59%**
	60	4.52	0.886	0.852	0.869	±2.00%	5.20	5.67	**92%**	**101%**
10Z16	34	2.56	1.140	1.073	1.107	±3.03%	2.31	3.32	**70%**	**77%**
	60	2.56	0.776	0.944	0.860	±9.76%	2.97	3.32	**90%**	**99%**
12Z10	34	6.79	2.432	2.316	2.374	±2.46%	2.86	5.56	**51%**	**57%**
	48	6.79	1.647	1.583	1.615	±2.00%	4.21	5.66	**74%**	**82%**
	60	6.79	1.475	1.405	1.440	±2.42%	4.72	5.56	**85%**	**93%**
12Z12	34	x	x	x	x	x	x	x	x	x
	48	5.48	1.519	1.412	1.466	±3.65%	3.74	4.72	**79%**	**87%**
	60	5.48	1.345	1.464	1.405	±4.23%	3.90	4.33	**90%**	**99%**
12Z14	34	3.25	1.710	1.559	1.635	±4.63%	1.99	3.43	**58%**	**64%**
	48	3.25	1.281	1.265	1.273	±0.64%	2.56	3.00	**85%**	**94%**
	60	3.25	1.070	1.096	1.083	±1.19%	3.00	3.43	**88%**	**96%**

Metric Conversion: 1 in. = 25.4mm, 1 kip = 4.448 kN, 1 kip/in = 175 kN/m

x: The tested ultimate load of lapped purlins is lower than the 80% of ultimate load of non-lapped purlins, no deflection are recorded.

[1] Test designation: for example, 12Z10 represents the specimen for 12 inch (305mm) Z-shaped purlins with 10 gauge (0.135 inch or 3.429mm) thickness.

Table C-6 Deflection and Flexural Stiffness Results of Lapped Purlins with Vertical Slotted Holes at the Maximum Measured Load

Test[1]	Lapped length (in.)	$P_{t\text{-}max}$ (kip)	Deflection Δ (in) at $P_{t\text{-}max}$			Dev.	K_{t-lap} (kip/in)	$K_{d-non\ lap}$ (kip/in)	$\frac{K_{t-lap}}{K_{d-non\ lap}}$	$\frac{K_{t-lap}}{K_{t-non\ lap}}$
			Test 1	Test 2	Avg.					
08Z10	34	12.71	1.771	1.673	1.722	±2.86%	7.38	15.76	**47%**	**51%**
	60	16.72	1.591	1.535	1.563	±1.78%	10.70	15.76	**68%**	**75%**
08Z13	34	7.70	1.619	1.616	1.618	±0.11%	4.76	10.34	**46%**	**51%**
	60	9.45	1.323	1.259	1.291	±2.46%	7.32	10.34	**71%**	**78%**
08Z16	34	4.17	1.368	1.180	1.274	±7.37%	3.27	6.41	**51%**	**56%**
	60	4.40	1.058	1.053	1.056	±0.24%	4.17	6.41	**65%**	**71%**
10Z10	34	10.81	3.281	3.217	3.249	±0.99%	3.33	8.37	**40%**	**44%**
	60	12.31	2.088	2.029	2.058	±1.44%	5.98	8.37	**71%**	**79%**
10Z13	34	5.81	2.479	2.144	2.312	±7.23%	2.51	5.39	**47%**	**51%**
	60	7.46	1.787	1.735	1.761	±1.49%	4.23	5.39	**79%**	**86%**
10Z16	34	2.81	1.413	1.259	1.336	±5.74%	2.10	3.14	**67%**	**74%**
	60	3.11	1.135	1.308	1.222	±7.07%	2.54	3.14	**81%**	**89%**
12Z10	34	7.82	3.031	3.054	3.042	±0.38%	2.57	5.49	**47%**	**51%**
	48	10.25	2.681	2.818	2.749	±2.51%	3.73	5.59	**67%**	**73%**
	60	10.91	2.736	2.619	2.678	±2.18%	4.08	5.49	**74%**	**82%**
12Z12	34	5.25	2.189	2.538	2.363	±7.36%	2.22	4.11	**54%**	**59%**
	48	7.70	2.365	2.410	2.387	±0.93%	3.23	4.49	**72%**	**79%**
	60	7.43	2.140	2.289	2.215	±3.36%	3.35	4.11	**82%**	**90%**
12Z14	34	3.54	1.931	1.910	1.921	±0.56%	1.84	3.21	**57%**	**63%**
	48	3.99	1.867	1.827	1.847	±1.08%	2.16	2.81	**77%**	**85%**
	60	4.84	1.737	1.996	1.866	±6.92%	2.60	3.21	**81%**	**89%**

Metric Conversion: 1 in. = 25.4mm, 1 kip = 4.448 kN, 1 kip/in = 175 kN/m

[1] Test designation: for example, 12Z10 represents the specimen for 12 inch (305mm) Z-shaped purlins with 10 gauge (0.135 inch or 3.429mm) thickness.

Appendix D Effective Flexural Rigidities

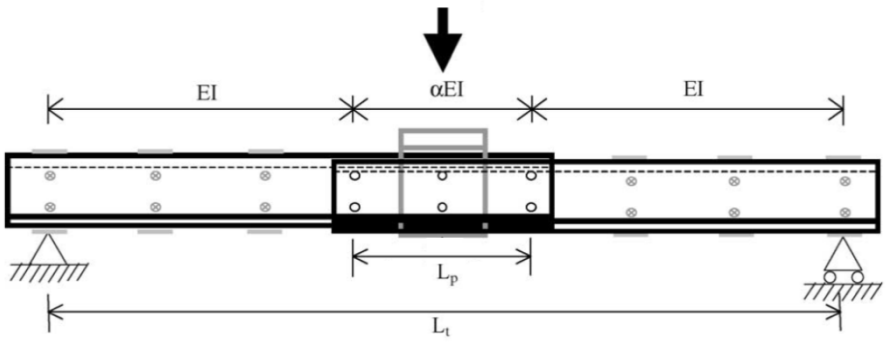

Figure D-1 Effective Flexural Rigidity Ratio (Ho and Chung 2004)

As shown in Figure D-1, the effective flexural rigidity of the lapped connection is assumed to be α times the flexural rigidity of the connected section, *EI*. Based on classical analytical method such as the complementary virtual work method, the mid-span deflection Δ of the test specimen may be expressed as follows (Ho and Chung 2004):

$$\Delta = [1 + (\beta^2 - 3\beta + 3)\beta\left(\frac{1-\alpha}{\alpha}\right)]\frac{PL^3}{48EI_e} \quad \text{(D.1)}$$

Where

β is the lap length to test span ratio equal to $\frac{L_p}{L_t}$;
P is the applied load;
L_t is the test span.

Re-arranging the expression,

$$K_t = \frac{P}{\Delta} = \frac{48EI_e}{L^3[1 + (\beta^2 - 3\beta + 3)\beta\left(\frac{1-\alpha}{\alpha}\right)]} \quad \text{(D.2)}$$

$$\alpha_t = \left(\frac{\frac{48EI_e}{K_t L^3} - 1}{(\beta^2 - 3\beta + 3)\beta} + 1\right)^{-1} \quad \text{(D.3)}$$

Where

K_t is the tested stiffness which calculated by using the service load P_s and the corresponding vertical deflection Δ_t.

Appendix E Force Distribution within Lapped Connection

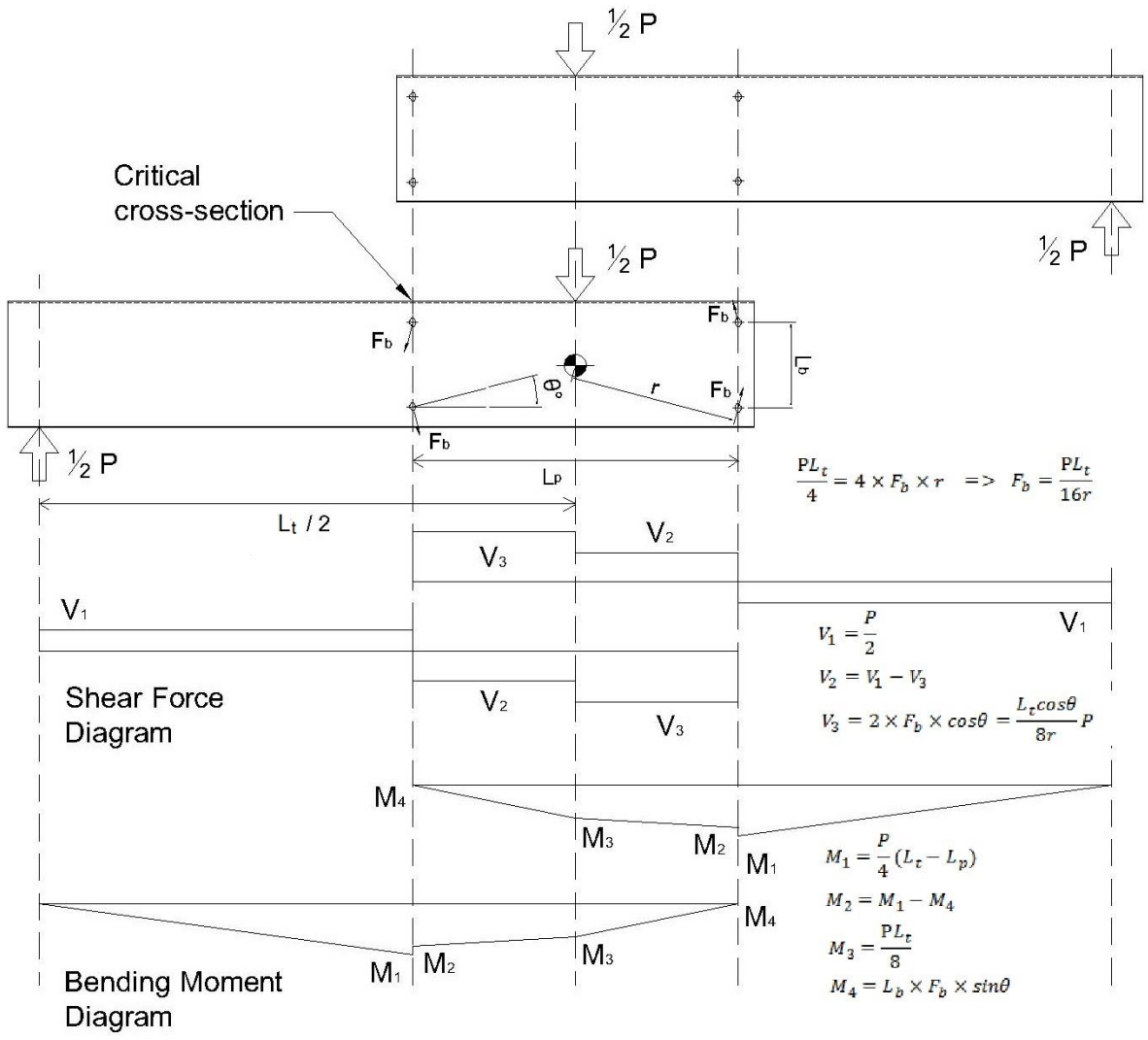

Figure E -1 Force Distribution within Lapped Connections (Chung and Ho 2005)

Appendix F
Load Deflection Curves

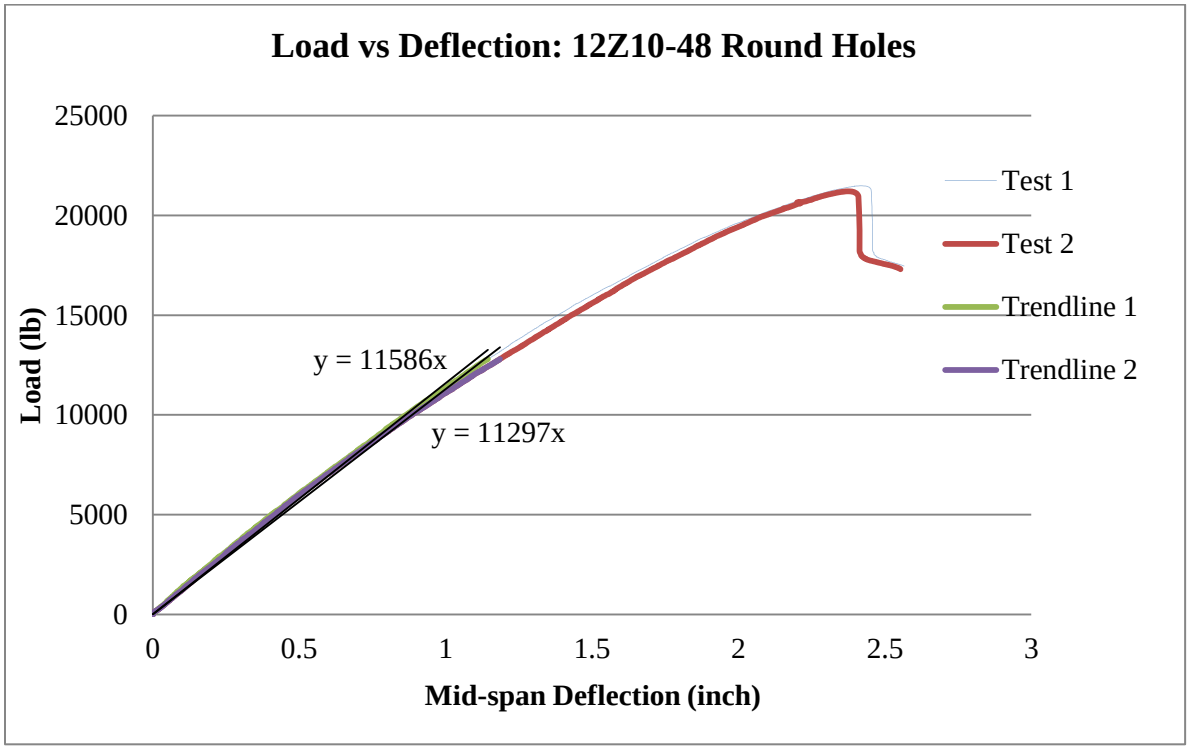
Load vs Deflection: 12Z10-48 Round Holes
25000
20000
15000
10000
5000
0
Load (lb)
0
0.5
1
1.5
2
2.5
3
Mid-span Deflection (inch)
y = 11586x
y = 11297x
Test 1
Test 2
Trendline 1
Trendline 2

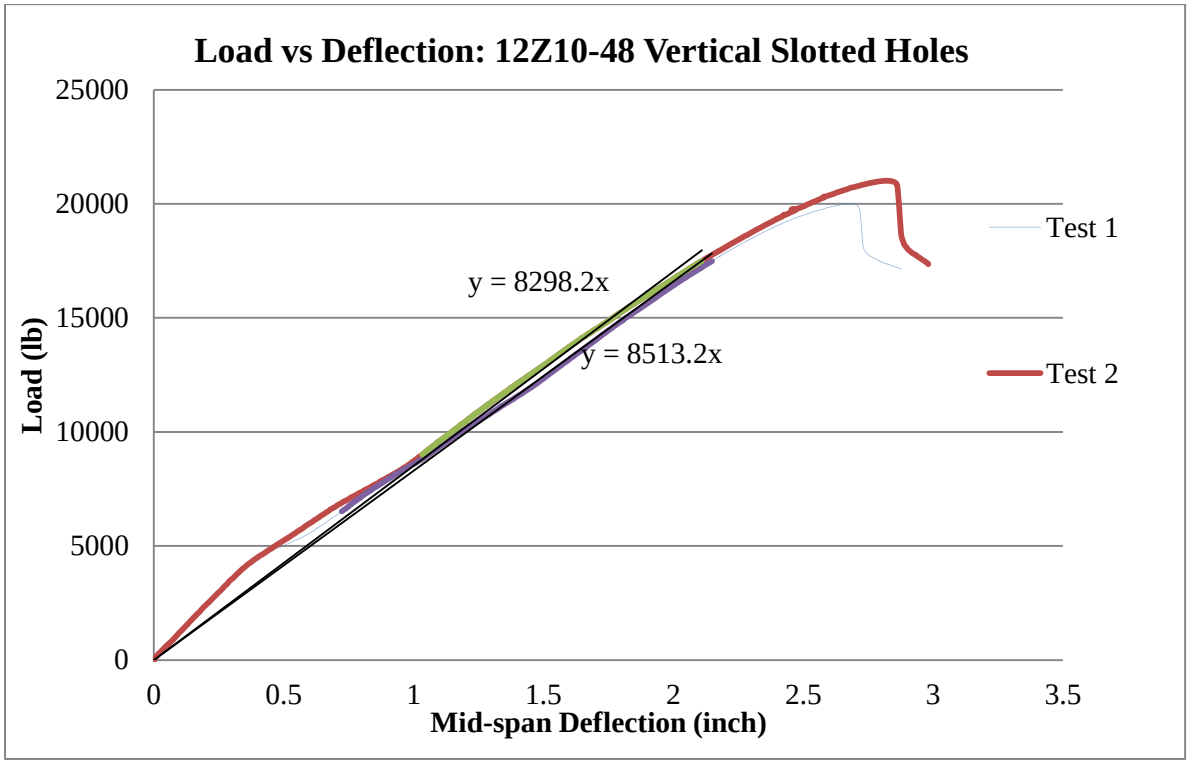
Load vs Deflection: 12Z10-48 Vertical Slotted Holes
25000
20000
15000
10000
5000
0
Load (lb)
0
0.5
1
1.5
2
2.5
3
3.5
Mid-span Deflection (inch)
y = 8298.2x
y = 8513.2x
Test 1
Test 2

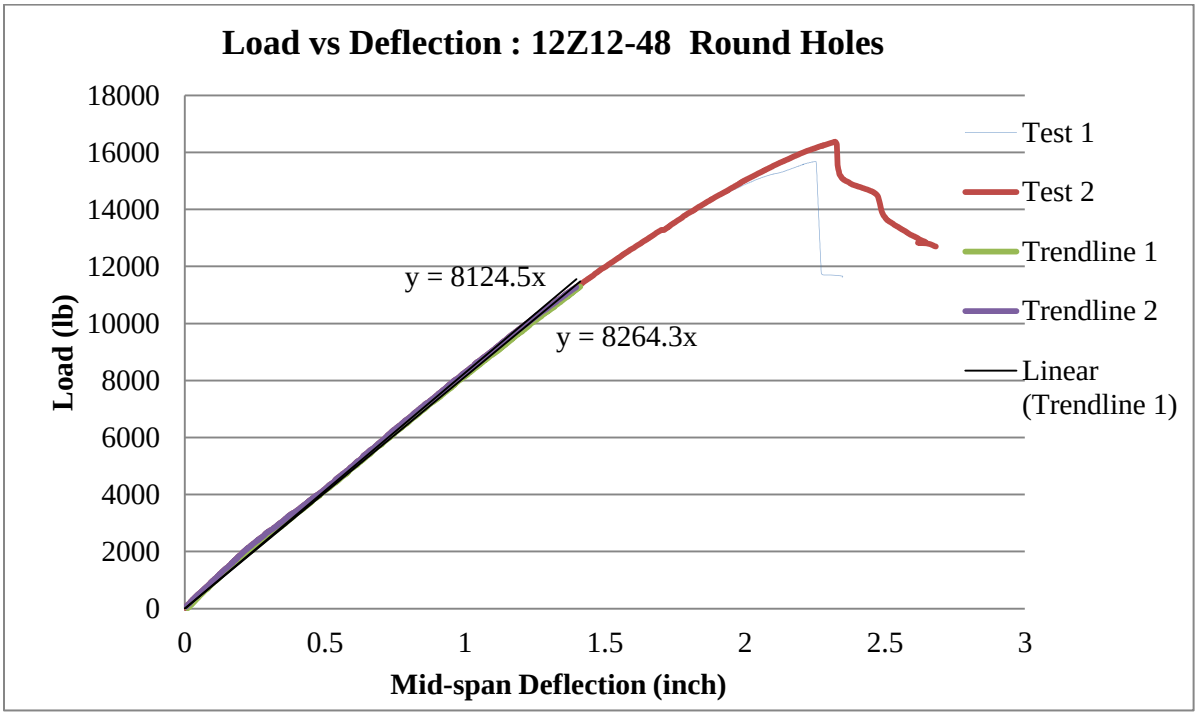
Load vs Deflection : 12Z12-48 Round Holes
18000
16000
14000
12000
10000
8000
6000
4000
2000
0
Load (lb)
0
0.5
1
1.5
2
2.5
3
Mid-span Deflection (inch)
y = 8124.5x
y = 8264.3x
Test 1
Test 2
Trendline 1
Trendline 2
Linear (Trendline 1)

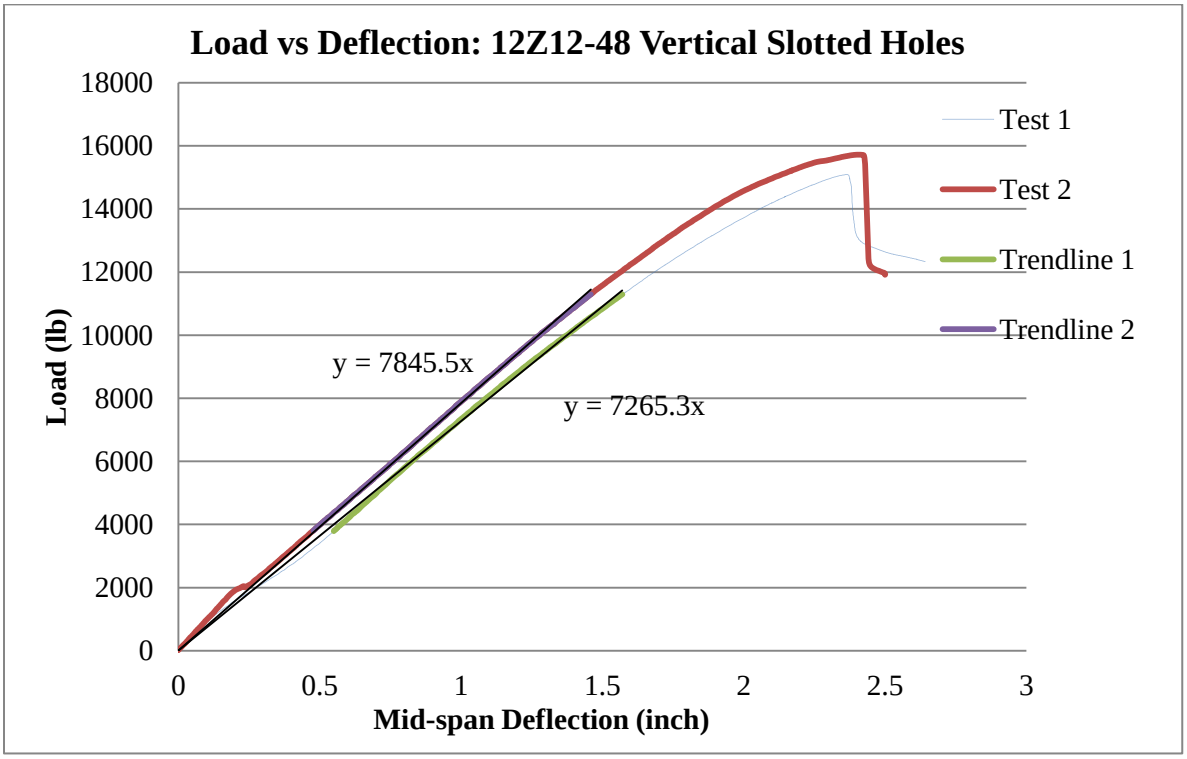
Load vs Deflection: 12Z12-48 Vertical Slotted Holes
18000
16000
14000
12000
10000
8000
6000
4000
2000
0
Load (lb)
0
0.5
1
1.5
2
2.5
3
Mid-span Deflection (inch)
y = 7845.5x
y = 7265.3x
Test 1
Test 2
Trendline 1
Trendline 2

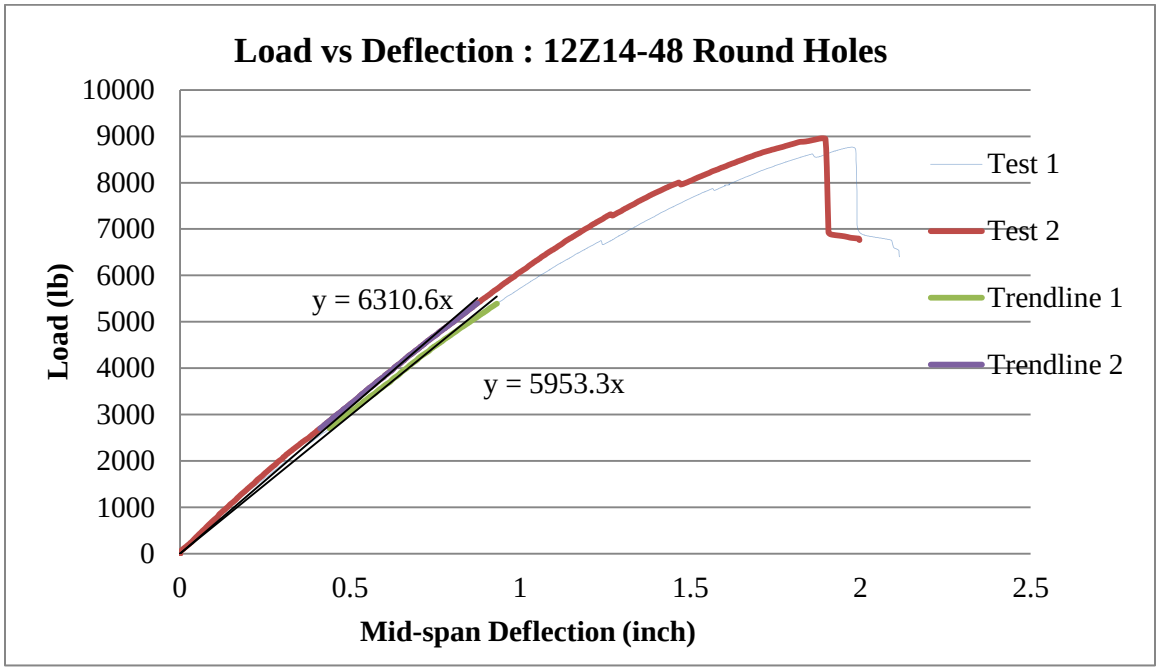
Load vs Deflection : 12Z14-48 Round Holes
10000
9000
8000
7000
6000
5000
4000
3000
2000
1000
0
Load (lb)
0
0.5
1
1.5
2
2.5
Mid-span Deflection (inch)
y = 6310.6x
y = 5953.3x
Test 1
Test 2
Trendline 1
Trendline 2

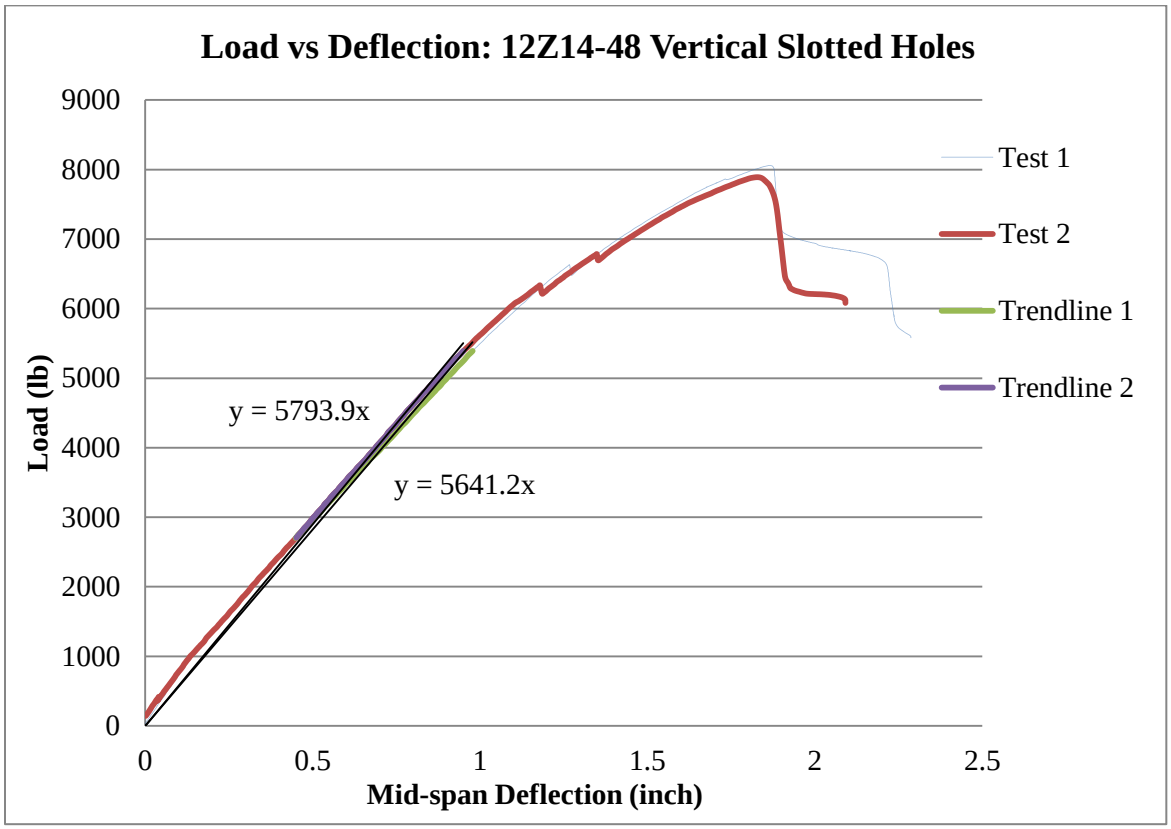
Load vs Deflection: 12Z14-48 Vertical Slotted Holes
9000
8000
7000
6000
5000
4000
3000
2000
1000
0
Load (lb)
0
0.5
1
1.5
2
2.5
Mid-span Deflection (inch)
y = 5793.9x
y = 5641.2x
Test 1
Test 2
Trendline 1
Trendline 2

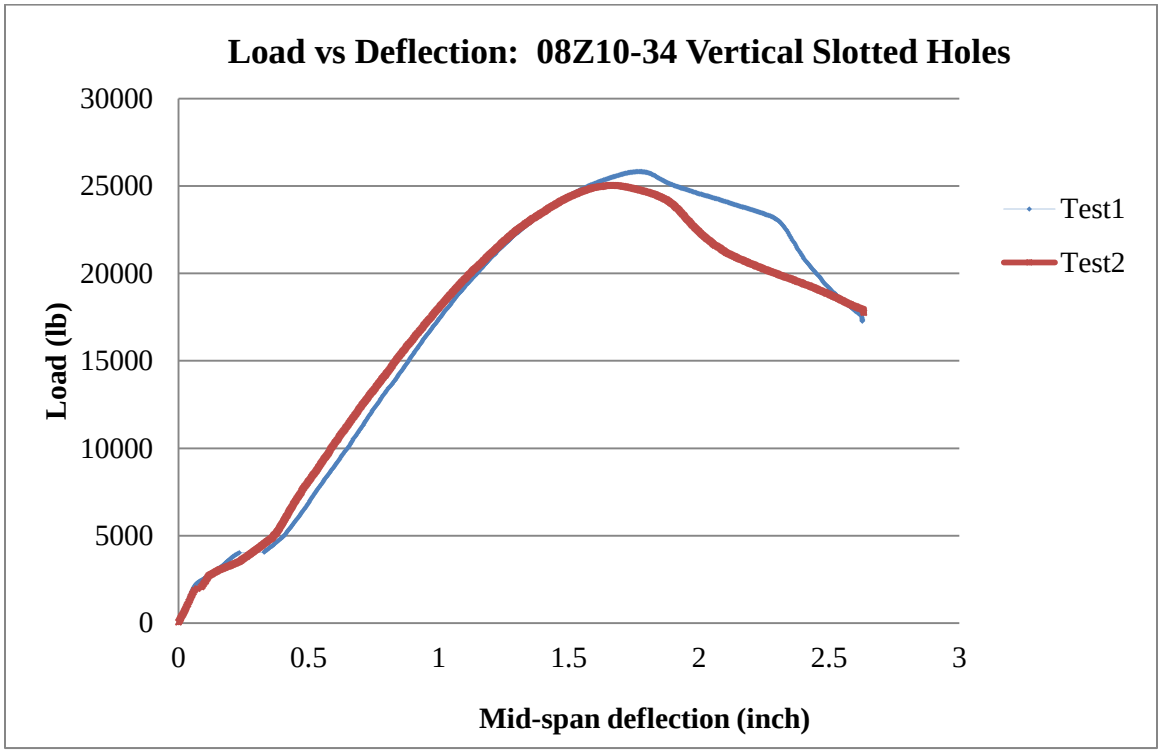
Load vs Deflection: 08Z10-34 Vertical Slotted Holes
30000
25000
20000
15000
10000
5000
0
Load (lb)
0
0.5
1
1.5
2
2.5
3
Mid-span deflection (inch)
Test1
Test2

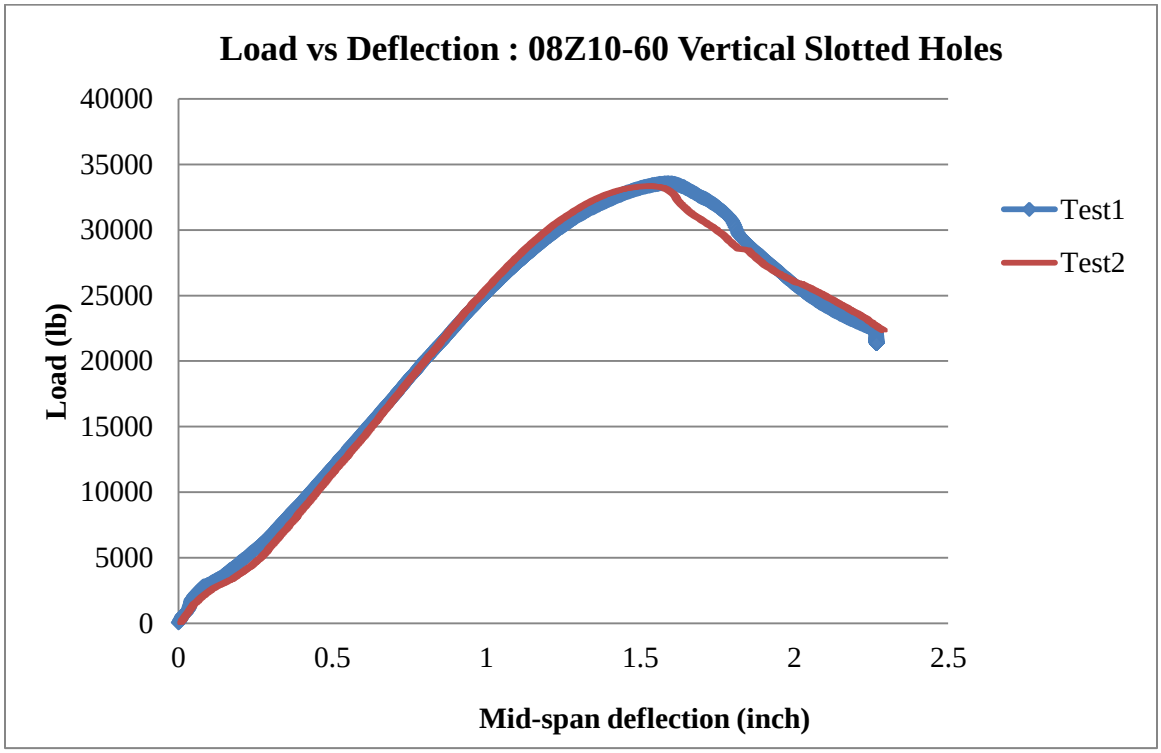
Load vs Deflection : 08Z10-60 Vertical Slotted Holes
40000
35000
30000
25000
20000
15000
10000
5000
0
Load (lb)
0
0.5
1
1.5
2
2.5
Mid-span deflection (inch)
Test1
Test2

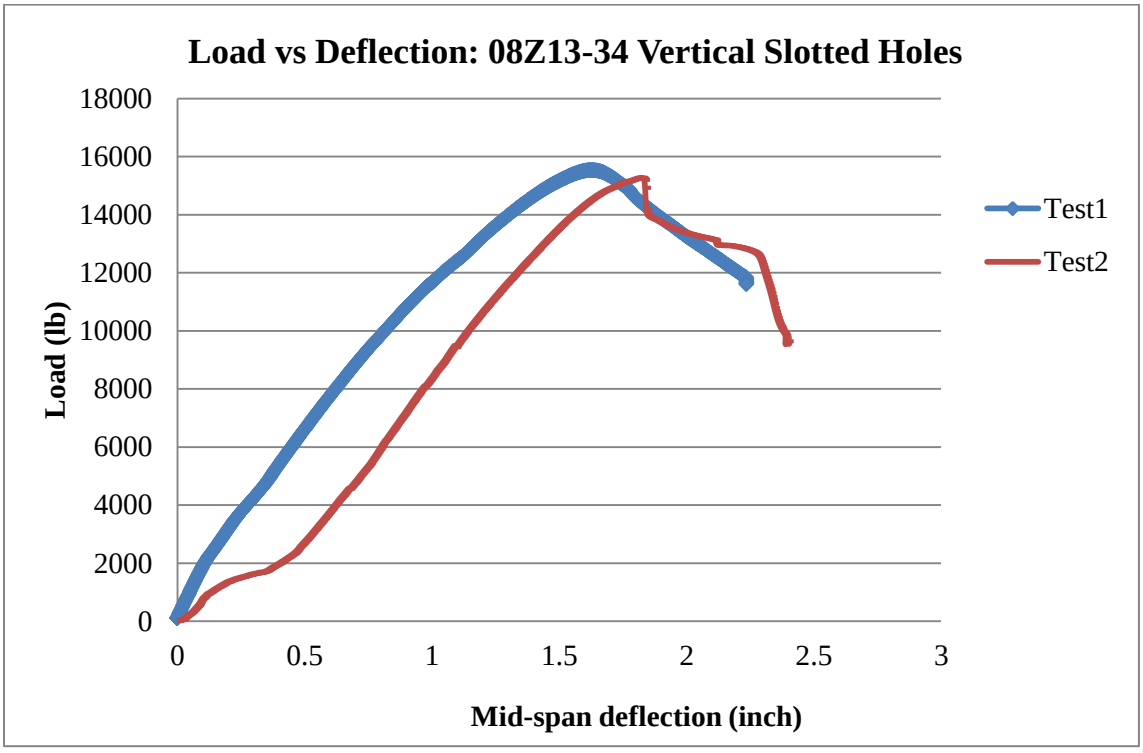
Load vs Deflection: 08Z13-34 Vertical Slotted Holes
18000
16000
14000
12000
10000
8000
6000
4000
2000
0
Load (lb)
0
0.5
1
1.5
2
2.5
3
Mid-span deflection (inch)
Test1
Test2

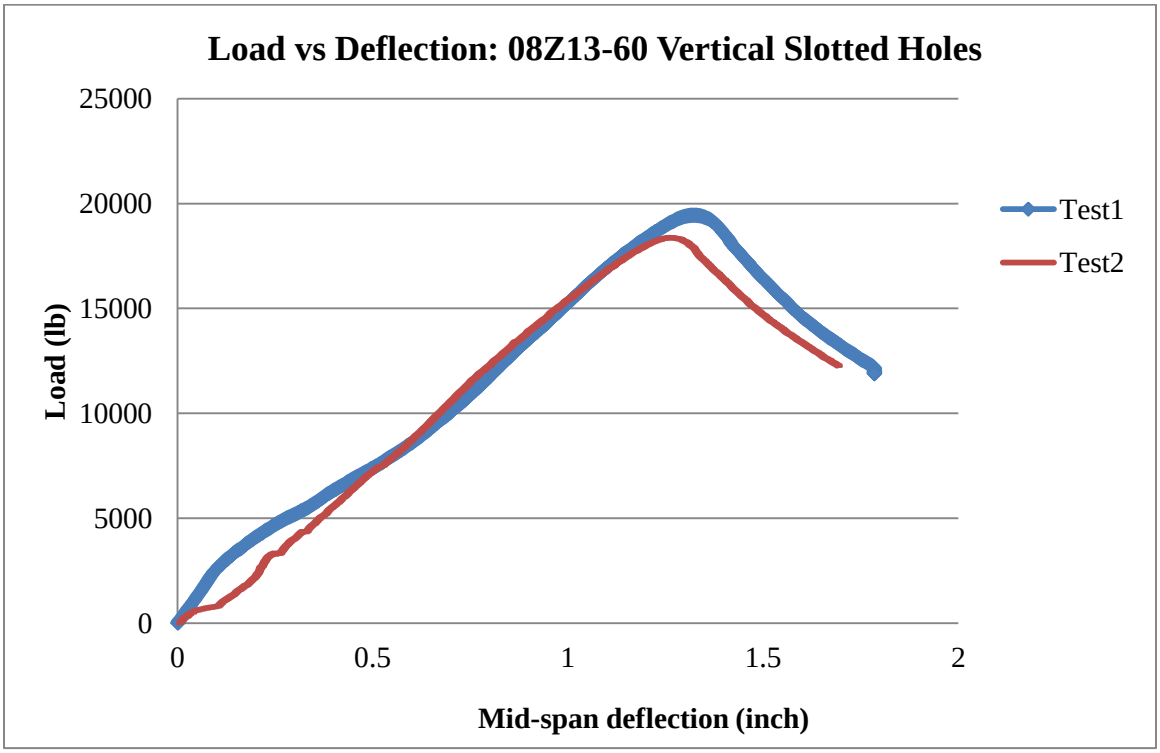
Load vs Deflection: 08Z13-60 Vertical Slotted Holes
25000
20000
15000
10000
5000
0
Load (lb)
0
0.5
1
1.5
2
Mid-span deflection (inch)
Test1
Test2

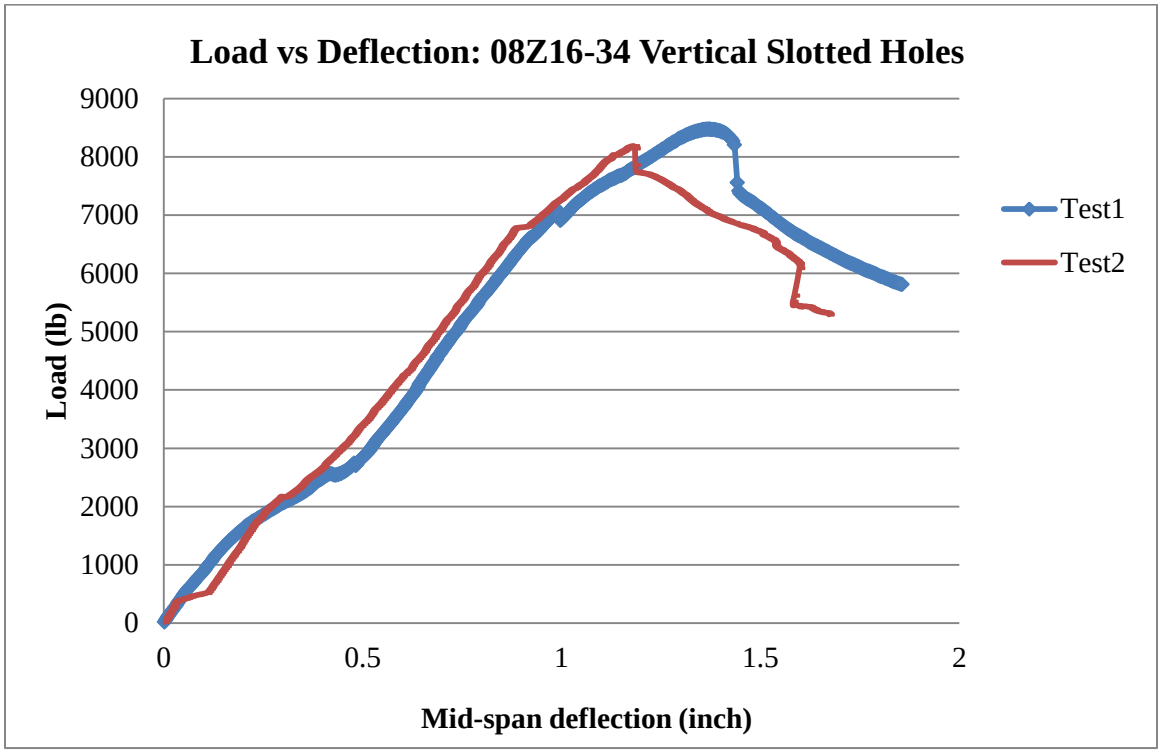
Load vs Deflection: 08Z16-34 Vertical Slotted Holes
9000
8000
7000
6000
5000
4000
3000
2000
1000
0
Load (lb)
0
0.5
1
1.5
2
Mid-span deflection (inch)
Test1
Test2

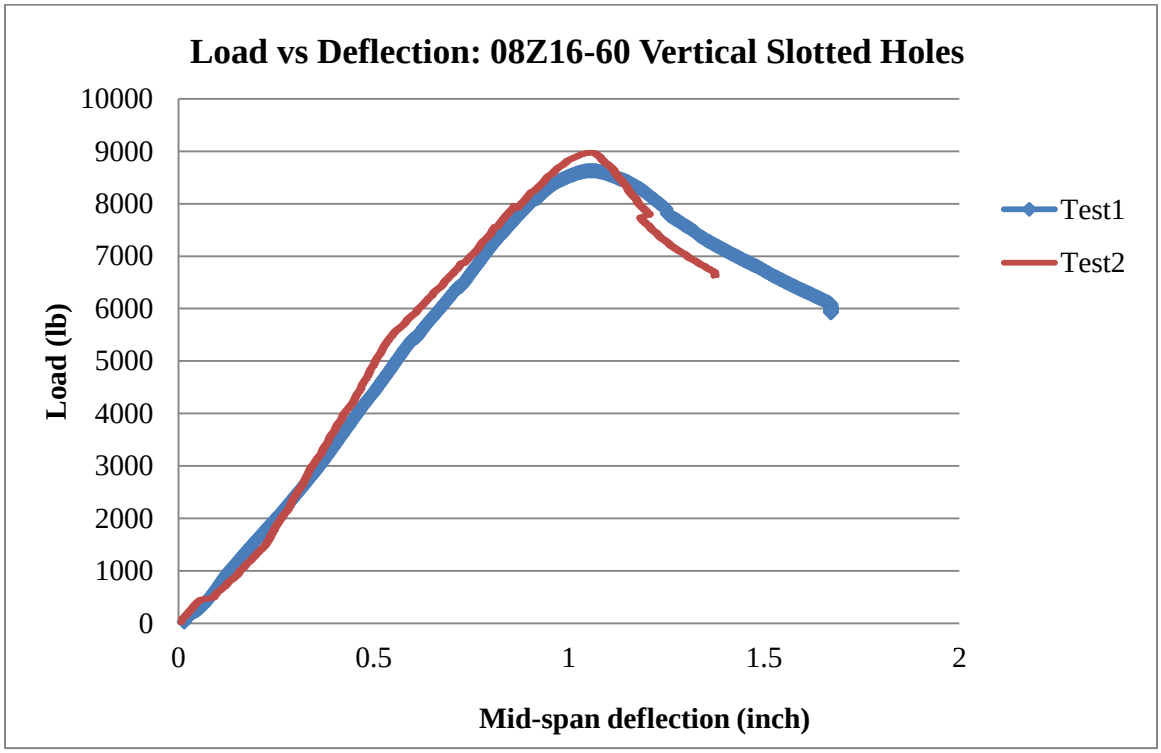
Load vs Deflection: 08Z16-60 Vertical Slotted Holes
10000
9000
8000
7000
6000
5000
4000
3000
2000
1000
0
Load (lb)
0
0.5
1
1.5
2
Mid-span deflection (inch)
Test1
Test2

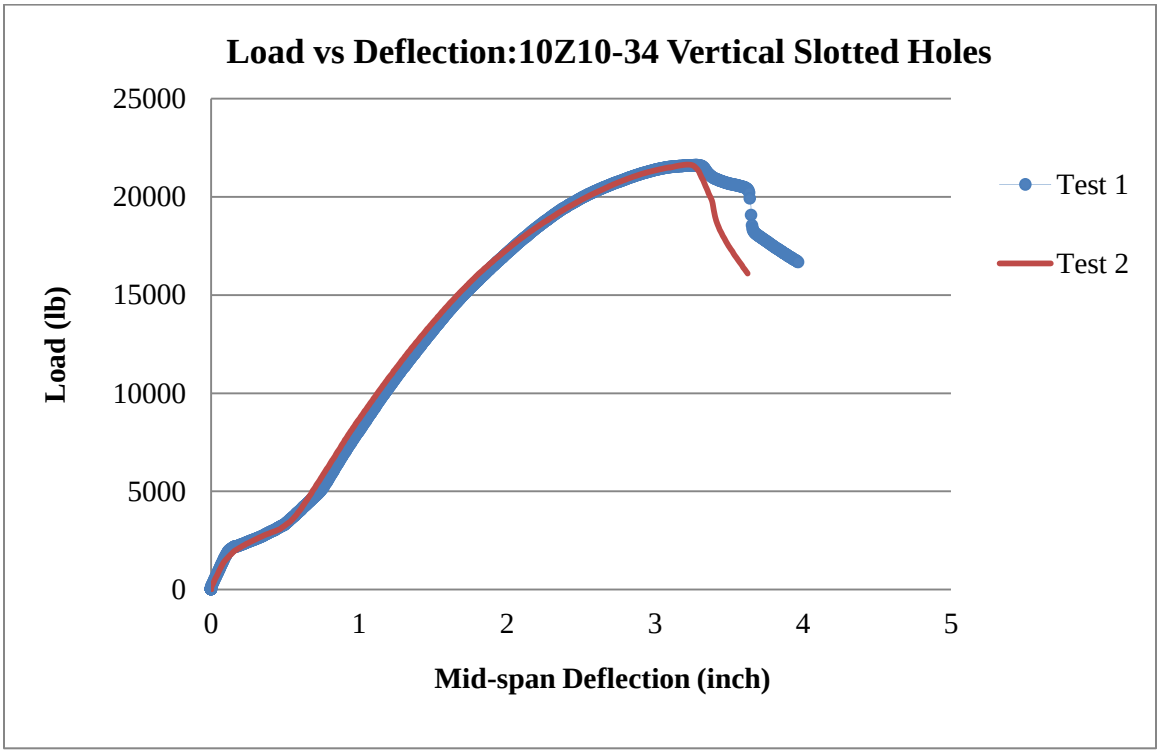
Load vs Deflection:10Z10-34 Vertical Slotted Holes
25000
20000
15000
10000
5000
0
Load (lb)
0
1
2
3
4
5
Mid-span Deflection (inch)
Test 1
Test 2

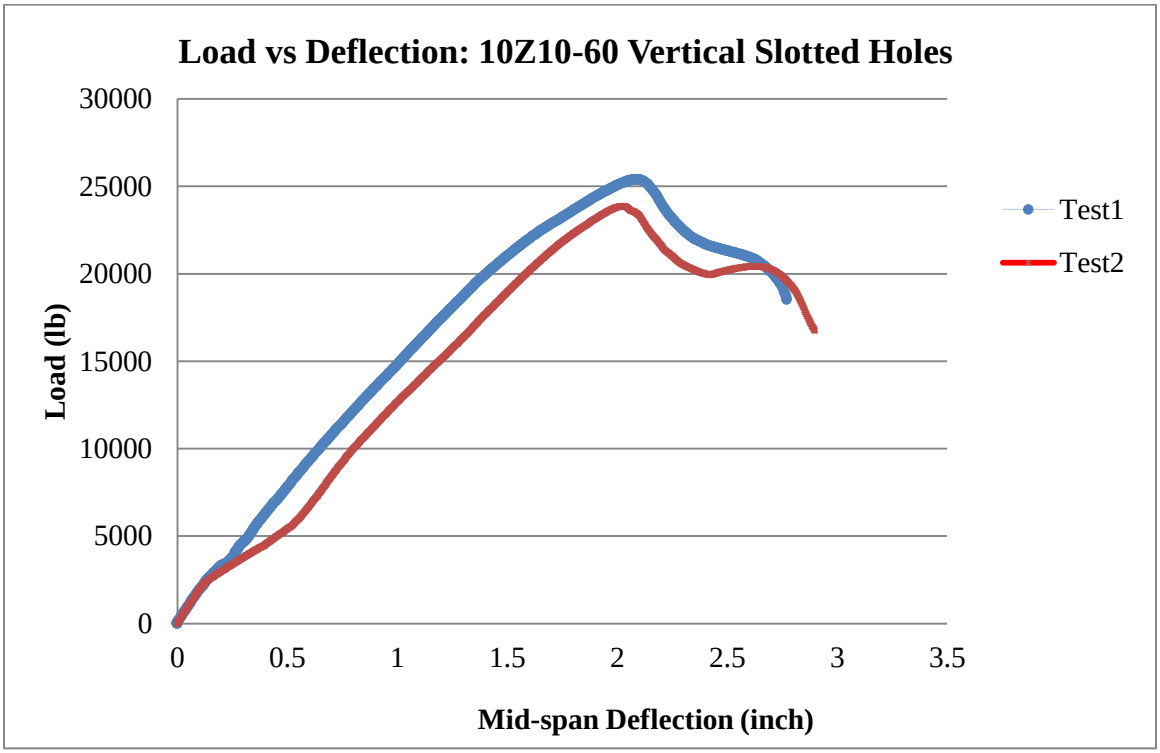
Load vs Deflection: 10Z10-60 Vertical Slotted Holes
30000
25000
20000
15000
10000
5000
0
Load (lb)
0
0.5
1
1.5
2
2.5
3
3.5
Mid-span Deflection (inch)
Test1
Test2

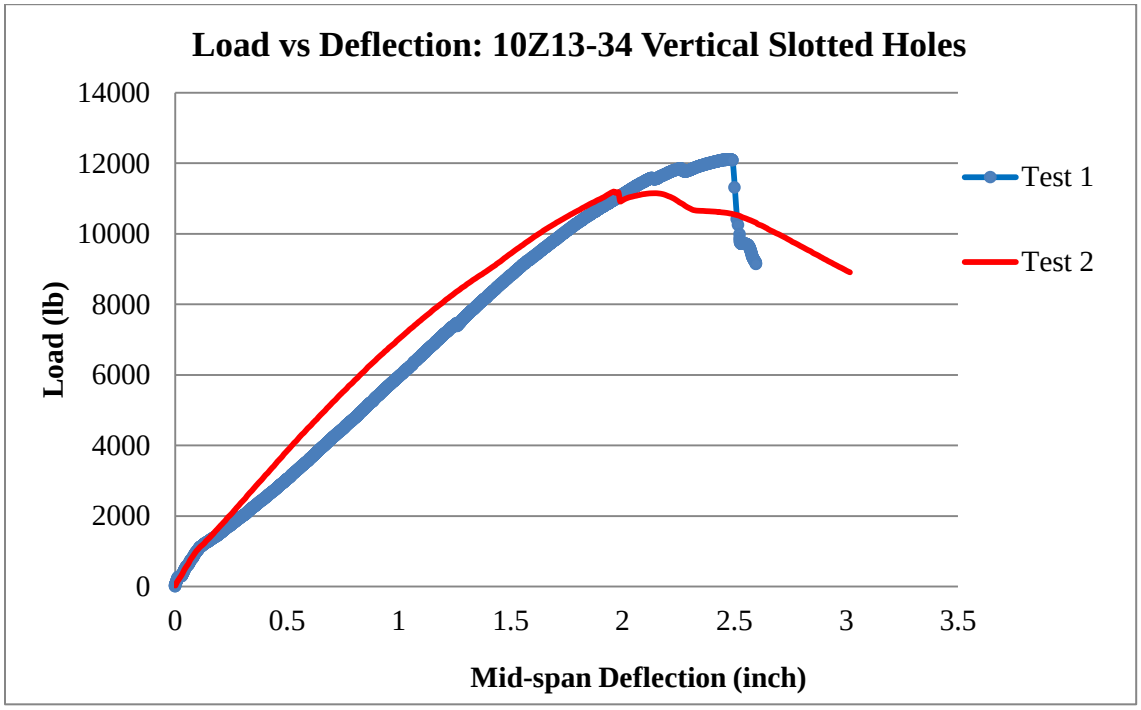
Load vs Deflection: 10Z13-34 Vertical Slotted Holes
14000
12000
10000
8000
6000
4000
2000
0
Load (lb)
0
0.5
1
1.5
2
2.5
3
3.5
Mid-span Deflection (inch)
Test 1
Test 2

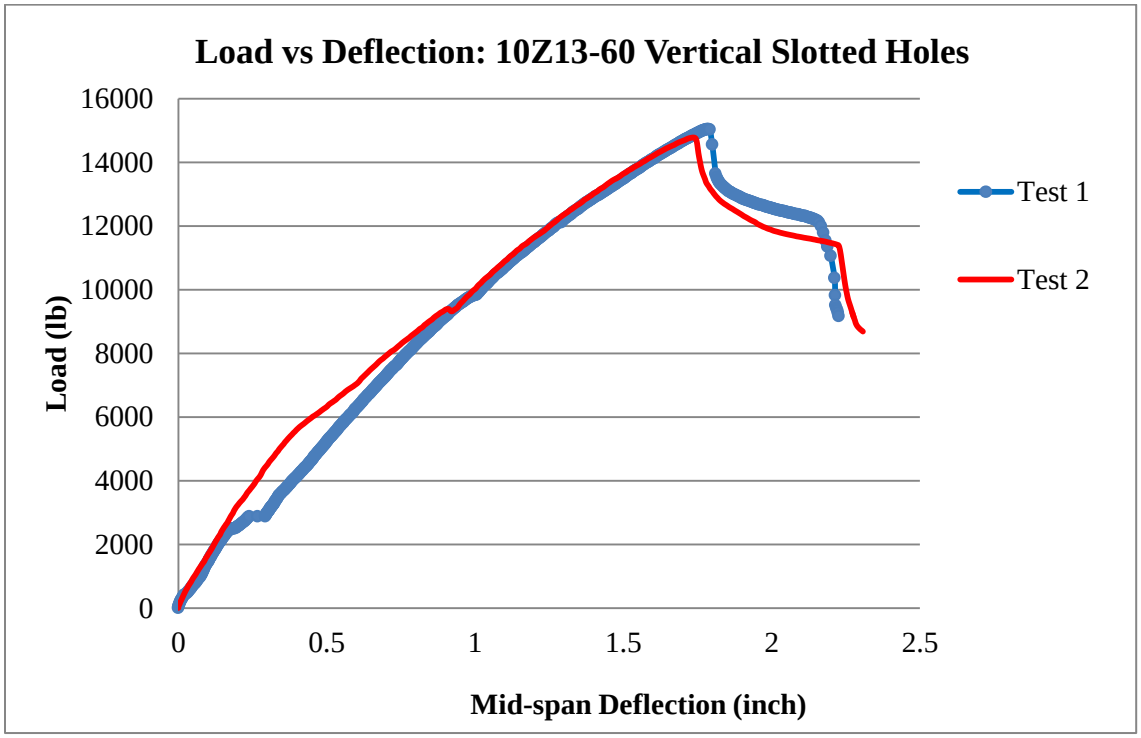
Load vs Deflection: 10Z13-60 Vertical Slotted Holes
16000
14000
12000
10000
8000
6000
4000
2000
0
Load (lb)
0
0.5
1
1.5
2
2.5
Mid-span Deflection (inch)
Test 1
Test 2

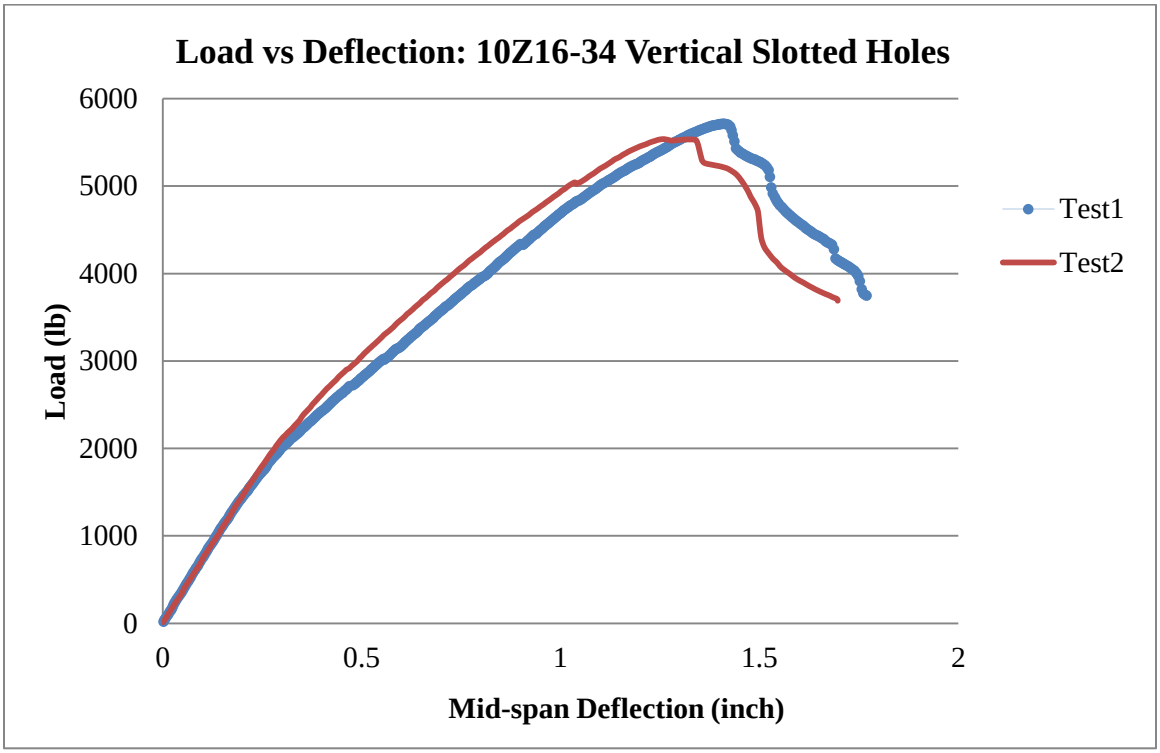
Load vs Deflection: 10Z16-34 Vertical Slotted Holes
6000
5000
4000
3000
2000
1000
0
Load (lb)
0
0.5
1
1.5
2
Mid-span Deflection (inch)
Test1
Test2

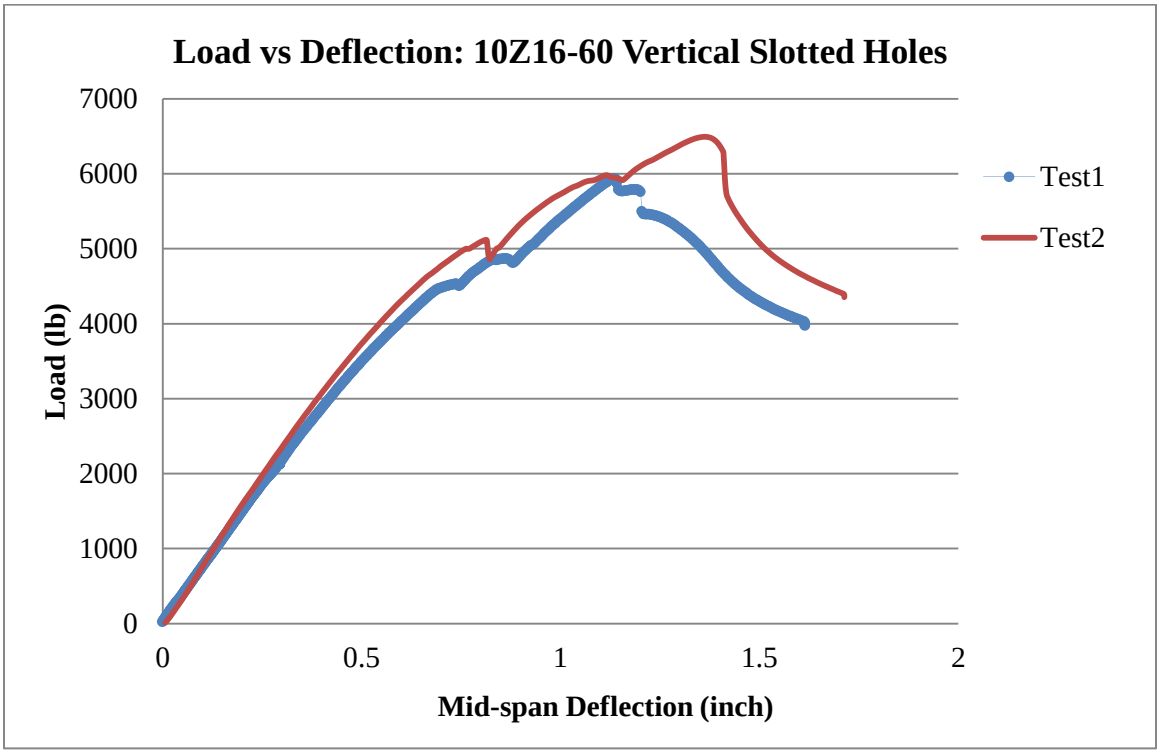
Load vs Deflection: 10Z16-60 Vertical Slotted Holes
7000
6000
5000
4000
3000
2000
1000
0
Load (lb)
0
0.5
1
1.5
2
Mid-span Deflection (inch)
Test1
Test2

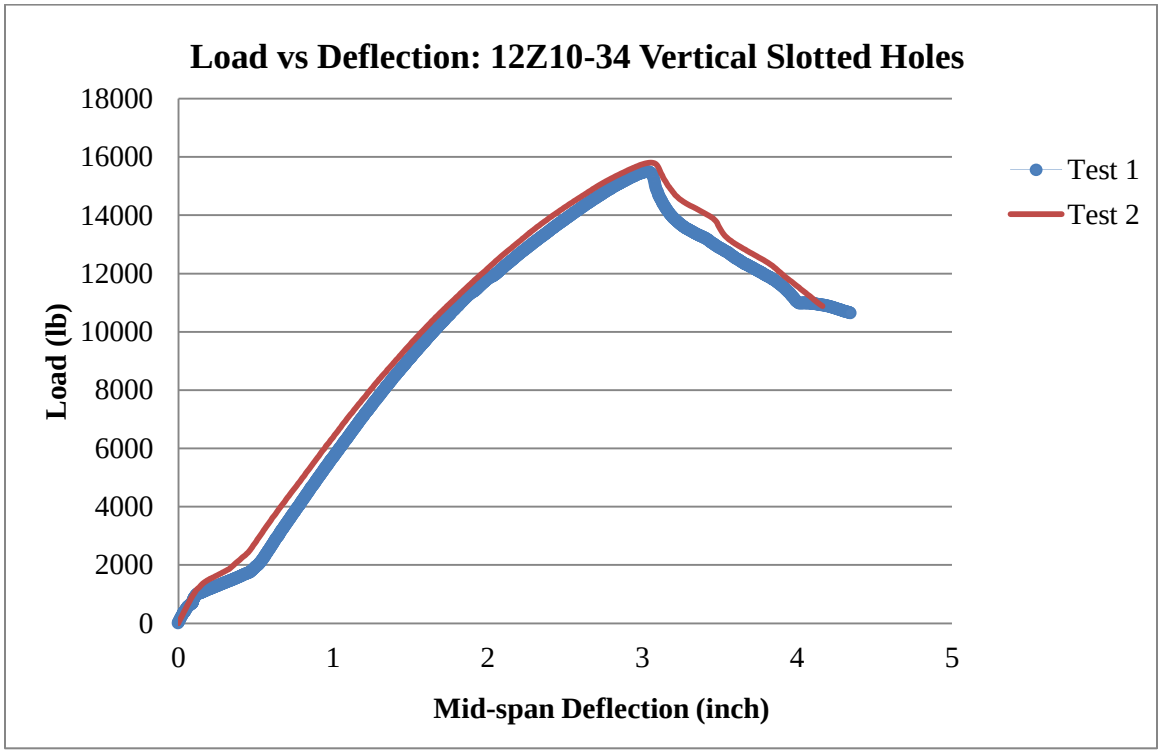
Load vs Deflection: 12Z10-34 Vertical Slotted Holes
18000
16000
14000
12000
10000
8000
6000
4000
2000
0
Load (lb)
0
1
2
3
4
5
Mid-span Deflection (inch)
Test 1
Test 2

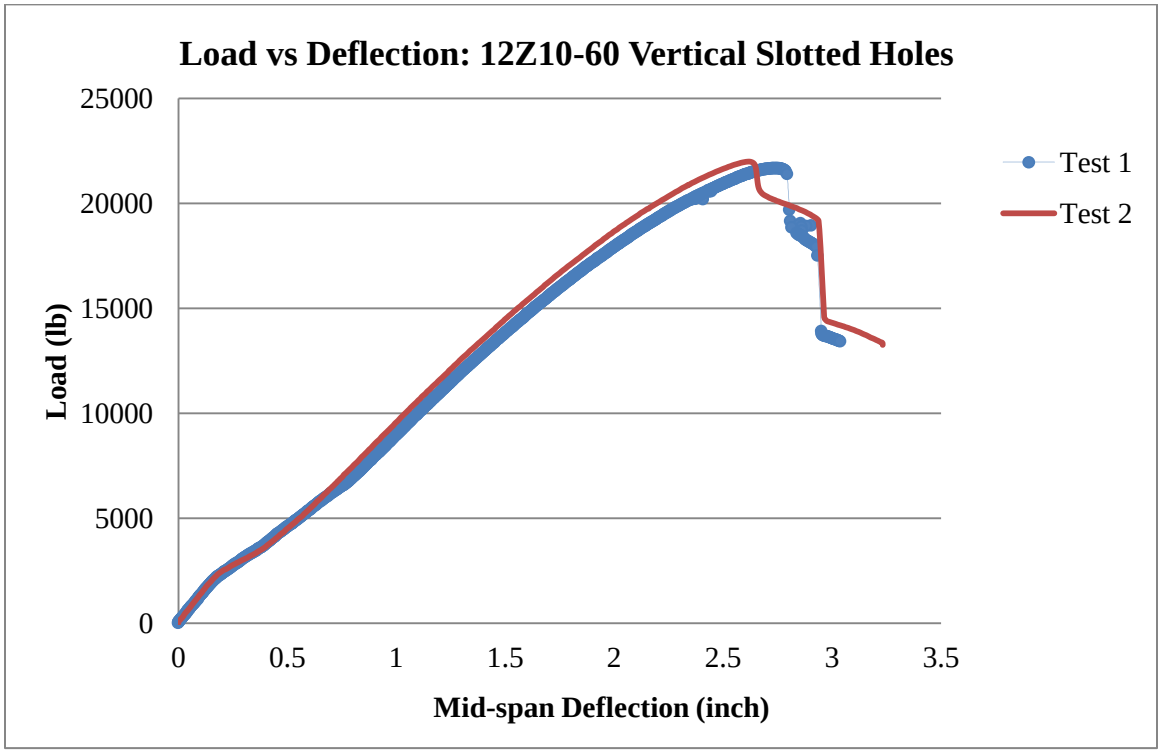
Load vs Deflection: 12Z10-60 Vertical Slotted Holes
25000
20000
15000
10000
5000
0
Load (lb)
0
0.5
1
1.5
2
2.5
3
3.5
Mid-span Deflection (inch)
Test 1
Test 2

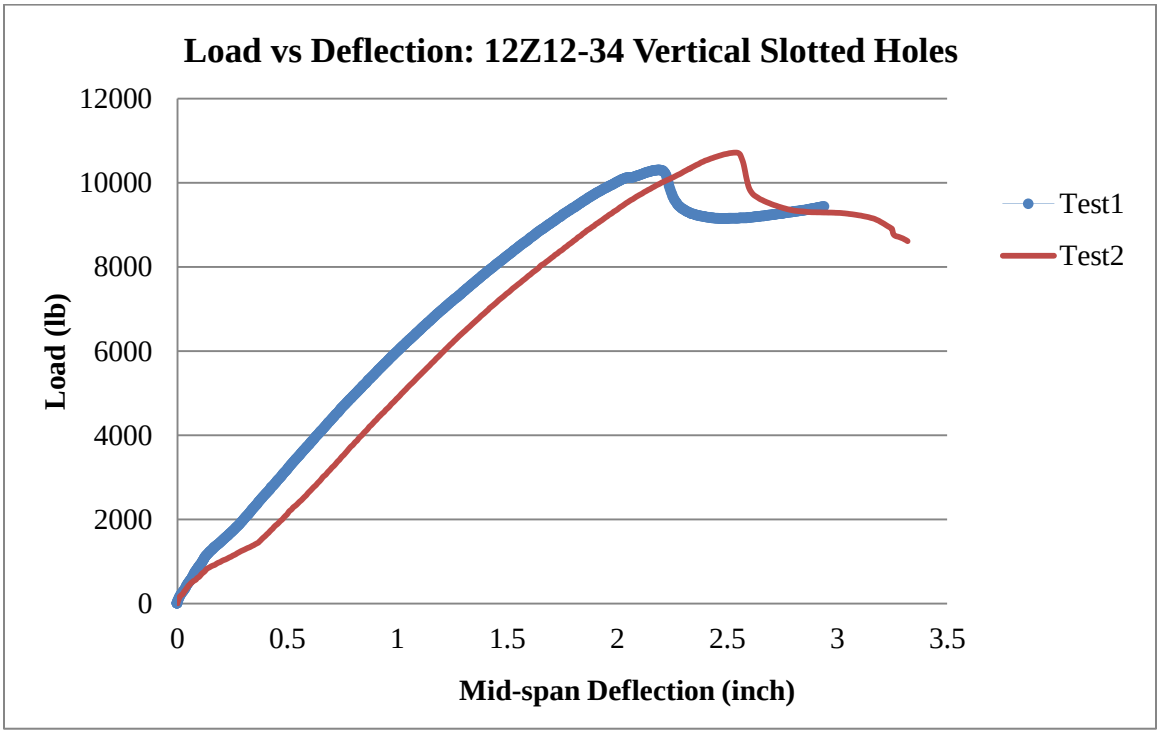
Load vs Deflection: 12Z12-34 Vertical Slotted Holes
12000
10000
8000
6000
4000
2000
0
Load (lb)
0
0.5
1
1.5
2
2.5
3
3.5
Mid-span Deflection (inch)
Test1
Test2

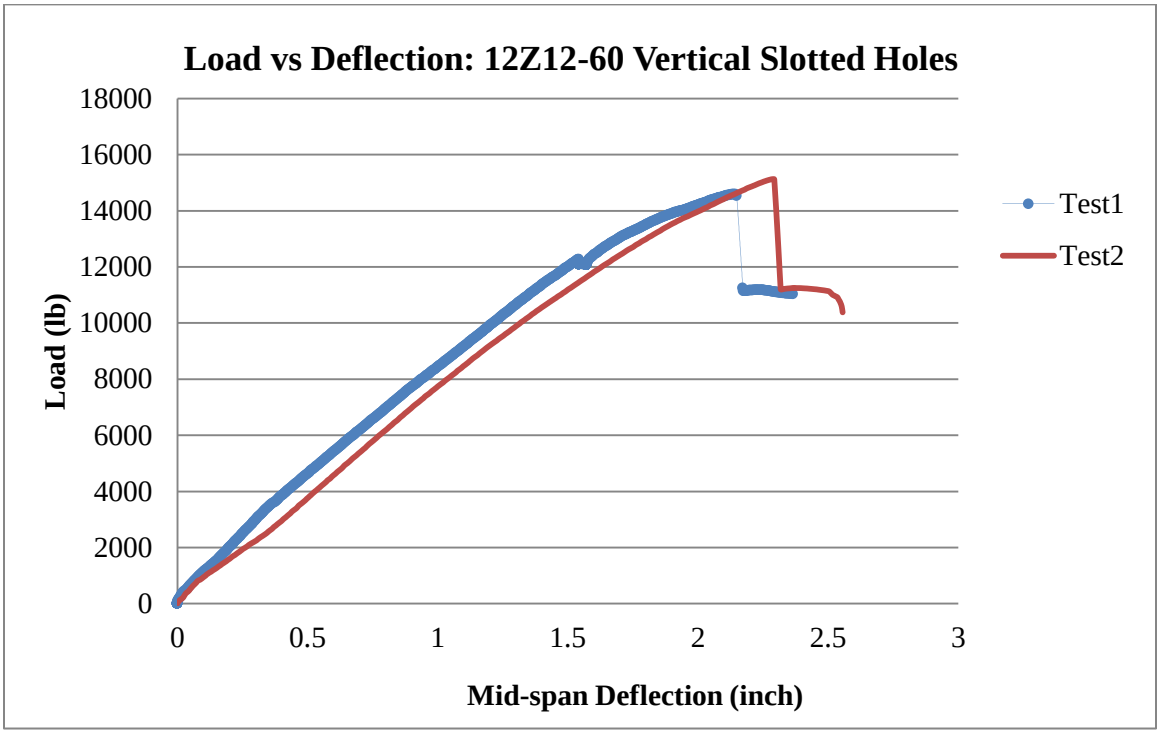
Load vs Deflection: 12Z12-60 Vertical Slotted Holes
18000
16000
14000
12000
10000
8000
6000
4000
2000
0
Load (lb)
0
0.5
1
1.5
2
2.5
3
Mid-span Deflection (inch)
Test1
Test2

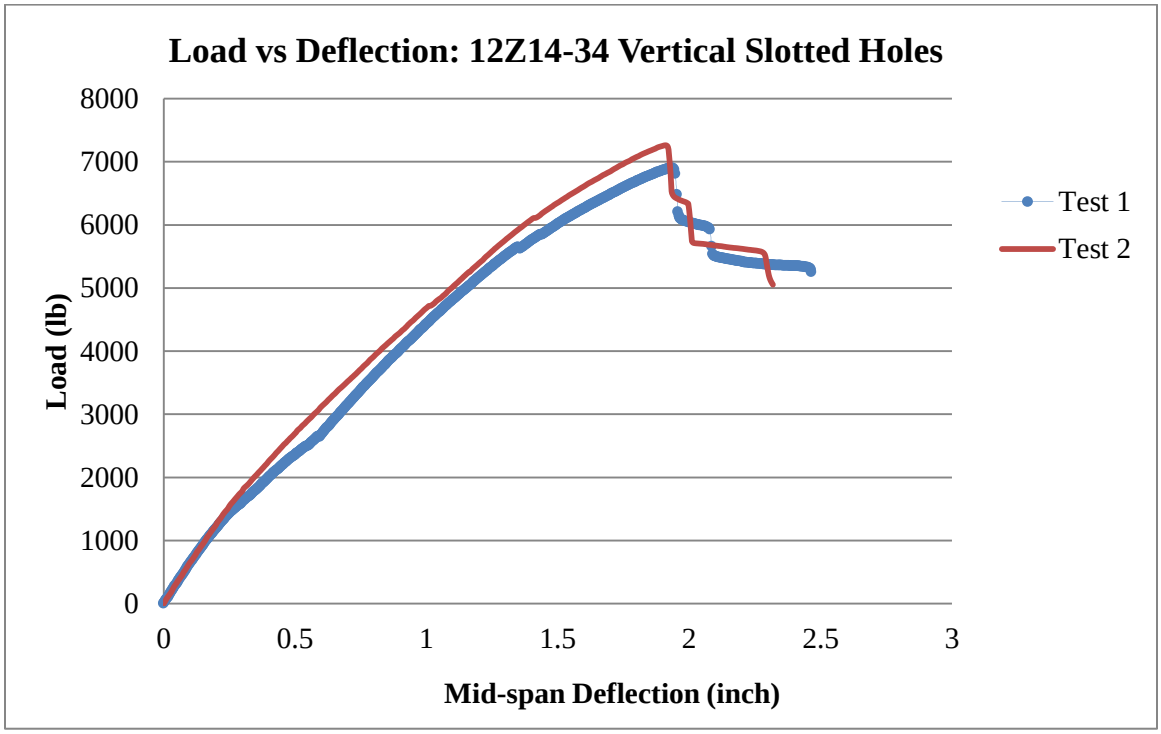
Load vs Deflection: 12Z14-34 Vertical Slotted Holes
8000
7000
6000
5000
4000
3000
2000
1000
0
Load (lb)
0
0.5
1
1.5
2
2.5
3
Mid-span Deflection (inch)
Test 1
Test 2

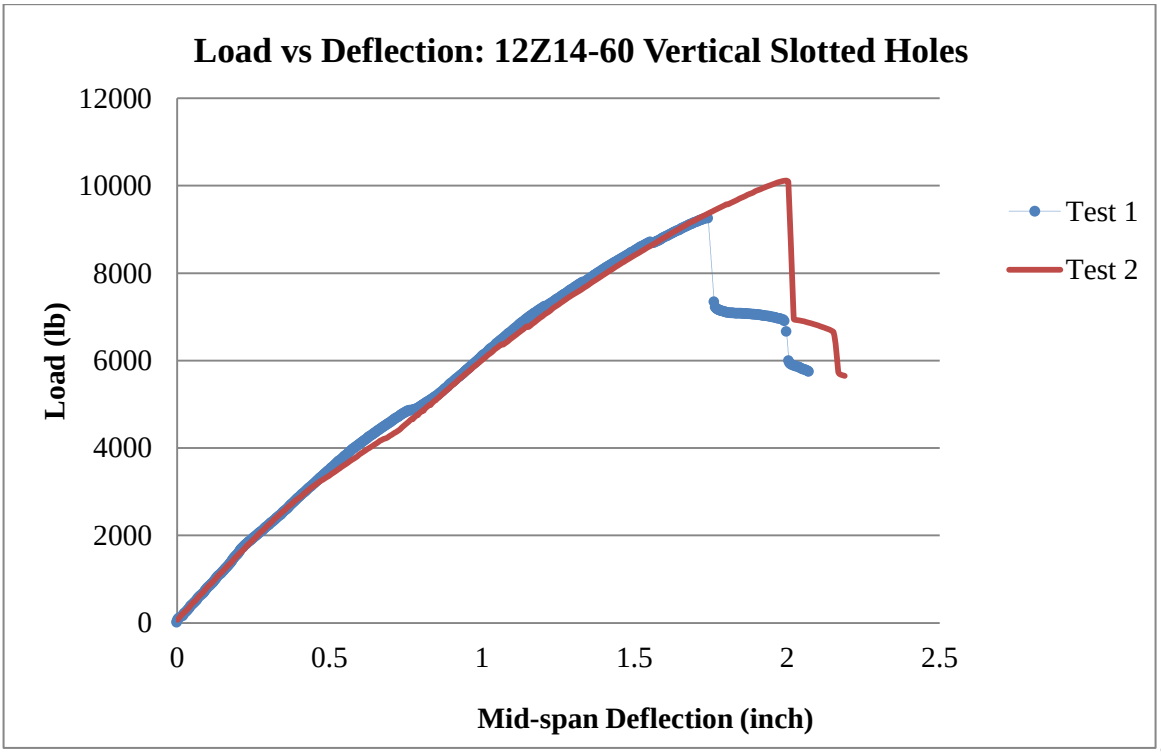
Load vs Deflection: 12Z14-60 Vertical Slotted Holes
12000
10000
8000
6000
4000
2000
0
Load (lb)
0
0.5
1
1.5
2
2.5
Mid-span Deflection (inch)
Test 1
Test 2

5